Assessment of Roll Stabilization Systems for Heavy Lift Ships

Nikhil Mathew

Master Thesis

presented in partial fulfillment
of the requirements for the double degree:
“Advanced Master in Naval Architecture” conferred by University of Liege
"Master of Sciences in Applied Mechanics, specialization in Hydrodynamics, Energetics and Propulsion” conferred by Ecole Centrale de Nantes

developed at University of Rostock
in the framework of the

“EMSHIP”
Erasmus Mundus Master Course
in “Integrated Advanced Ship Design”

Ref. 159652-1-2009-1-BE-ERA MUNDUS-EMMC

Supervisor: Prof. Dr.-Ing. habil. Nikolai Kornev, University of Rostock

Internship Supervisor: Mr. Helge Rathje, SAL Heavy Lift GmbH

Reviewer: Prof. Dr.-Ing. Domnisoru L. Leonard, University of Galati

Rostock, February 2016

ABSTRACT

Heavy-lift ships are vessels designed to move very large loads that cannot be handled by normal vessels, and lately heavy lift ships have been widely used in the offshore industry for offshore installation projects which requires large operational time window. As majority of the lifting operations are done at zero speed condition the dependency on roll motion is very high, which make it necessary to install roll stabilization system on such vessels.

There are many roll stabilization systems which are being commonly used in the maritime industry, but, most of the stabilization systems become obsolete at zero speed condition and hence the only effective systems left are passive fins and anti roll tanks. But, both these systems have constraints ,like, anti-roll tanks utilizes large stowage area of the vessel which effect the profit of the company, as well as, retrofitting of these systems are really complicated. Similarly, passive fins have the limitation on its size, as the size of the fins increases the resistance. So a new stabilization system has to be designed which is effective, economical and has the possibility to be fitted to a vessel whenever required without affecting its stowage area or the hull form resistance. As a solution it was found that if there is a possibility to fit a large plate on the vessel, then, it will act as a damping system which can reduce the roll motion. Even though, the system seems simple, there can be 'n' number of possibilities which make it necessary to perform an optimization analysis.

Before running the optimization, it is necessary to accurately estimate the roll motion by considering the non-linearity due to viscosity. Majority of the motion analysis softwares used in the industry are potential solvers, which do not analyze the viscous component. So to consider the non linear viscous damping, a roll decay test is performed but, since experimental tests are expensive, numerical simulation using RANSE solver (Star CCM+) was used. Finally, by using roll decay results and ITTC recommendations, the non-linear damping coefficient is estimated and the non linear roll RAO of the vessel is computed accurately using a potential solver. Now the optimization using genetic algorithm can be performed for finding the best plate which gives minimum roll RAO and minimum structure weight. So by considering the oscillatory drag coefficient of the plate it's possible to estimate the roll RAO of the vessel with plate and using simple beam theory the best plate structure for a pressure distribution was calculated which is used to compute the weight of the structure.

Finally, the best plate configuration obtained is compared with all the possibilities of fixing a passive anti roll U-tank in the vessel and for designing the U-tank the theory put forth by Lloyd in 1989 is used. Ultimately the most feasible solution out of the above is proposed.

ACKNOWLEDGEMENTS

Firstly, I would like to express my sincere gratitude to my supervisors **Mr. Helge Rathje**, Senior Project Engineer, SAL Heavy Lift GmbH and **Prof. Dr.-Ing. habil. Nikolai Kornev**, Head of the department, Department of modeling and simulation, University of Rostock, for their continuous support throughout this thesis work and also for taking part in major decisions, giving necessary advices, guidance and arranging all the facilities needed which made life easier.

Besides my advisors, I would like to express my deepest sense of gratitude to *Mr. Jonathan Schmidt*, Senior Project Engineer, *Mr. Bin Wang (EMship Alumni),* Project Engineer, *Mr. Sebastian W.*, Project Engineer, *Mr. Arthur Stuckert*, Project Engineer and *Mr. Tilo Klappenbach*, Project Engineer, in SAL Heavy Lift GmbH, as well as, *Dr.-Ing Hannes Kroger*, Department of modeling and simulation, University of Rostock, for their guidance and help which were extremely valuable for this study.

I also like to thank *Mr. Matthias Walter*, Department of modeling and simulation, and the faculty of Department of Naval Architecture, University of Rostock for supporting and facilitating everything required for running the CFD computations.

Finally, I want to thank my family: my parents, my brother and my sister for supporting me spiritually throughout writing this thesis and my life in general.

This thesis was developed in the frame of the European Master Course in “Integrated Advanced Ship Design” named “EMSHIP” for “European Education in Advanced Ship Design”, Ref.: 159652-1-2009-1-BE-ERA MUNDUS-EMMC.

Table of Contents

List of Figures

List of Tables

List of Abbreviations

CAD	-	Computer Aided Design
CFD	-	Computational Fluid Dynamics
DNV-GL	-	Det Norske Veritas & Germanischer Lloyd
DOF	-	Degrees of freedom
DP	-	Dynamic positioning
DTMB	-	David Taylor model basin
FEA	-	Finite Element Analysis
FEM	-	Finite Element Method
GA	-	Genetic Algorithm
ITTC	-	International Towing Tank Conference
MOGA	-	Multi Objective Genetic Algorithm
RAO	-	Response Amplitude Operator
RANSE	-	Reynolds Averaged Navier Stokes Equations
VCG	-	Vertical center of gravity
VOF	-	Volume of Fluid Method
WAF	-	Wake amplification factor

List of Symbols

Lwl	–	Length of waterline of the vessel
B	–	Breadth of the vessel
C_b	–	Block coefficient of the vessel
C_m	–	Midship sectional coefficient of the vessel
GM	–	Metacentric height
Φ	–	Angle of roll
ρ	–	Density of fluid
g	–	Acceleration due to gravity
M_{ij}	–	Mass component of the vessel
A_{ij}	–	Added mass coefficient
B_{ij}	–	Damping coefficient
C_{ij}	–	Stiffness coefficient
F_i	–	Force acting on the vessel
ω	–	Encounter frequency of the incident wave
k	–	Radius of gyration
I_{xx}	–	Mass moment of inertia
Δ_{vessel}	–	Displacement of the vessel
B_F	–	Frictional damping coefficient
B_W	–	Wave making damping coefficient
B_E	–	Eddy making damping coefficient
B_{BK}	–	Bilge keel damping coefficient
Φ_n	–	Peak values of roll decay test
Φ_a	–	Maximum angle of roll
xt	–	Length of the tank
qf	–	Coefficient of linear damping of the tank
r_d	–	Distance between CG of the vessel and the axis of the connecting tube
h_r	–	Distance between water level and the axis of the connecting tube
w_r	–	Width of the side tank of anti roll U tank
w	–	Distance between the axes of side tanks
h_d/h	–	Height of the tank
$\Delta\Phi$	–	Difference between peak values
Φ_m	–	Mean of peak values
$\bar{\bar{M}}$	–	Mass matrix
$\bar{\bar{A}}$	–	Added mass matrix
$\bar{\bar{B}}$	–	Damping coefficient matrix
$\bar{\bar{C}}$	–	Stiffness matrix
$\bar{F}$	–	Force vector
$\bar{f}$	–	Force amplitude vector
$\bar{\epsilon}$	–	Vector of phase angles of the force w.r.t wave elevation

$\bar{X}$	–	Response vector
$\bar{\theta}$	–	Vector of phase angle of the motion w.r.t wave elevation
x_g, y_g, z_g	–	Center of gravity w.r.t the reference point
H	–	Wave height.
a, b, c	–	Decay coefficients
A_d	–	Coefficient representing wave-making component
ω_n	–	Natural frequency
C_{44}	–	Stiffness coefficient for roll
B_{44n}	–	Damping coefficient from potential solver for roll
ω_t	–	Natural frequency of the tank
yo, yi, zo, zi	–	Coordinates of U tank - check figure 26
τ	–	Response of the water column
τ_{max}	–	Maximum response of the water column
C_d	–	Drag coefficient
V	–	Velocity of the fluid on the plate
F_d	–	Drag force
B_{44p}	–	Linearized damping coefficient from the drag of the plate
L_p	–	Length of the plate
B_p	–	Breadth of the plate
Z_p	–	Position of the plate
X_{ap}	–	Orientation of the plate about x axis
AR	–	Aspect ratio
$C_{dtheeta}$	–	Drag coefficient for a given angle of attack
C_{d90}	–	Drag coefficient for 90^o angle of attack
P_d	–	Pressure due to the drag or viscosity
P_w	–	Pressure due to the wave
N	–	Number of stiffeners
F	–	Shear force
M	–	Bending moment
Bs	–	Breadth of the pontoon arm structure
b_p	–	Breadth of the element plate
t_p	–	Thickness of the element plate
h_s	–	Stiffener height
t_s	–	Stiffener thickness
y	–	Distance from the neutral axis
Q	–	Moment of area
I	–	Moment of Inertia
R_{eh}	–	Permissible stress from DNV-GL rules
σ_a	–	Allowable stress
F_n	–	Vertical force on the plate
KC	–	Keulegan–Carpenter number

Declaration of Authorship

I declare that this thesis and the work presented in it are my own and have been generated by me as the result of my own original research.

Where I have consulted the published work of others, this is always clearly attributed.

Where I have quoted from the work of others, the source is always given. With the exception of such quotations, this thesis is entirely my own work.

I have acknowledged all main sources of help.

Where the thesis is based on work done by myself jointly with others, I have made clear exactly what was done by others and what I have contributed myself.

This thesis contains no material that has been submitted previously, in whole or in part, for the award of any other academic degree or diploma.

I cede copyright of the thesis in favour of the University of Rostock

Date: 15/01/2016 *Signature*

1. INTRODUCTION

Heavy-Lift Ships are vessels designed to move very large loads that cannot be handled by normal ships. These vessels were initially used as unloading facilities at inadequately equipped ports and later developed into a large domain which at present includes offshore installations. Most of the heavy lift vessels are utilized in this sector for the transportation and installation of subsea structures, water spools & jumpers, offshore platform jackets, topsides and water mooring systems for floating installations. Since these vessels have large holds and deck capacities, they allow them to handle these types of installation projects efficiently.

Figure 1. SAL heavy lift vessel during offshore installation, from http://sal-heavylift.com.

Majority of the offshore installation process require relatively large operational time window which highly depends on the motions of the vessel on different sea states. For a well-positioned vessel with dynamic positioning the most sensitive motions will be heave and roll, out of which roll motion has high significance as it hinders double banking operations, as well as, make it tough to position the offshore structure accurately.

So it is necessary to find a solution to reduce the roll motion of the vessel which is both economical and feasible. At present there are many roll stabilization systems which are popular in the industry, but they become obsolete when the forward velocity is zero. Hence a stabilization system has to be designed which is effective at zero speed condition and is also economical, feasible and easy to fit whenever required. Hence in this thesis a new stabilization system is designed and is compared with other conventional systems.

1.1 SAL Heavy Lift GmbH

SAL Heavy Lift is one of the world's leading carriers, specialized in sea transport of heavy lift and project cargo. SAL has 16 modern heavy lift fleets out of which the largest vessels are the type 183 vessels having a lifting capacity of 2000t. There are two vessels under this class, MV SVENJA (12/2010) and MV LONE (03/2011) as shown in Figure 2.

Figure 2. SAL heavy lift ship type 183. Available in http://sal-heavylift.com

1.2 SAL TYPE 183

SAL type 183 are the largest ships available in SAL Heavy Lift fleet and these vessels are been used for numerous offshore installations along with other heavy lift operations. MV SVENJA has been equipped with Dynamic Positioning (DP) I system and MV LONE with DP II system. Both these vessels have identical vessel particulars and it is as shown in table 1.

Table 1. Vessel particulars of SAL Type 183.

Vessel Particulars	Value
Displacement	21846 t
Length of Waterline (Lwl)	153m
Breadth (B)	27.5m
Draft (used during offshore installation)	8.5 m
Block Coefficient (Cb)	0.596
Sectional Area Coefficient (Cm)	0.981
VCG (from Keel)	11.5m
Considered GM	1.55m

These vessels may experience large resonant roll motions during the offshore installation processes and it's of high priority to find a feasible solution to mitigate this problem.

2. GENERAL DISCRIPTION

2.1 OBJECTIVE

To design an optimum roll stabilization system for SAL Heavy Lift Ships Type 183.

2.2 SCOPE OF THE PROJECT

- Study of different roll stabilization systems (Literature Survey)
- Finding the feasible solutions
- Estimation of roll motion of the ship
  - Ikeda Method (Empirical Formulation)
  - Roll decay test (RANSE solver)
    - Validation of CFD model using DTMB 5415 test results
    - Computation of roll damping coefficient using RANSE solver
  - Estimation of nonlinear roll RAO of the vessel
  - Comparison of the results obtained
- Design and comparison of the feasible solutions
  - Design of Anti-Roll U tank considering all possibilities
  - Design of roll stabilization system using the plate
    - Optimization of the plate (Genetic Algorithm)
      - Hydrodynamic – Potential solver and viscous component
      - Structure – Simple beam theory
    - Validation of roll motion result with RANSE solver
  - Comparison of both solutions
- Proposing the best solution

2.3 DESIGN SEA STATE

The roll stabilization system designed is intended to reduce the roll motion of the vessel when facing a beam sea with same time period as the natural period of the vessel with a wave height of 3m.

2.4 SOFTWARES USED

Several softwares have been used in this whole thesis and they have been listed in table 2.

Table 2. Softwares used in this thesis.

Software Name	Purpose of Software
Maxsurf	CAD Modeling
Rhino	CAD Modeling
Star CCM+	Solver (Reynolds-averaged Navier–Stokes solver)
WAMIT	Solver (Potential Flow)
modeFRONTIER	Optimization tool
Hyperworks	FEA Analysis Software
Matlab	Coding

Maxsurf and Rhino is been used for modeling the vessels and exporting the models into the required formats. Since roll motions have high dependency on the viscosity of the fluid a RANSE (Reynolds Averaged Navier Stokes Equations) solver is required for accurately estimating the Roll RAO of a vessel and in this thesis the CFD solver developed by CD-Adapco, Star CCM+ which is a widely used computational tool in the industry, has been used.

However, RANSE solvers can't be used for optimization as its time consuming, so a potential solver, WAMIT, motion analysis software developed by MIT, is utilized for optimization runs. As potential solvers don't take into account the viscous part, this component is calculated externally and then is used in the equation motion and solved this is done using different codes made in Matlab. Also a structural optimization code was developed code in Matlab and to validate the result FEA software Hyperworks, developed by Altair Engineering is used.

The main objective of this thesis is to design a roll stabilization system which is optimum for the vessel and to do so optimization run clubbing different softwares is required. To run the optimization in a seamless manner, the modeFRONTIER software developed and marketed by conglomerate ESTECO, is used. It is an integration platform for multi-objective and multi-disciplinary optimization, in other words, it acts like a black box with various optimization algorithms programmed into it and has a user friendly platform to integrate different programs or softwares with high ease.

3. LITERATURE SURVEY

The rigid ship has generally six degrees of freedom (DOF) which are called as surge, sway, heave, roll, yaw and pitch (see Figure 3). Out of these, surge, sway and yaw don't have restoring forces, hence these motions are not oscillatory and it's possible to constrain these motions using effective mooring system or DP system during operations. On the other hand, roll, pitch and heave have restoring components which make them oscillate about their own axis and it is normally not possible to constrain these motions completely.

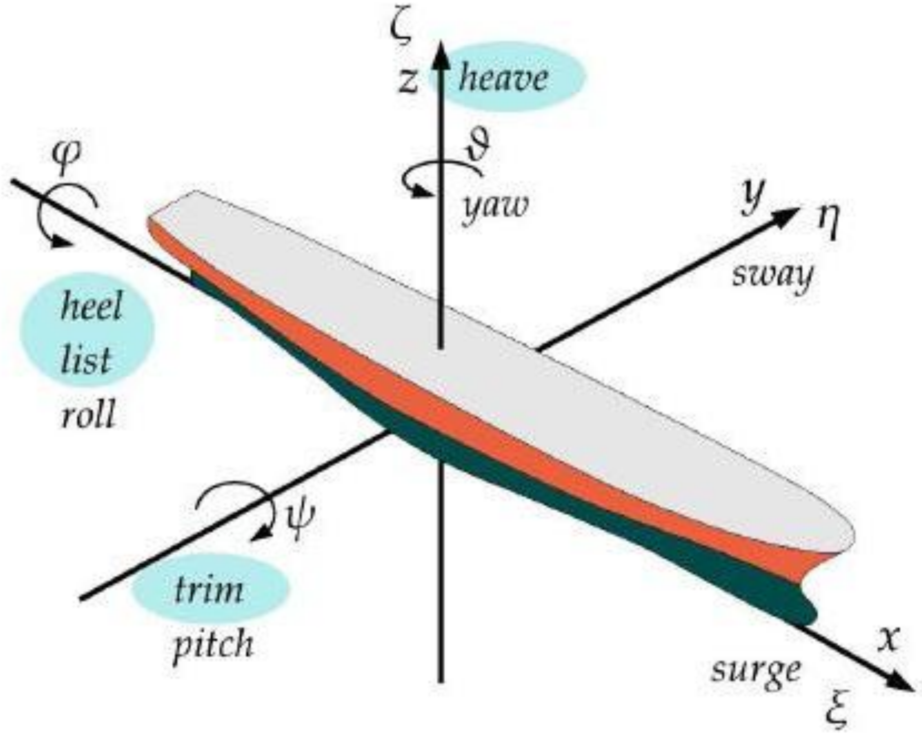

Figure 3. Ship Motions with 6 degrees of motions [1].

In this thesis priority is given to mainly one degree of motion i.e. roll motion. Roll Motion is a highly non-linear motion due to the influence of viscosity which makes it complicated to estimate. Hence the theoretical background behind the roll motion and the methods to estimate roll motion of a vessel will be discussed in detail in this section along with the stabilization systems used to reduce the roll motion.

3.1 COMPUTATION OF ROLL MOTION

A roll motion can be represented as

$$(M_{44} + A_{44})\ddot{\Phi} + B_{44}\dot{\Phi} + C_{44}\Phi = F_4 e^{i\omega t} \tag{1}$$

Where

Φ	–	Angle of roll
M_{44}	–	Moment of inertia of the vessel I_{xx}
A_{44}	–	Added moment of inertia for roll motion
B_{44}	–	Damping coefficient of roll motion
C_{44}	–	Coefficient of restoring moment
F_4	–	Moment causing roll
ω	–	Encounter frequency of the incident wave

The roll motion Φ can be estimated by solving the above equation. Each degree of freedom has similar formulations along with coupled components. The details of solving 6- DOF have been explained in later sections and here each component of roll motion is explained.

M_{44} is the mass dependent factor for roll motion, so $M_{44}=I_{xx}$ – mass moment of inertia about x-axis. I_{xx} can be expressed for a vessel as

$$M_{44} = I_{xx} = \Delta_{vessel} \times k^2 \tag{2}$$

Where k is the radius of gyration and for most heavy lift vessels it is nearly equal to 0.4 times the breadth of the vessel.

C_{44} is the stiffness of the system or in other words is the restoring moment of a vessel i.e. $\Delta. g. GZ = \Delta. g. GM\ sin\Phi = \Delta. g. GM\ \Phi$, this is true for small angles, if high angles have to be used then using the help of KN chart a GZ curve can be made which later can be written as a function of Φ by fitting a curve. Hence C_{44} can be deduced from the hull form directly.

While A_{44}, B_{44} and F_4 can't be estimated from the hull specification alone, those are hydrodynamic components which are estimated by taking into account the presence of wave around the vessel. There are several methods to estimate the hydrodynamic components and normal practice is to use potential flow solvers.

Potential solvers use the assumptions that the flow is steady, incompressible and inviscid, which results in simpler formulations resulting in faster computation. In this thesis the potential solver used is WAMIT which is a radiation diffraction program, developed based on three-dimensional panel method. In WAMIT, the free-surface condition is linearized and the radiation and diffraction velocity potentials on the body wetted surface are determined from the solution of an integral equation obtained by using Green's theorem with the free-surface source-potential as the Green function [13]. For further details on the solver refer [13].

Hence using WAMIT the following quantities can be evaluated:

- Hydrostatic coefficients (C_{44})
- Added-mass and damping coefficients for all modes (A_{44} & B_{44})
- Wave exciting forces and moments using the Haskind relations (F_4)
- Motion amplitudes and phases for a freely-floating body ($\Phi e^{i\omega t}$)
- Hydrodynamic pressure and fluid velocity on the body surface

But as the inviscid flow assumption is taken for the hydrodynamic calculations, it is found that the damping coefficient estimated has only the wave radiation part which is not sufficient enough as the damping is highly influenced by the viscosity of the fluid and it is neglected. Viscosity of fluid makes the roll motion highly nonlinear and that make the prediction of roll motion difficult.

While a vessel is rolling there are different damping effects due to the viscosity and they are drag, friction, flow separation and appendage effects. Hence the damping of the vessel in rolling is usually estimated using two common procedures:

I. Semi-empirical methods
II. Free oscillation model tests

Semi-empirical methods are developed based on an extensive series of model tests where an empirical formula is obtained after combining the test results with some theoretical considerations. The Ikeda-Himeno roll prediction method is the most popular method used in the industry for evaluation of roll damping for ship-like bodies. This method has been explained in detail in section 3.2.1.

A free oscillation model test, or roll decay test, is considered as the most reliable tool for predicting roll damping of a vessel. But these require experimental tests which are too expensive. Hence, numerical simulation of the test in a RANSE solver will be a feasible solution. Since RANSE solvers take into account the viscosity it is indeed possible to estimate all the complexity occurring during rolling.

So it is possible to estimate the roll motion more accurately by estimating M_{44} from the vessel particulars, C_{44} A_{44} and F_4 using potential solver and B_{44} by using roll decay test or semi empirical methods.

3.2 DAMPING COEFFICIENT

3.2.1 Semi-Empirical Method

As discussed before, since the roll damping of ships has significant effects of viscosity, it is difficult to calculate it theoretically. Therefore experimental results or some prediction methods are used to estimate the roll damping. Ikeda prediction method is one of the widely used methods in many ship motion computer programs.

In Ikeda's method, the roll damping is divided into the frictional (B_F), the wave (B_W), the eddy (B_E) and the bilge keel (B_{BK}) components at zero forward speed, and at forward speed, the lift (B_L) is added. Since most of the heavy lift operations are done at zero speed condition the lift component B_L can be neglected [2].

$$B_{44}=B_w + B_F + B_E + B_{BK} \tag{3}$$

In the initial stage each component except the friction component is predicted for each cross section with unit length and the values are summed up along the ship length, but, that gave inconsistent results for similar hull forms due to the different methods of integration. Hence, a new method was developed by utilizing Ikeda's method and methodical series ships. So in this approach, the formulations are made using Taylor Standard Series hull forms. When the roll damping of a hull form is to be calculated, the calculation is done for a similar Taylor Standard Series hull form which is methodically obtained by changing length, beam, draft, midship sectional coefficient and longitudinal prismatic. This approach tends to give more precise results.

For the calculation required in this thesis, the wave making component is excluded as it can be accurately calculated using a potential solver. So the empirical formulation of three components B_F , B_E and B_{BK} are used from Ikeda Method, refer[2] for the formulations.

3.2.2 Free oscillation model tests

It is normal practice to perform a free oscillation test or roll decays test (in this case) to find the damping of a system. To perform a free oscillation test the body is offset away from its equilibrium position, here its roll angle, and the body is let free to oscillate on its own. The body oscillates in its natural period and if the system experiences damping then the amplitude of oscillation reduces w.r.t time as shown in Figure 4. ITTC put forth some recommendations to estimate the damping coefficient of a vessel from roll decay test results. The damping moment can be expressed as

$$B_{\Phi} = B_1\dot{\Phi} + B_2\dot{\Phi}^{\,2} + B_3\dot{\Phi}^{\,3} \tag{4}$$

which is a nonlinear representation. Computing the roll motion using the above formulation can't be done in frequency domain due to the square and cube terms of time dependent variable. In such cases normally time domain analysis is done to estimate the results with nonlinearity, but, the computing time is way too high. Hence for comparatively easy computation the time dependent variable is linearized. This help in taking into account the roll dependent non-linear part which is the key element while computing roll motion. To show how the linearization is done let's consider terms until the second order.

$$B_{\Phi} = B_1\dot{\Phi} + B_2\dot{\Phi}^{\,2} \tag{5}$$

$$\Phi = \Phi_a \cos{(\omega t)} \tag{6}$$

$$\dot{\Phi} = -\omega\, \Phi_a \sin{(\omega t)} \tag{7}$$

$$B_{\Phi} = -B_1\omega\, \Phi_a \sin(\omega t) - B_2(\omega\, \Phi_a \sin{(\omega t)})^2 \tag{8}$$

It's known that,

$$\sin(\omega t)|\sin(\omega t)| = \sum_{n=0}^{\infty} \frac{8\sin{((2n+1)\omega t)}}{\pi(2n+1)(4\times(2n+1)^2)} = \frac{8}{3\pi}\sin(\omega t) - \frac{8}{15\pi}\sin(3\omega t) + .. \tag{9}$$

Considering only the linear part of the equation,

$$B_{\Phi} = -B_1\omega\, \Phi_a \sin(\omega t) - B_2(\frac{8}{3\pi}\omega^2\Phi_a{}^2 \sin(\omega t)) \tag{10}$$

Then, $$B_{\Phi} = B_{44}\dot{\Phi} \tag{11}$$

$$B_{44} = B_1 + \frac{8}{3\pi}\,\omega\Phi_a B_2 \tag{12}$$

Similarly, the following equation can be obtained after linearizing the time dependent term of the 3rd order term,

$$B_{44} = B_1 + \frac{8}{3\pi}\,\omega\Phi_a B_2 + \frac{3}{4}\omega^2\Phi_a^2 B_3 \tag{13}$$

Here

Φ_a – Maximum angle of roll

The estimation of B_{44} using the ITTC recommendation will be explained below using a sample reading shown in Figure 4.

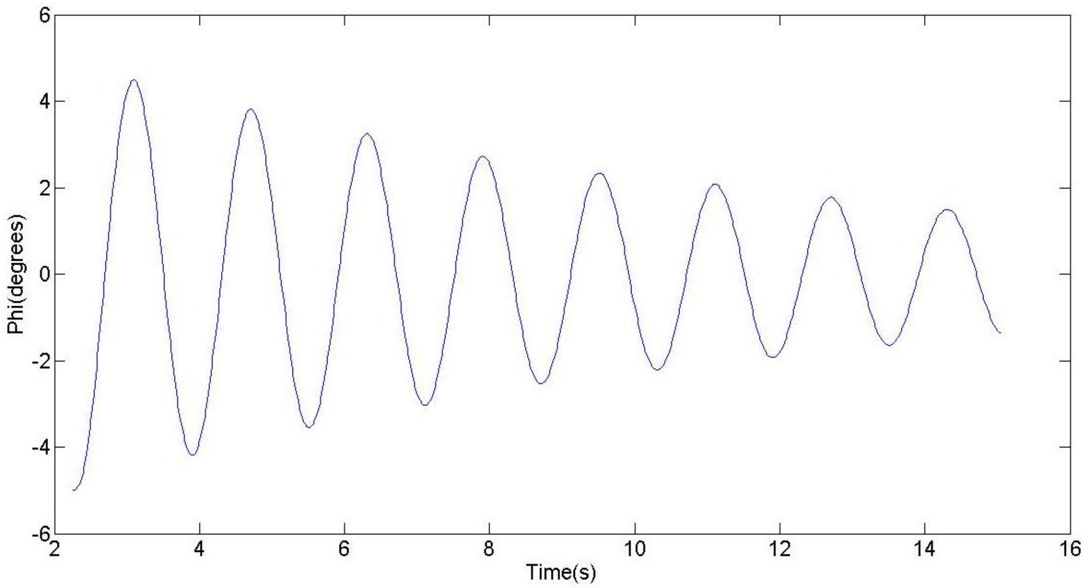

Figure 4. Roll decay test result of DTMB 5512 model for initial angle 5 degrees at Fn=0.069.

Find the peak values i.e. first let's take only the positive side and later the negative side. Find

$$\Delta\Phi = \Phi_n - \Phi_{n+1} \tag{14}$$

$$\Phi_m = \frac{\Phi_n + \Phi_{n+1}}{2} \tag{15}$$

So a series of data is obtained and a plot $\Delta\Phi$ vs Φ_m can be made as shown in Figure 5

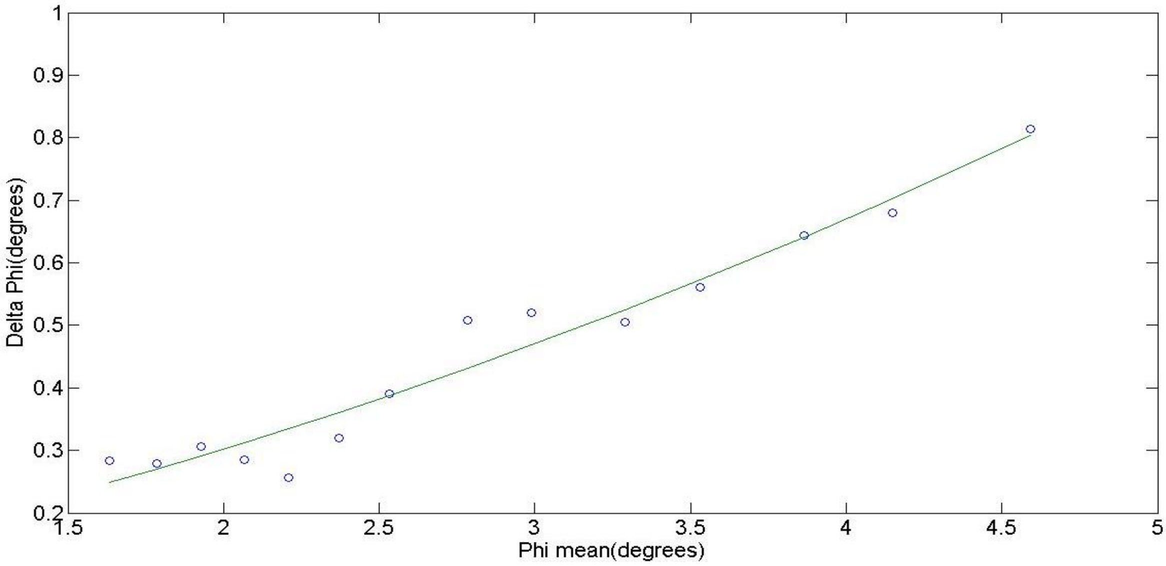

Figure 5. Curve fitted to the roll decay test result in Figure 4.

Fit a polynomial curve in such a way that curve equation can be written as

$$\Delta\Phi = a\Phi_m + b{\Phi_m}^2 + c{\Phi_m}^3 \tag{16}$$

The coefficients a, b and c are called decay coefficients. The relation between these coefficients and the damping coefficients can be derived by integrating Eq. (1) without the external force term over the time period of a half roll cycle and then equating the energy loss due to damping to the work done by the restoring moment [12]. The result can be expressed in the form:

$$\Delta\Phi = \frac{\pi\omega}{2C}\,\Phi_m\,(B_1 + \frac{8}{3\pi}\,\omega\Phi_m B_2 + \frac{3}{4}\omega^2\Phi_m^2 B_3) \tag{17}$$

Hence,

$$B_{44} = \frac{2C}{\pi\omega}\frac{\Delta\Phi}{\Phi_m} \tag{18}$$

$$B_{44} = \frac{2C}{\pi\omega}\frac{a\Phi_m + b{\Phi_m}^2 + c{\Phi_m}^3}{\Phi_m}$$

$$B_{44} = \frac{2C}{\pi\omega}(a + b\Phi_m + c{\Phi_m}^2) \tag{19}$$

3.3 ROLL STABILIZATION SYSTEMS

The ship damping systems are being used since the middle of the last century. In general, the damping devices produce the moment acting against the perturbation moment and counteract the oscillations. Roll stabilization systems can be broadly classified into

1. **Passive systems:** In which no separate source of power or no special control system is required like the anti – rolling tanks (passive), fixed fins & passive moving weight system.

2. **Active systems:** The moment opposing roll is produced by moving masses or control surfaces by means of power like the active fins, Anti–rolling tanks (active), active moving weight and the gyroscope.

The active system are expensive but is designed for different seas states, however, passive system are cheap and is designed only for a specific environmental condition. Hence each system has its own pros and cons and a brief study of different system is required to choose the right system. The common devices used in the industry are

- Damping tanks,
- Bilge keels and
- Active fins and rudders

3.3.2. Damping Tanks or Anti-Roll Tanks

Anti-roll tanks are the most commonly used devices to stabilize the roll motion of ships. The principle used is that shifting weight of the fluid exerts a roll moment on the ship and, by suitable design, this can be made to damp the wave-excited roll motion. Anti-roll tanks can be classified as either passive or active, depending on whether the fluid is allowed to move entirely due to the motion of the ship or is moved with a pump. Passive anti-roll tanks have the advantage of having no moving parts and requiring little maintenance. Moreover, they operate well at slow speeds. Further details are given in section 3.4.

3.3.2. Bilge Keel

The bilge keel stabilizing device (Fig. 6) is a very simple and efficient way to reduce the roll oscillations. The bilge keels are metallic plates which are installed along streamlines. The stabilizing moment is created due to the force on keel. The force exerted is increased due to the vortex shredding on the edge of the plate. The most important geometric parameters of bilge keel are the ratio of the keel area to LB and the distance between the keel center and the ship gravity center referred to the ship beam (see Fig. 6).

Figure 6. Bilge keels.

When designing a bilge keel there are important decisions to consider. To minimize hydrodynamic drag the bilge keel should be placed in way of a flowline where it does not oppose cross-flow. For such a usage the ends of the bilge keel should be tapered and properly faired into the hull. Also, a bilge keel should not protrude from the hull so far that the device could be damaged when the vessel is alongside a pier, even with a few degrees of adverse heel. Bilge keels on commercial vessels should not protrude below the baseline either, where they could be damaged or fouled by grounding.

3.3.3 Rudder Roll and Active Fins

The rudders and active fins are very efficient to reduce the roll oscillations of fast passenger and combat ships. They can be either active or passive and are maintained at the ship bilge. The stabilizing moment arises due to dynamic lift force on the fins or rudders which are proportional to the ship speed squared. Therefore the rudders have no effect when the ship speed decreases. The actively controlled rudders installed in horizontal plane are called active fins (Fig. 7). They can be retracted during mooring.

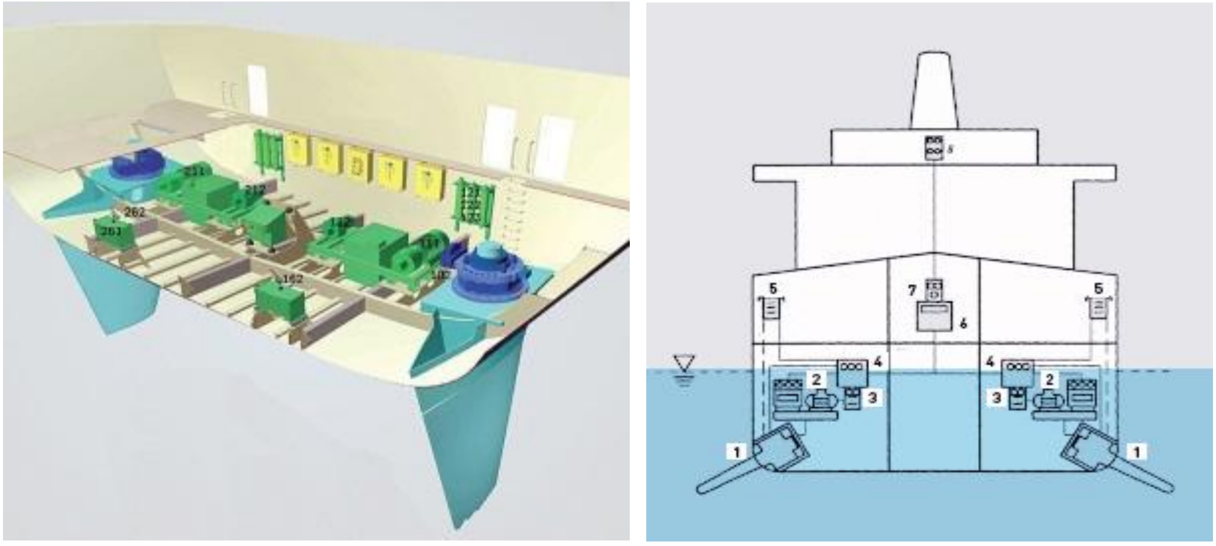

Figure 7. Active rudder roll (left) and active fins (right) [1].

3.3.4 Summary

A brief summary of all the common systems used in the industry are illustrated in table 3

Table 3. Summary of roll stabilization systems [1].

Type	Efficiency	Speed	Impact on Design	Mechanical Problems	Costs
Active Fins	60% - 90%	12knots	Significant space required	Fin Cavitation, Hydraulic control	0.5-2.0 Million Euros
Rudder roll	40% - 60%	12knots	Need more robust steering gear	Additional steering gear design	0.2-0.4 Million Euros
Bilge Keels	10% - 20%	All speeds	Increase resistance	Could be damaged	Shipyard
Anti-Roll tanks	40% - 75%	All speeds	Water weight 1-2% of displacement	None in flume, Remote valves at U-shape	50-80 Thousand Euros

It could be seen that active fins and rudder rolls need forward velocity to be effective and since the working condition for the current case is zero speed, the only possible systems are anti roll tanks, passive fins and bilge keels. The vessel SAL 183 already has bilge keels and retrofitting a passive fin can affect the resistance and in addition, it needs dry docking to fit the system on to the vessel. So the only feasible solution is antiroll tanks and it is discussed in detail.

3.4 ANTI-ROLL TANKS

Passive anti-roll tanks use a hydrodynamically controlled flow of liquid within a designed tank to create a stabilizing moment opposing the wave moment causing the ship to roll. By careful selection of the right tank configuration (proper size, shape, location, liquid level and amount of internal damping) a tank can be made to have the same resonant roll period of the ship, and the fluid flow within the stabilizer will lag naturally behind the resonant movement of the ship by 90 degrees as shown in Figure 8.

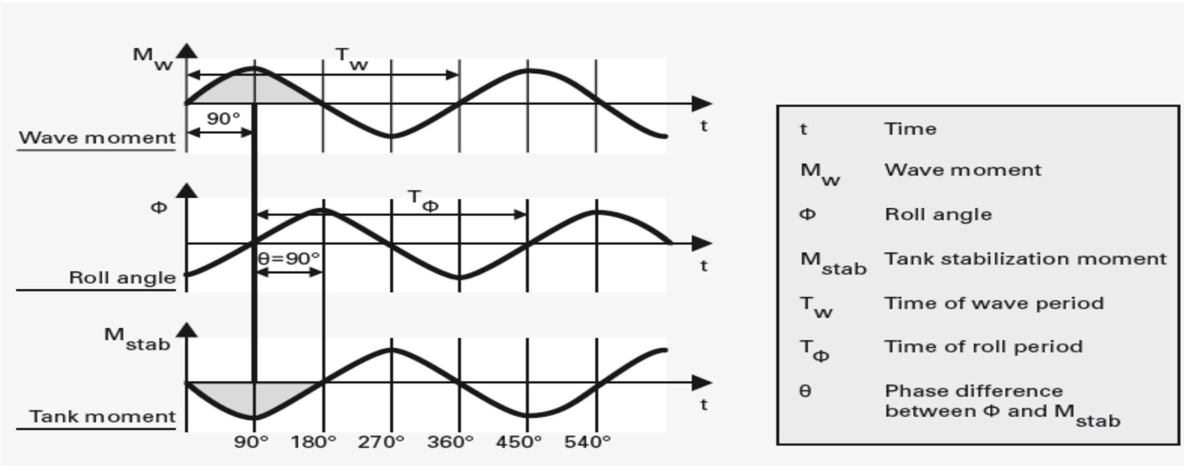

Figure 8. Wave moment and the tank moment diagram. Available in hoppe-marine.com.

Hence near resonance, the movement of the liquid in the tank will create a stabilizing force directly opposing the forces created by the passing wave. Different types of passive antiroll tanks are free surface tanks and U-tube tanks.

3.4.1 Free Surface Tanks

A single partially filled tank that extends across the full breadth of the vessel. Its shape, size and internal baffles allow the liquid inside to slosh from side to side in response to the roll motion of the ship. The phasing of the roll moments acting on the ship and the resultant liquid motion will be such that it reduces the roll motion. These tanks have the added advantage that it is possible to vary tank natural frequency by changes in water level and thus accommodate changes in ships metacentric height. Free surface tanks are commonly referred to as "flume"

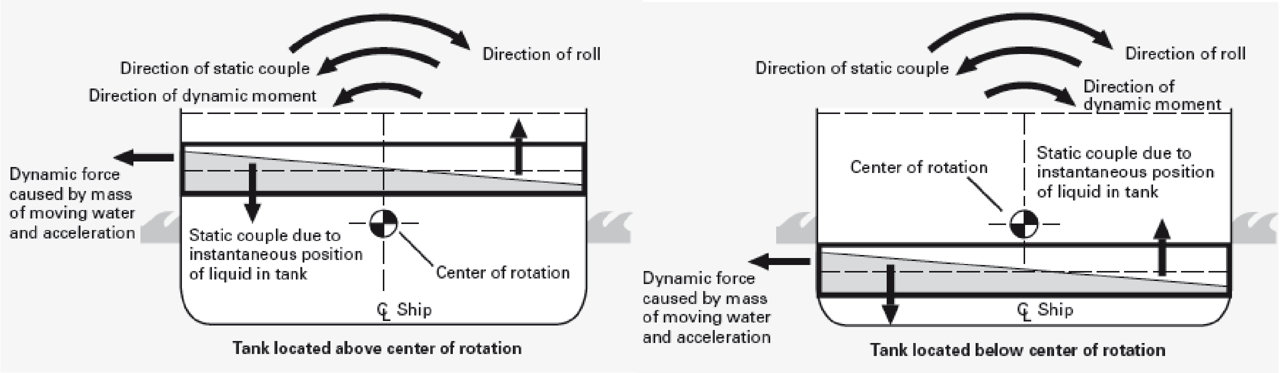

tanks.

Figure 9. Forces generated by Fume Tank. Available in hoppe-marine.com.

A basic flume tank is relatively simple in construction and design, even though controlled systems add a bit more complexity. This system can complicate the vessels stability as we are purposefully adding free surface effect into the vessel which can lead to capsizing of a vessel if environmental conditions stray too far from the design conditions. Also flume tanks require both free volumes, often internally in the vessel, and displacement - ~2% of the vessels overall mass.

3.4.2 U-tube tanks

These are partially filled tanks consisting of two wing tanks connected at the bottom by a substantial crossover duct or ventilation duct. The air columns above the liquid in the two tanks are also connected by a duct.

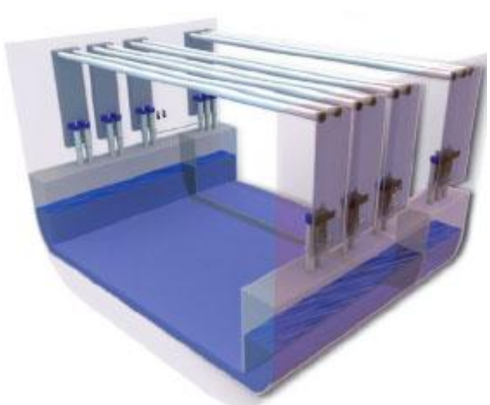

Figure 10. Anti- Roll U- Tank

As in the free surface tanks, as the ship begins to roll the fluid flows from wing tank to wing tank causing a time varying roll moment to the ship and with careful design this roll moment is of correct phasing to reduce the roll motion of the ship. They do not restrict fore and aft passage as space above and below the water-crossover duct is available for other purposes.

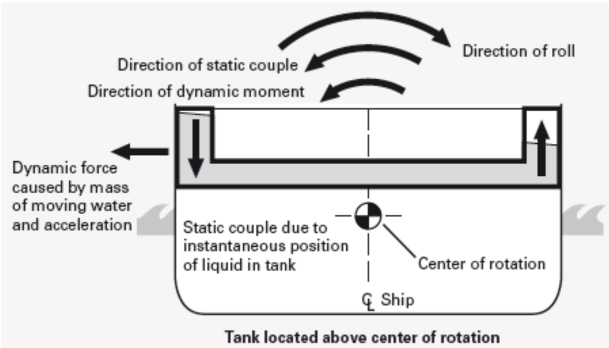

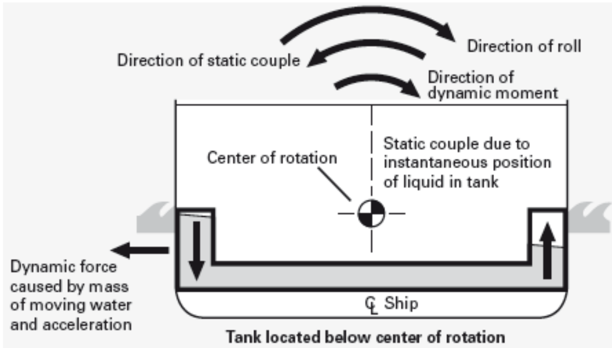

Figure 11. Forces generated by U- tank. Available from hoppe-marine.com

U-connected tanks can be moderated by controlling the ventilation valves as well as the water level, allowing for a greater amount of control of the tanks effects. These tanks are generally fitted as deep tanks, lowering their VCG, and providing a greater degree of safety in operation over the flume variety. Flume tanks are more suitable for small vessels and for large vessels like in the present case where space is a big concern, U tanks are the best solution.

3.4.3. Modelling of U-tube tanks

Mathematical modeling of U-tube tank was developed by Lloyd (1989) for single degree of roll motion by neglecting nonlinear terms. Gawad et al. [6] made theoretical investigation to study the effect of tank location, tank mass, tank damping on maximum roll RAO using the formulation by Lloyd (1989) equations. Holden et al. (2010) have done the nonlinear mathematical modeling of the U-tube tank using Lagrangian energy method and compared the results with experimental results. Earlier research findings have highlighted the roll response at resonance and also reported the influence of tank parameters on the roll response behavior. Here the method proposed by Gawad [6] will be discussed.

A configuration of a simple passive U-tube tank is represented in Figure 11. The tank consists of two side reservoirs and a connecting duct of constant cross-section. The origin O is at the midpoint of the connecting duct and is the point about which moments are summed.

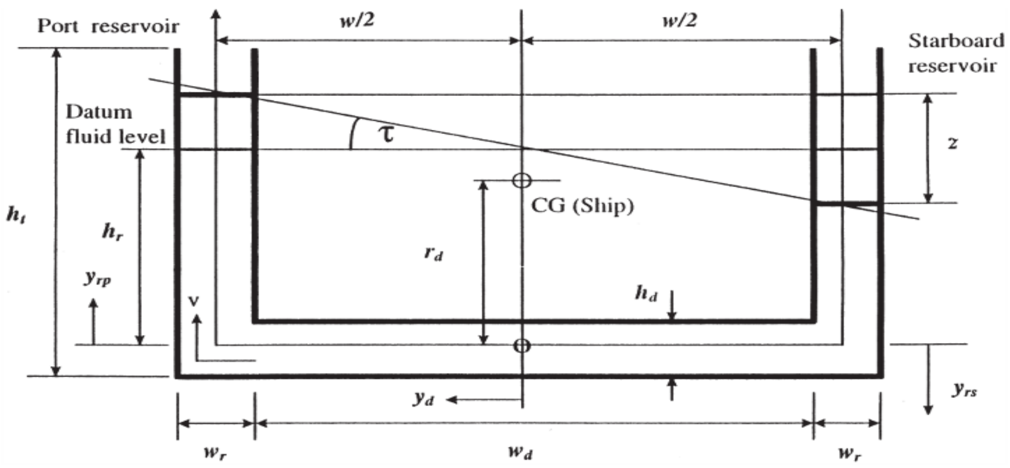

Figure 12. Schematic diagram of a U-tank [6]

The equation of motion of the tank liquid is derived under two simplifying assumptions:

1. The relative motion of the liquid in the U-tube is one-dimensional and
2. Coupling between the 6-DOF equations of motion of the ship and tank-liquid motion takes place through the roll motion only.

However, because the equations of motion of the ship themselves are coupled, there are indirect interactions between the tank-liquid motion and the remaining degrees of freedom. Thus, the equation governing the tank angle τ takes the form

$$a_{\tau\tau}\ddot{\tau} + b_{\tau\tau}\dot{\tau} + c_{\tau\tau}\tau + [a_{\tau4}\ddot{\Phi} + c_{\tau4}\Phi] = 0 \tag{20}$$

Where,

Φ – Roll angle of the vessel

$$a_{\tau4} = Q_t(r_d + h_r) \tag{21}$$

$$c_{\tau4} = Q_t\, g = c_{\tau\tau} \tag{22}$$

$$a_{\tau\tau} = Q_t w_r(\frac{w}{2h_d} + \frac{h_r}{w_r}) \tag{23}$$

$$b_{\tau\tau} = Q_t q_f w_r(\frac{w}{2h_d^2} + \frac{h_r}{w_r^2}) \tag{24}$$

$$Q_t = \frac{1}{2}\rho_t w_r w^2 x_t \tag{25}$$

xt - Length of the tank

qf –Coefficient of linear damping of the tank – Normally between 0.14 and 0.17 [10]

r_d, h_r, w_r, w, h_d are geometrical parameters as shown in the Figure 12. Along with the above equation we have the equation of motion of the vessel with passive tanks, i.e.

$$(M_{44} + A_{44})\ddot{\Phi} + B_{44}\dot{\Phi} + C_{44}\Phi + [a_{4\tau}\ddot{\tau} + c_{4\tau}\tau] = Me^{i\omega t} \quad (26)$$

Where,

A_{44} – Virtual mass moment of inertia for roll motion

B_{44} – Damping coefficient of roll motion

C_{44} – Stiffness for roll motion

$a_{4\tau} = a_{\tau 4}$

$c_{4\tau} = c_{\tau 4}$

The method to solve the above 2 equations has been explained in section 6.1.

3.5 FEASIBLE SOLUTIONS

Finally, the only option left among the conventional stabilization systems are the antiroll tanks and since flume tanks have safety problems and require a separate compartment near the centreline, the only possible solution left is the U-tanks. There are several possibilities of fixing an antiroll U tank into an exciting vessel i.e. by modifying an exciting tank arrangement or by fitting a new set of tanks into the vessel where there is free space. Both of these affect the vessel specification, either it reduces the stowage area of the vessel as the free space available is in the cargo hold, or reduce the lifting capacity of the vessel as the ballast tanks are used to provide a counter moment while lifting. So fixing an antiroll tank into the existing vessel has its own contras.

Even though the above solution is effective there are drawbacks which make it necessary to find another solution which doesn’t affect the vessel specifications. This led to think about all other possibilities and the idea of placing a plate few distances away from the centre line of the vessel was put forth, which is simple and economical. Hence the above two roll stabilization systems are designed and their effectiveness are studied and compared in this thesis.

4. ROLL DECAY TEST IN RANSE SOLVER

It's not always possible to perform an experimental test whenever required, as these tests are expensive. In such cases CFD softwares are used which is less expensive but might require high end computational capabilities like large clusters which will support such simulations. The results obtained from such simulations may have computational errors which results in unrealistic values or values which are highly deviated from the reality. Hence before using such simulation softwares it is necessary to validate the model using experimental results and later utilize the model for similar simulations which don't have any results to validate.

4.1 VALIDATION USING DTMB MODEL

The initial step for performing a CFD simulation for solving a given problem, as discussed before is validation. It is necessary to check whether the results obtained through experiments are the same as the results obtained from the software. If the results obtained are satisfactory then the CFD tool is used for similar analysis.

As explained in section 3.2, it is possible to estimate the roll RAO of a vessel using a potential solver if a roll decay test is conducted. However, roll decay test is rarely conducted in the industry, so the available experiment results are the results from the roll decay test done by IIHR, University of IOWA, on DTMB model 5512, which is a 1/46.6 DTMB model 5415.

4.1.1 DTMB Model 5512

Model 5415 was conceived as a preliminary design for a navy surface combatant in 1980. The hull geometry includes both a sonar dome and transom stern; however, no full-scale ship exists.

IIHR did decay test with both bare hull and also with bilge keel (not all the appendages). The tests were done for different initial angles (0, -2.5, -3.0, -4.0, -5.0, -7.5, -10.0, -12.5, -15.0, -20.0 degrees) and Froude numbers (0.069, 0.096, 0.138, 0.190, 0.280, 0.34, 0.41). The model along with its particulars is provided below.

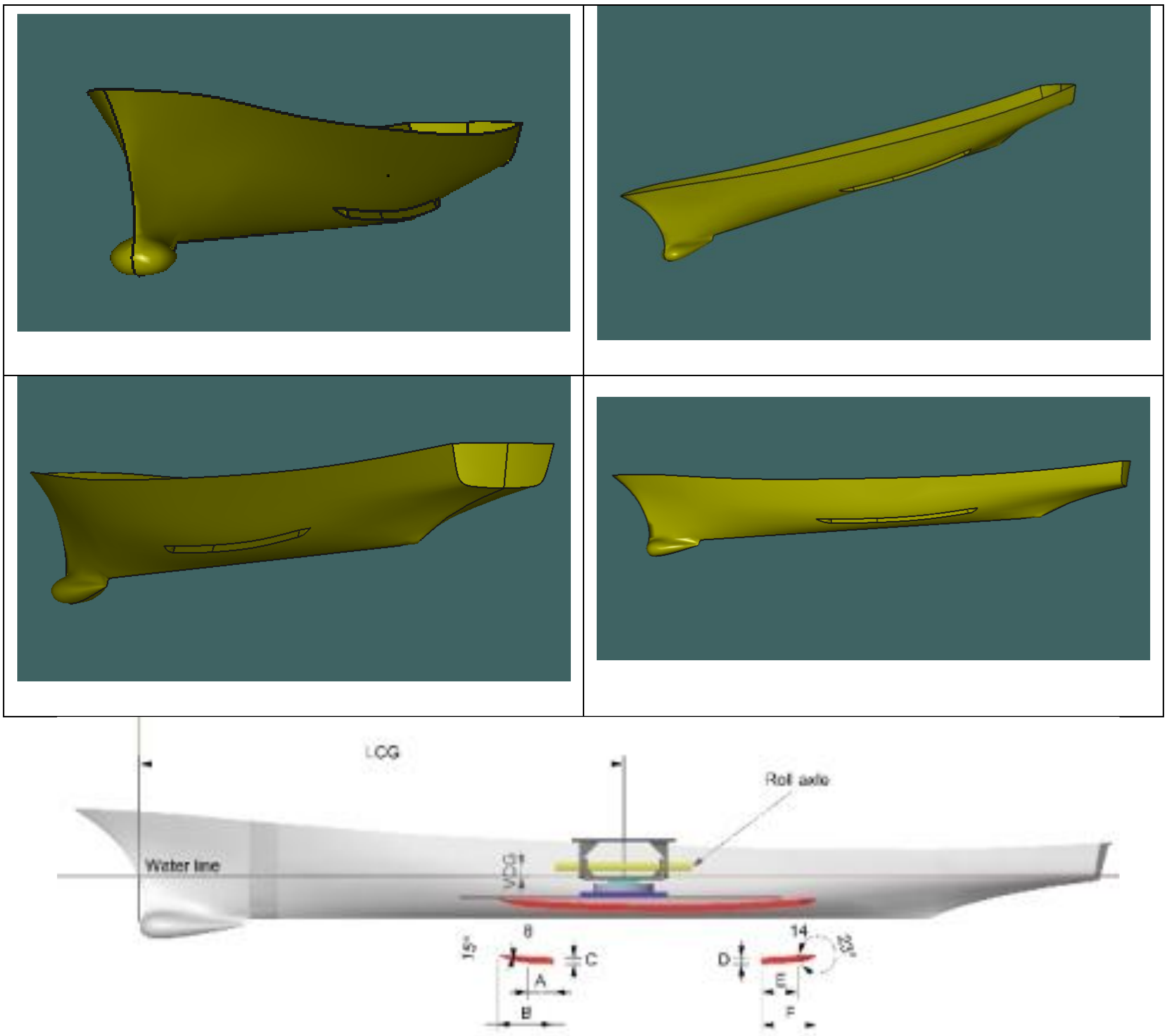

Figure 13. DTMB model 5415

Table 4. Particulars of DTMB model 5415 [3]

Particulars	Value	Unit
Scale	01:46.6	-
Lpp	3.048	m
Lwl	3.052	m
Bwl	0.41	m
Tm	0.136	m
Mass	83.35	Kg
COG-X	-0.0157	m
COG-Y	0	m
COG-Z	0.084	m
Ix	1.98	Kg×m^2
Iy	53.88	Kg×m^2
Iz	49.99	Kg×m^2

4.1.2 Modelling In Star-CCM+

For validation the initial analysis is done on the DTMB (David Taylor Model Basin) 5415 model which was provided by the IIHR. There are different test results which can be used for this simulation. Since the ultimate aim is to find the damping of vessel at zero forward velocity and with bilge keel, the DTMB test condition with bilge keel and a Froude number of 0.069 is used here.

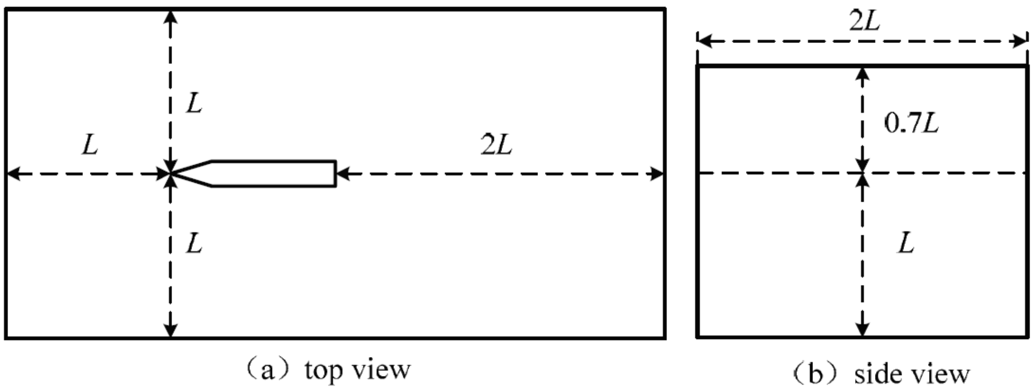

Figure 14. DTMB model 5415

The first step of a CFD simulation is to define the fluid domain. So a rectangular domain was defined as shown in Figure 14, following the recommendation provided in reference [5]. Then the vessel model is introduced and is rotated about the water plate to the given angle, here its 10 degrees and the region between the domain & the vessel is extracted and meshed. The perpendicular surface in the aft of the model is given the boundary condition as Pressure Outlet and rest all surfaces are given the condition as velocity inlet.

Since this is a multi-phase problem, VOF method is used to simulate the water surface and an unsteady, implicit turbulent model (K-Omega SST) for simulating the fluid flow. Fluid velocity of 0.377 m/s is defined in x direction so that the Froude number of 0.069 is obtained.

For this analysis dynamic mesh has been used, hence the vessel is defined with 6 degrees of freedom but only rotational motion about x-axis is unconstraint. Different mesh configurations were tried and the mesh configuration which gave good results is shown in Figure 16. Since the flow around the hull form is of high priority, initially the meshes were aligned along the vessel axis, but, that created errors in defining a flat water surface. These errors were created due to the usage of VOF method. When the VOF method is used, each element is considered to have a fraction of fluid in each cell and when the cell rotates the change in inclination of the fluid due to gravity is not considered, an example is shown in Figure 15.

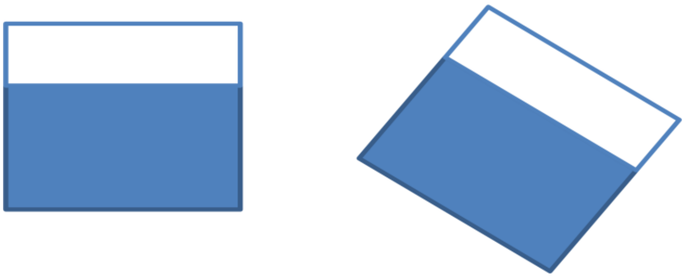

Figure15. Defining volume of fluid in a cell using VOF method

Hence, to have the perfect definition of waterline in the initial condition the mesh is aligned along the global axis. To define the waterline throughout the simulation, high refinement in y direction and z direction is given to the mesh. If the roll decay test is carried out for 10 degrees then refinement in y direction and z direction is given for a rectangular block of height 2L*sin(10°) as shown in Figure 16, where L is the length of the model. This gave better results.

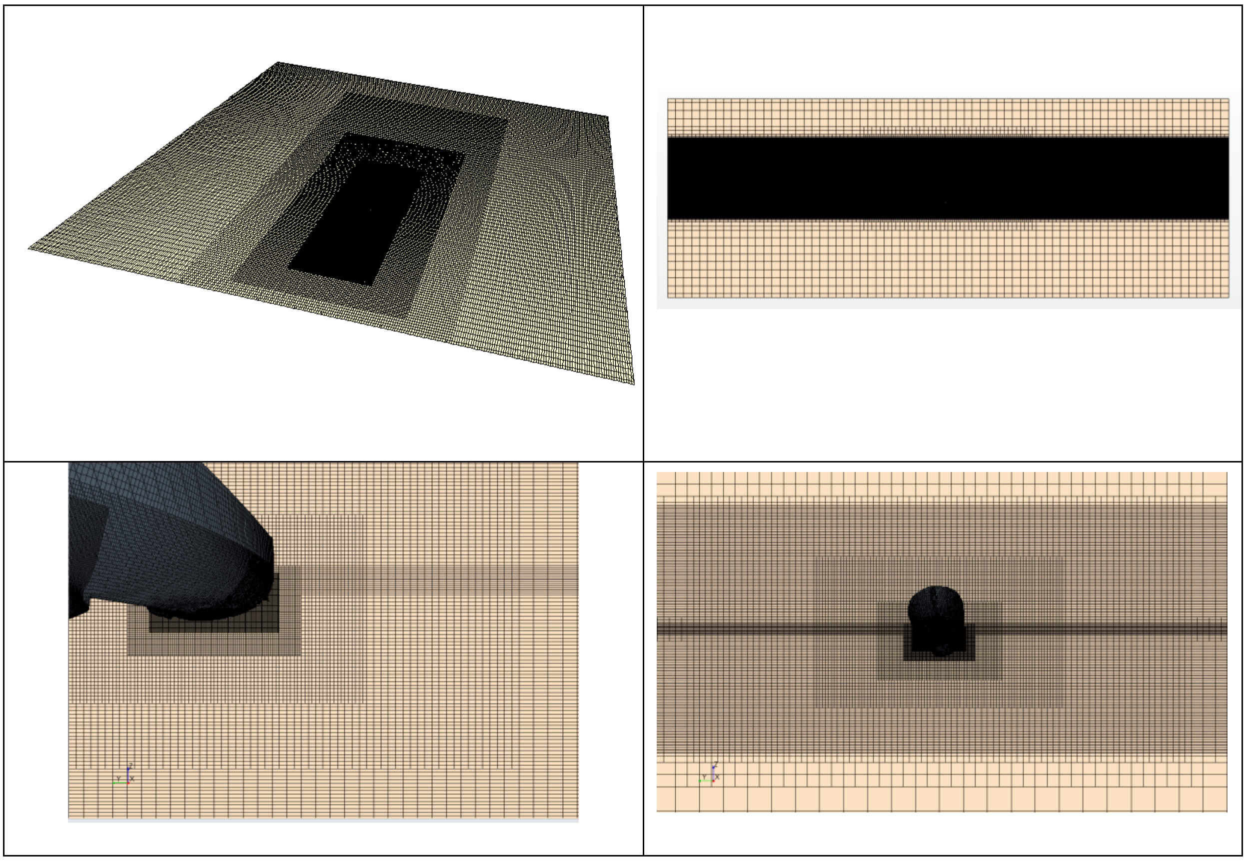

Figure 16. Star CCM mesh for DTMB model 5415

Computation of eddy dissipation near the bilge keel, bow and the aft is of high importance hence really fine meshes are defined near those, using block refinement. Also for reducing the error due to sudden change in mesh size a gradual increase of mesh was provided with minimum10 cells between each refinement which can be seen in Figure 16. Also prism layers were provided in such a way that the y-plus value was below five.

Other main priorities which determine the accuracy of the results are the time step and the internal iterations required for the solver. It was found that with 15 internal iterations and a time step of 0.005 secs the results obtained had less error. The recommendation was to use the time step of 1/100 of the natural period of the vessel [5] i.e. 0.018 but since the errors were large, 0.005 secs were used. Later using time step of 0.001 secs the analysis was ran but the results were converged. Finally the simulation was executed with a ram time of 0.2 secs after which the body was set free and then orientation of the vessel about x axis is computed and compared.

4.1.3 Results

Several analyses were done and the best results are compared with the experimental results as shown in Figure 17.

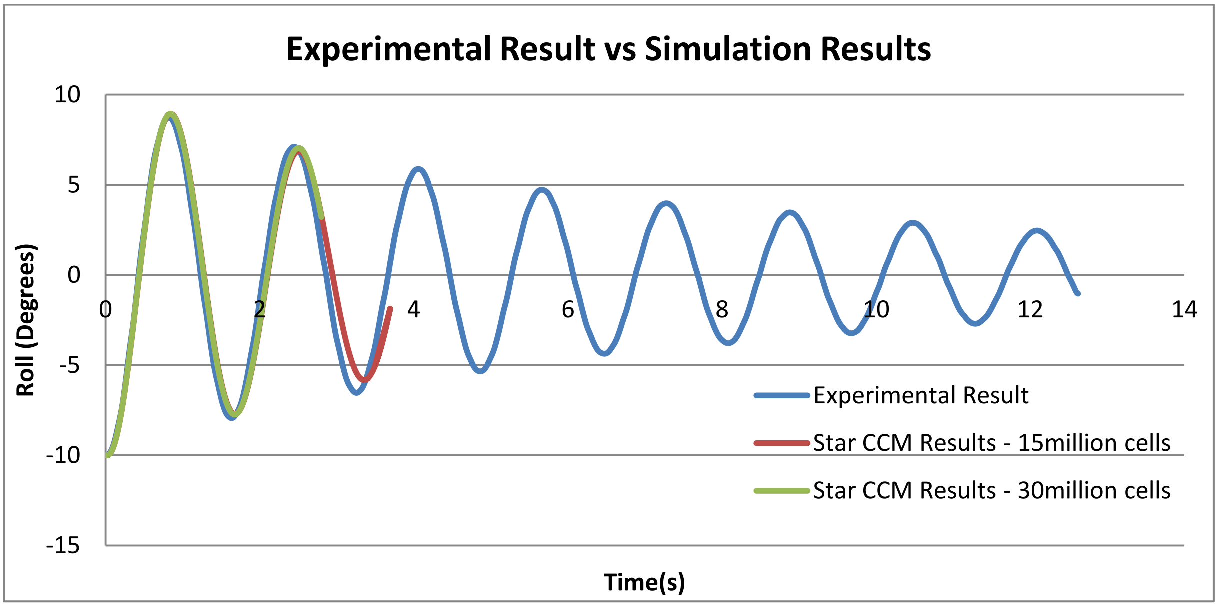

Figure 17. Comparison between experimental result and simulation results

It could be seen that the simulation results for the first 2 oscillations are exactly the same but later it deviates away. To study whether it’s due to the issue of convergence the same simulation was ran with twice the cell number but the results were identical. So those errors can be due to the error caused by the oscillation of the mesh. Anyhow, it is evident that this model can give good results for the first few oscillations and hence similar approach was used for estimating the roll decay coefficient of SAL type 183.

4.2 SAL TYPE 183

The above process was done to find the most apt model to simulate the roll decay test on SAL 183 so that the decay coefficients can be calculated for estimating the roll RAO accurately. The details of the vessel and the particulars of SAL 183 during offshore installation are shown in section 1.2.

4.2.1 SAL Type 183 Model

SAL TYPE 183 model provided didn't have bilge keels modeled, since in this study bilge keel is of high importance, it was designed from the sectional drawings. The bilge keel had a mean breadth of around 35 cm and a total length of 39.212 m along the midship. The model with bilge keel is shown in Figure 18.

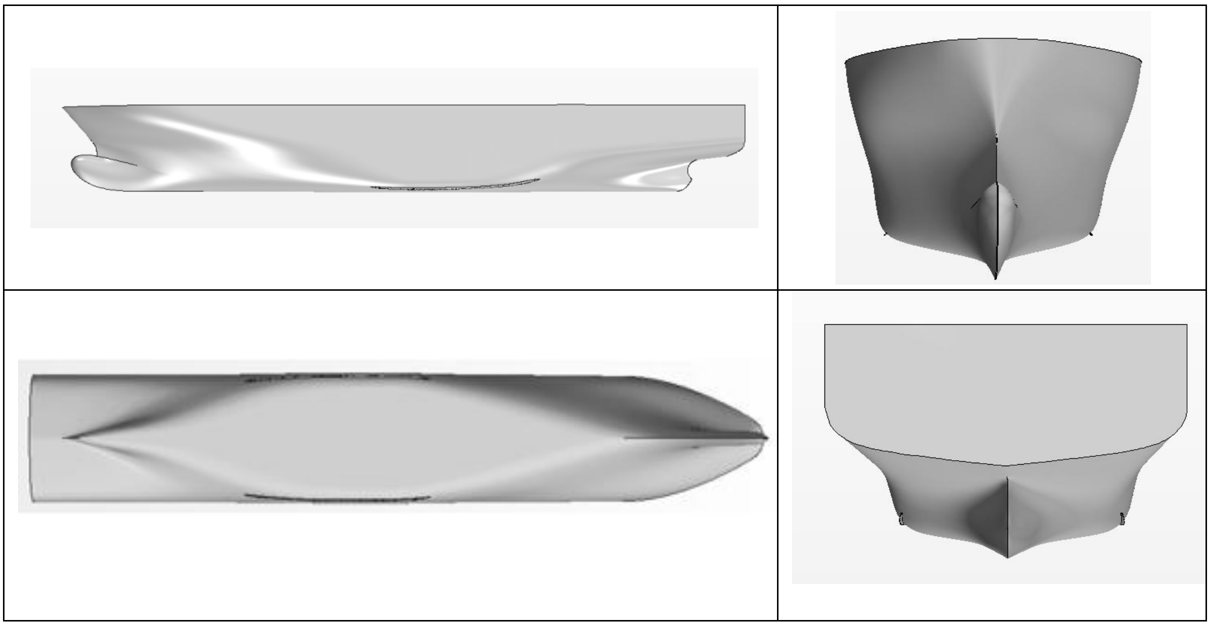

Figure 18. SAL 183 model

4.2.2 Modelling In Star-CCM+

To perform the roll decay test on SAL 183 the same approach used before for simulating the roll decay test on DTMB model 5415 is considered. There are few differences in meshing, as this computation is done at higher Reynolds number (the real size vessel). Firstly the mesh refinement required is too high which increased the mesh number drastically. For DTMB model good results were obtained for 15 million cells while in this case it was obtained for 37 million cells (see Figure 19). Next is the fluid velocity, the simulation is to be ran at zero speed condition but since there were errors due to reverse flow on boundaries, a velocity of 0.1 m/s was given. The other main constrain is the y-plus value, as the real vessel is used. Reducing y-plus below 100 was not possible due to the meshing limitation, hence, the wall function is considered for this simulation.

Star CCM has provided a limiting value of 10000 for turbulent viscosity ratio which is sufficient for a laminar or low turbulent flow. But when the Reynolds number is high, turbulent viscosity ratio goes beyond this limit and since the value is limited to 10000 the results obtained may have errors so a higher denomination values has to be assigned for the ratio while performing such computations. In this approach the time step used was 0.01 secs with 20 internal iterations and it gave good results.

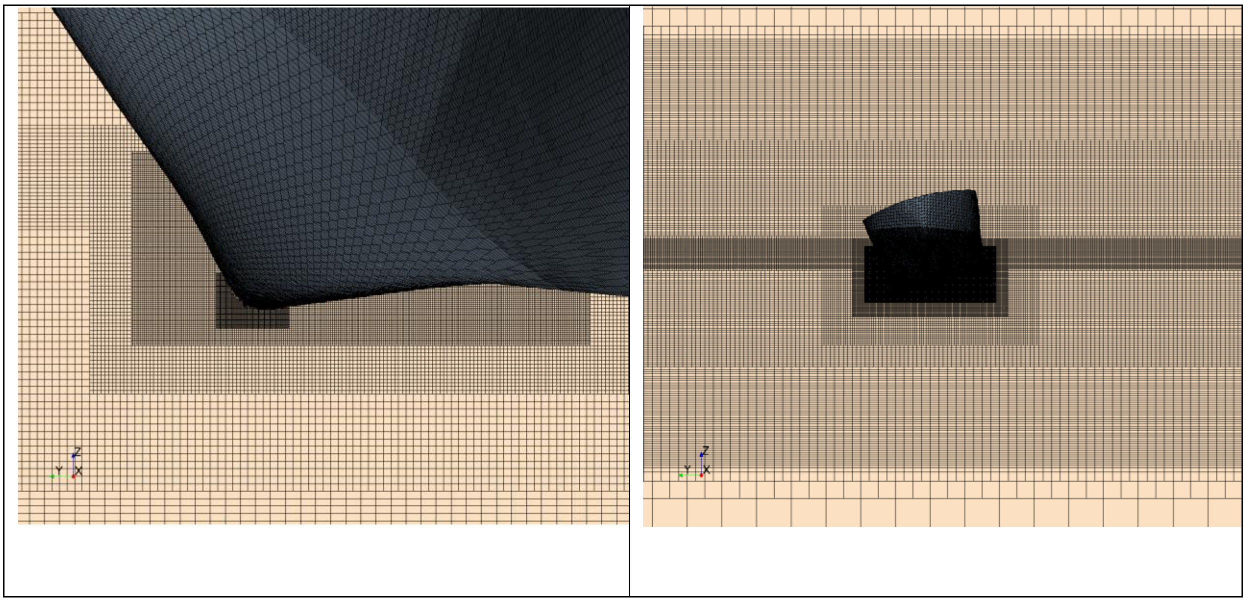

Figure 19. Meshing used for roll decay test of SAL 183model

It could be seen in Figure 17 that in the region of error the time period of the oscillation changed. Hence it was taken as a criterion that the time period of the oscillation has to be constant for different meshes and close to the natural frequency calculated using WAMIT.

Since only one oscillation is considered, it was necessary to perform roll decay test for several initial angles and the above approach helped in finding the apt mesh and also converged solutions for each case.

4.2.3 Roll Decay Test Results

The roll decay test was done for different initial angles so that a set of peak values are obtained for estimating the decay coefficients using the curve fitting method explained in section 3.2.2. If the computation was faster and gave accurate results after the initial few oscillations, then just few numbers of initial angles would have been sufficient. But due to time constrain and other issue one oscillation for different initial angles is considered here (See Figure 20).

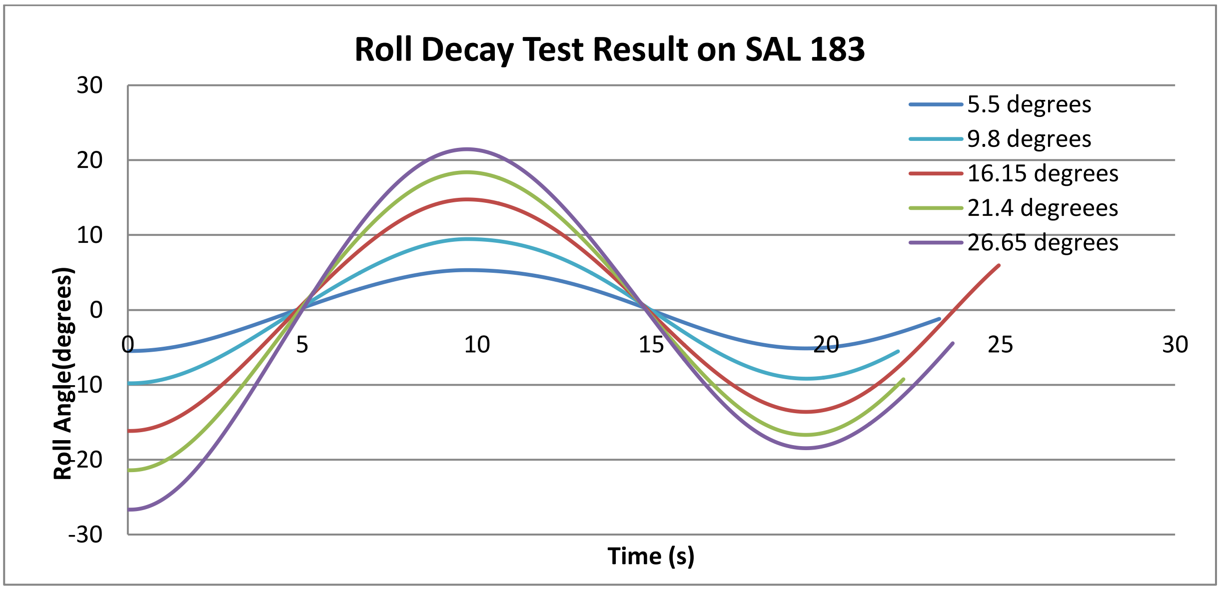

Figure 20. Roll decay test results

For the roll decay test the model is initially rotated about the water plane and when the CG of the vessel is too high from the waterline (here 3 m above waterline), the centre of rotation changes and this can create a different roll value than expected. So it is necessary to find the initial angle of rotation w.r.t the centre of rotation.

To do so, the time period of peak points of the roll decay results are extracted and the difference will be the natural period of the vessel. Then the roll angle at half time period of the first oscillation is extracted which will be the initial angle w.r.t the centre of rotation. Since these values determine the decay coefficients the above estimation method is of high importance.

4.2.4 Curve Fitting

As per the procedure explained in 3.2.2 the peak values of the roll decay test results are obtained and their differences are calculated and plotted. The difference is normally taken between values on the same side but here since the number of oscillations is less the difference between the consecutive peaks are also considered, but the difference is multiplied by two and plotted. The resulting graph can be seen in Figure 21 were these points are fitted to a polynomial equation.

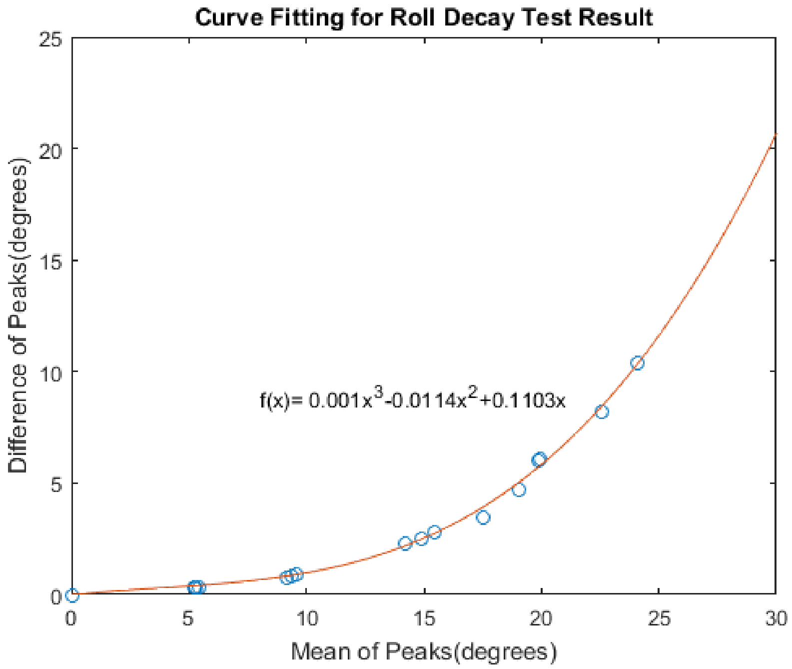

Figure 21. Curve fitting

Finally the values of roll decay coefficients a, b, c are obtained and they are

$$a=0.1103 \qquad b=-0.0114 \qquad c=0.001$$

which will be used for further calculations.

5. NONLINEAR ROLL RAO

The initial objective of this thesis is to estimate the Roll RAO of a vessel accurately. It's important to consider the non linearity explained in the previous sections and finally find the accurate RAO. To take into account the nonlinearity additional considerations has to be taken into account and it's been discussed in this section.

5.1 ALGORITHM USED

When a vessel is free to float in a sea there are 6 degrees of motion as explained in section 3. Equation (1) is considered only when the body has one degree of freedom. When the vessel is free to move in all 6 degrees of motion, the effect of coupling between different motions has to be taken into account. Then the equation of motion for a given degree of freedom 'i' can be written as

$$\sum_{j=1}^{6}(M_{ij} + A_{ij})\ddot{X}_j + B_{ij}\dot{X}_j + C_{ij}X_j = F_i e^{i(\omega t)} \tag{27}$$

The ij terms are the coupling term between two motions, unless i=j. The above equation can be written in matrix form which is explained in the later sections.

Coupling terms are vital when the RAO of a free floating vessel is to be estimated and these terms are calculated using potential solvers. The only term which is not accurately estimated in a potential solver is the damping coefficient of roll motion i.e. B_{44}. By clubbing the output from a potential solver and the methods explained in previous section 3.2.2 to estimate damping coefficient, the roll RAO can be estimated accurately.

5.1.1 Solving Equation of Motion

Before discussing the algorithm used to determine the non linear roll RAO it's necessary to understand how the equation of motion is solved. The equation of motion in matrix form can be written as,

$$\left(\bar{\bar{M}} + \bar{\bar{A}}\right)\ddot{\bar{X}} + \bar{\bar{B}}\dot{\bar{X}} + \bar{\bar{C}}\bar{X} = \bar{F}e^{i(\omega t)} \tag{28}$$

Where,

$\bar{\bar{M}}$ - Mass matrix – see section 5.1.1

$\bar{\bar{A}}$ – Added mass matrix– see section 5.1.1

$\bar{\bar{B}}$ – Damping coefficient matrix– see section 5.1.1

$\bar{\bar{C}}$ – Stiffness matrix– see section 5.1.1

$\bar{F}$ – Force vector– $\bar{F} = \bar{f}e^{i\bar{\epsilon}}$

$\bar{f}$ – Force amplitude vector

$\bar{\epsilon}$ – Vector of phase angles of the force w.r.t wave elevation

$\bar{X}$ – Response vector

ω – Angular frequency of the wave

t - time

Since $\bar{X}$ is a harmonic function it can be written as,

$$\bar{X} = \bar{x}e^{i(\omega t+\bar{\theta})}$$

$$\dot{\bar{X}} = i\ \omega\bar{x}e^{i(\omega t+\bar{\theta})}$$

$$\ddot{\bar{X}} = -\ \omega^2\bar{x}e^{i(\omega t+\bar{\theta})}$$

Where,

$\bar{\theta}$ – Vector of phase angle of the motion w.r.t wave elevation

The equation (28) can be written as

$$-\left(\bar{\bar{M}} + \bar{\bar{A}}\right)\omega^2\bar{x}e^{i(\omega t+\bar{\theta})} + \bar{\bar{B}}i\ \omega\bar{x}e^{i(\omega t+\bar{\theta})} + \bar{\bar{C}}\bar{x}e^{i(\omega t+\bar{\theta})} = \bar{f}e^{i(\omega t+\bar{\epsilon})} \tag{29}$$

Cancelling $e^{i(\omega t)}$ from both side

$$-\left(\bar{\bar{M}} + \bar{\bar{A}}\right)\omega^2\bar{x}e^{i\bar{\theta}} + \bar{\bar{B}}i\ \omega\bar{x}e^{i\bar{\theta}} + \bar{\bar{C}}\bar{x}e^{i\bar{\theta}} = \bar{f}e^{i\bar{\epsilon}} \tag{30}$$

$$\bar{x}e^{i\bar{\theta}} = \frac{\bar{F}}{\bar{\bar{C}} - \left(\bar{\bar{M}} + \bar{\bar{A}}\right)\omega^2 + i\ \bar{\bar{B}}\ \omega} \tag{31}$$

Or we can write the above as

$$\bar{\bar{R}} = \bar{\bar{C}} - \left(\bar{\bar{M}} + \bar{\bar{A}}\right)\omega^2 + i\ \bar{\bar{B}}\ \omega \tag{32}$$

Then the motion vector, $\bar{X} = \bar{F}\ \times\ \bar{\bar{R}}^{-1}$ (33)

Here $\bar{X}$, is a vector of complex numbers, the absolute of each element will give the amplitude of the motion and the argument of the complex number will give the phase angle.

5.1.2 Input from WAMIT

The main output after WAMIT analysis is a *.out file which consist of all the elements required to create the matrices used in section 5.1.1. A typical analysis result can be seen in Appendix A1. It's necessary to know how to create the matrices required for solving the equation of motion of a vessel from the WAMIT output file.

When the point of reference at which RAO calculated is different from the center of gravity the following will be the mass matrix.

$$\bar{\bar{M}}= \begin{bmatrix} m & 0 & 0 & 0 & mz_g & -my_g \\ 0 & m & 0 & -mz_g & 0 & mx_g \\ 0 & 0 & m & my_g & -mx_g & 0 \\ 0 & -mz_g & my_g & I_{11} & I_{12} & I_{13} \\ mz_g & 0 & -mx_g & I_{21} & I_{22} & I_{23} \\ my_g & mx_g & 0 & I_{31} & I_{32} & I_{33} \end{bmatrix}$$

where,

m=ρV, V is the volume of the vessel – obtained from WAMIT

x_g, y_g, z_g - Center of gravity w.r.t the reference point – obtained from WAMIT

I_{11}, I_{22}, I_{33} - Mass moment of inertia with respect to each motions i.e. roll, pitch & yaw and the coupling components

The coefficients which are outputted in WAMIT can't be used directly to solve the equation of motion. It is required to be multiplied with some factors as shown below.

$$\bar{\bar{A}}=\rho \begin{bmatrix} A_{11} & A_{12} & A_{13} & A_{14} & A_{15} & A_{16} \\ A_{21} & A_{22} & A_{23} & A_{24} & A_{25} & A_{26} \\ A_{31} & A_{32} & A_{33} & A_{34} & A_{35} & A_{36} \\ A_{41} & A_{42} & A_{43} & A_{44} & A_{45} & A_{46} \\ A_{51} & A_{52} & A_{53} & A_{54} & A_{55} & A_{56} \\ A_{61} & A_{62} & A_{63} & A_{64} & A_{65} & A_{66} \end{bmatrix}, \quad \bar{\bar{B}}=\rho\omega \begin{bmatrix} B_{11} & B_{12} & B_{13} & B_{14} & B_{15} & B_{16} \\ B_{21} & B_{22} & B_{23} & B_{24} & B_{25} & B_{26} \\ B_{31} & B_{32} & B_{33} & B_{34} & B_{35} & B_{36} \\ B_{41} & B_{42} & B_{43} & B_{44} & B_{45} & B_{46} \\ B_{51} & B_{52} & B_{53} & B_{54} & B_{55} & B_{56} \\ B_{61} & B_{62} & B_{63} & B_{64} & B_{65} & B_{66} \end{bmatrix}$$

$$\bar{\bar{C}}=\rho g \begin{bmatrix} 0 & 0 & 0 & 0 & 0 & 0 \\ 0 & 0 & 0 & 0 & 0 & 0 \\ 0 & 0 & C_{33} & C_{34} & C_{35} & 0 \\ 0 & 0 & C_{43} & C_{44} & C_{45} & C_{46} \\ 0 & 0 & C_{53} & C_{54} & C_{55} & C_{56} \\ 0 & 0 & 0 & 0 & 0 & 0 \end{bmatrix}, \qquad \bar{F}= \rho g H/2 \ [F_1 \quad F_2 \quad F_3 \quad F_4 \quad F_5 \quad F_6]$$

where , H is the wave height.

The force estimated is outputted with an amplitude and phase. The phase is given with respect to the wave elevation. So each element can be written as $F_j = f_j e^{i\epsilon_j}$, so $\bar{F}$ is a vector with complex numbers

Using the above matrices and the formulation explained in section 5.1.2 the response of the vessel can be estimated. But to estimate the non linear roll RAO the following procedure has to be followed

5.1.3 Flow Chart

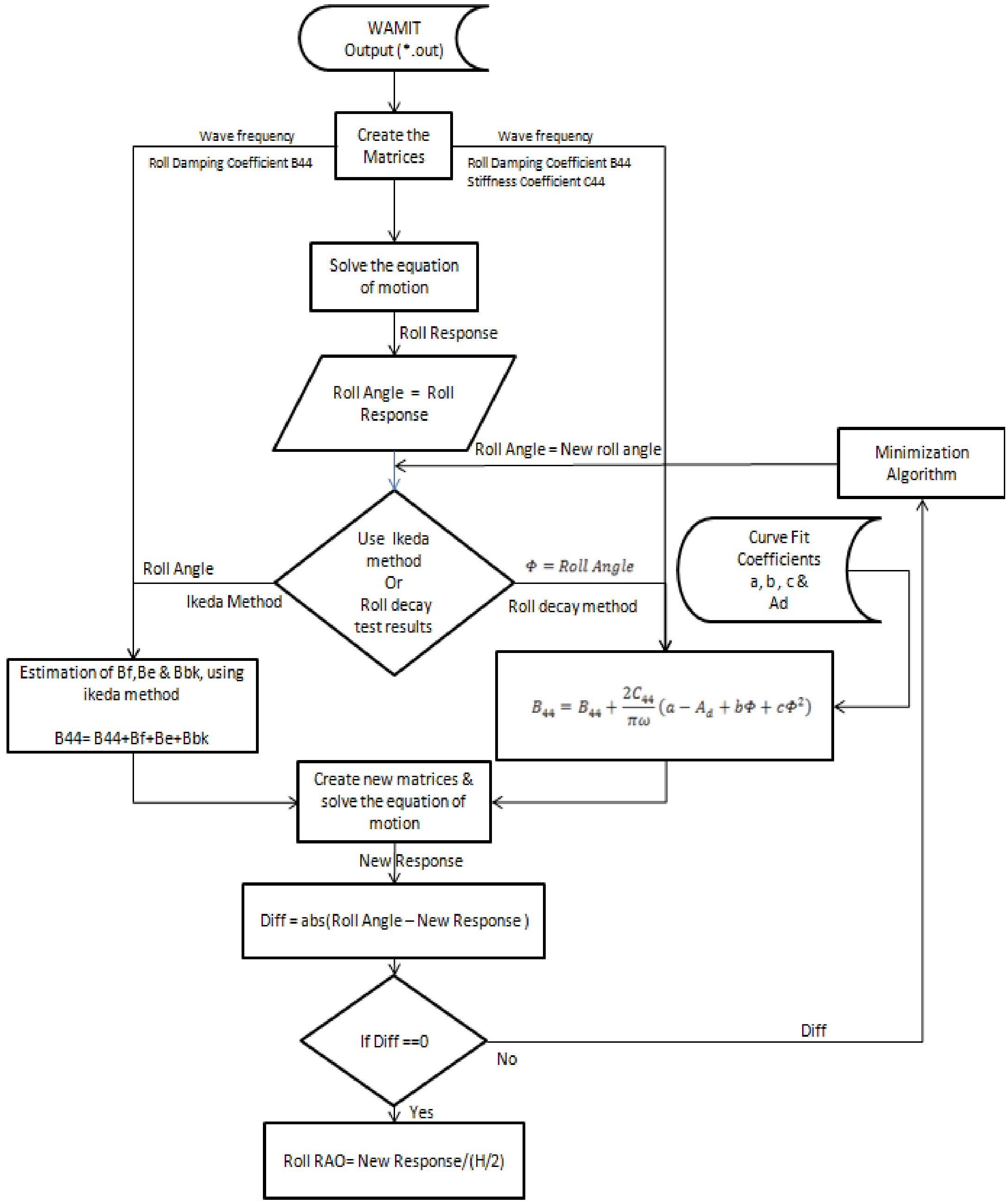

Figure 22. Nonlinear RAO estimation algorithm.

5.1.4 Description

In the previous sections it was explained how the equation of motion can be solved from the WAMIT output. So to start with, the matrices are created and the roll response is found without considering the viscous damping and it is initiated to the value ‘roll angle’. The only element to be changed in the matrices is the roll damping coefficient B_{44} and to find the accurate viscous roll damping there are two methods, one is Ikeda Method and the other is using the roll decay test results. Both procedures are explained below

Ikeda Method

In Ikeda formulation, damping coefficient is divided into 4 parts wave making (B_w), friction (B_F), eddy making (B_E) and bilge Keel ($B_{BK)}$. Since the wave making part or the radiation component is accurately estimated using the potential solver, only the other 3 components are calculated using the Ikeda formulation and these components of damping are highly dependent on the roll angle. Hence the input required to find the 3 components are the roll angle for which damping has to be found and the wave frequency. The details of Ikeda formulation can be seen in reference [6].

Since the damping coefficient estimated by WAMIT is the damping due to radiation and the other 3 components are needed to be added to the same element i.e. B_{44} the following formulation is used. $B_{44\,=}$ $B_{44+}B_F$ $+B_{w+}$ B_{BK}

Using roll decay test results

From roll decay test, the decay coefficients a, b, c are obtained from the curve fitting process explained in section 3.2.2. The damping obtained using these coefficients consist of all the components i.e. eddy making, wavemaking, friction, bilge keel etc. Also when the roll decay test is done the roll frequency is equal to the natural frequency. So to use these coefficients for calculating damping coefficient for other frequencies, some considerations has to be taken into account.

Major part of the damping coefficient is purely dependent on the roll angle, which can be utilized for the other frequencies. While the damping coefficient due to wave making is dependent on the frequency, so this component has to be eliminated. To do so let’s consider the equation (19)

$$B_{44} = \frac{2C}{\pi\omega}(a + b\Phi_m + c{\Phi_m}^2)$$

Here ‘a’ is the linear part which is not dependent on the angle. So from equation 17 we have

$$a\Phi + b\Phi^2 + c\Phi^3 = \frac{\pi\omega}{2C_{44}}\ \Phi\ (B_1 + \frac{8}{3\pi}\ \omega\Phi B_2 + \frac{3}{4}\omega^2\Phi^2 B_3)$$

$$B_1 = \frac{2C_{44}}{\pi\omega}\ a \tag{34}$$

In the above equation B_1 is the linear damping coefficient and the damping due to wave making is also linear. So if the wave making component at natural frequency can be expressed as a decay coefficient then it’s possible to find a new set of decay coefficient which doesn’t have the wavemaking component. The coefficient representing the wavemaking component A_d can be written as

$$A_d = \frac{\pi\omega_n}{2C_{44}} B_{44n} \tag{35}$$

Where,

ω_n - Natural frequency

C_{44}- Stiffness coefficient for roll

B_{44n}- Damping coefficient from potential solver for roll

Finally the damping coefficient excluding the wave making part can be written as

$$B = \frac{2C_{44}}{\pi\omega\Phi}(a\Phi - A_d\Phi + b\Phi^2 + c\Phi^3) = \frac{2C_{44}}{\pi\omega}(a - A_d + b\Phi + c\Phi^2) \tag{36}$$

$$B_{44} = B_{44} + \frac{2C_{44}}{\pi\omega}(a - A_d + b\Phi + c\Phi^2) \tag{37}$$

Hence if the roll angle, frequency of the wave and the stiffness coefficient is known then the damping coefficient B_{44} can be obtained.

Minimization Algorithm

The new damping coefficient is found w.r.t the initiated roll angle. Then the equation of motion is solved and new response is obtained. Then the new roll response is compared with the roll angle used for finding the damping coefficient. If the difference between the roll angles is not equal to zero then a new roll angle is inputted using a minimization algorithm. The minimization algorithm tries to input the value of roll angle in such a way that the difference tends to zero after few iterations. In matlab ‘fminbnd’ is the function used for this purpose. Finally the roll angle at which the difference is zero is outputted. By this approach it is possible to take into account the non –linearity.

5.2 RESULTS & DISCUSSION

Roll RAO of the vessel SAL 183 was calculated using both Ikeda method, as well as, roll decay test results. To understand the nonlinear effect of roll RAO of the vessel on wave height, the RAO was estimated for 1m and 3m wave height and the results are plotted in the Figure 23.

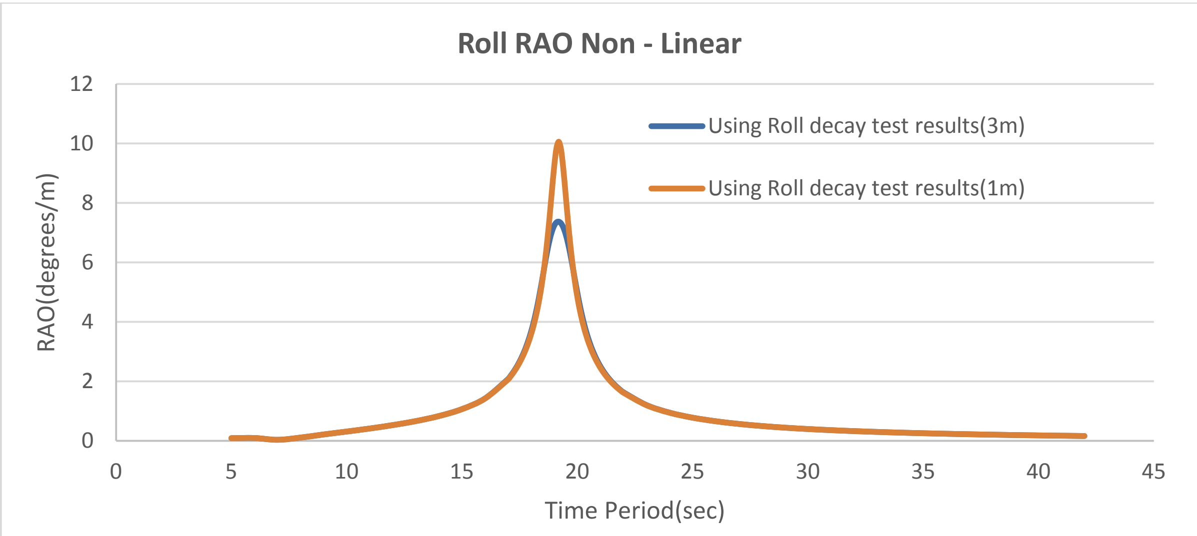

Figure 23. Roll RAO of SAL 183 for 1m and 3m wave height.

It is clearly seen from the plot that as the wave height increases the damping increases which causes a reduction in roll RAO. Also a comparison study was done with both the methods for 3m wave height and the results are as shown in Figure 24.

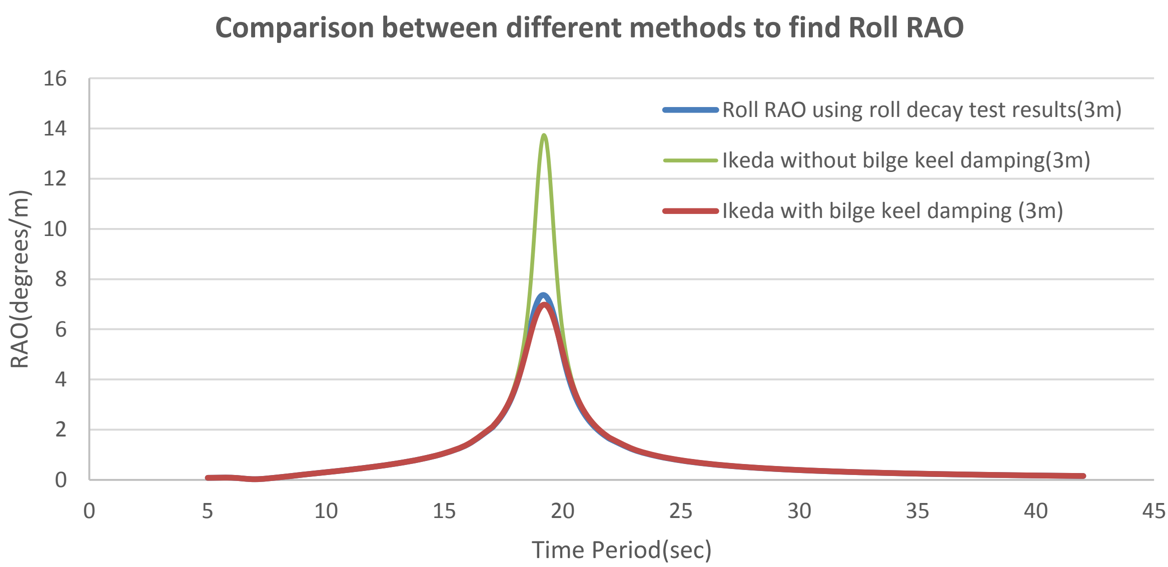

Figure 24. Comparison of roll RAO using different approaches.

The comparison depicts that the damping estimation using Ikeda damping with bilge keel component and roll decay test is giving really close results. This shows that Ikeda damping is best suited for initial analysis as the time and computational effort required for Ikeda method is really less. However, it’s always better to perform a roll decay test as the results obtained from these are always accurate.

6. ANTI-ROLL U-TANK

Anti – roll U tank is one of the best solution for the current problem, as the whole volume were the U tank is placed is not lost and it is possible to control water inside the tank which make it more safe when compared with flume tanks. While designing a U tank it is important to tune tank and it means that the natural frequency of the tank has to be made equal to the natural frequency of the vessel. From equation 20 we have

$$a_{\tau\tau}\ddot{\tau} + b_{\tau\tau}\dot{\tau} + c_{\tau\tau}\tau + [a_{\tau 4}\ddot{\Phi} + c_{\tau 4}\Phi] = 0$$

It's known that the natural frequency of the tank ω_t is a function of the mass component and the stiffness component and it can be written as,

$$\omega_t = \sqrt{\frac{c_{\tau\tau}}{a_{\tau\tau}}} = \sqrt{\frac{2\mathrm{gh_d}}{w\,\mathrm{w_r} + 2\mathrm{h_d h_r}}} \qquad (38)$$

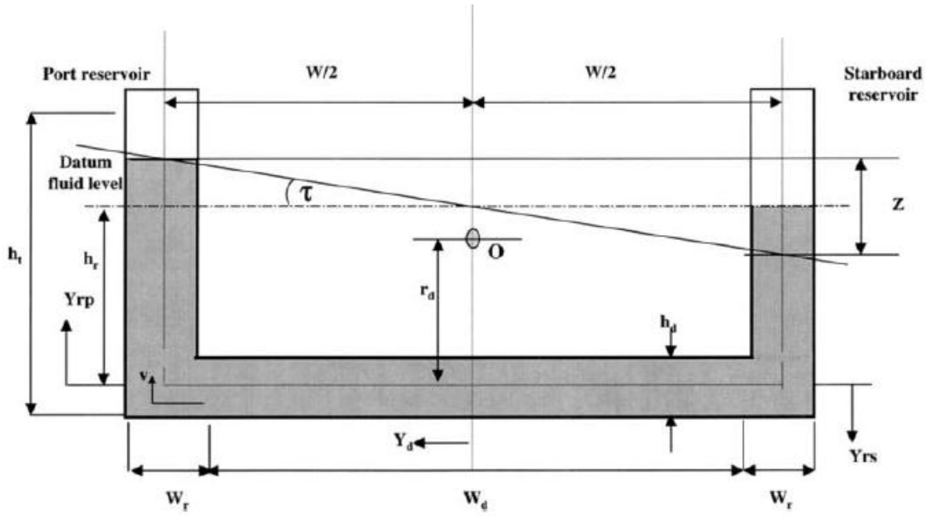

Figure 25. Cross-section of an anti-roll U tank

It's interesting that the natural frequency of the tank is not dependent on the length of it instead it's a function of the cross sectional geometry and the water filled i.e. $\mathrm{h_r}$. So it's possible to say that for a given cross-section the natural frequency of the tank depends only on the water level filled which simplified the designing process of an anti roll U tank. However it's necessary to know how different anti roll U tank configurations effect the motion of the vessel which is explained in next section.

6.1 GENERAL ALGORITHM

To estimate the effect of anti roll U tank on the motion of the vessel, the same algorithm used in section 5 is used, but, the matrices used have a small change. The equation of anti roll U tank is as following (from section 3.4.3).

$$a_{\tau\tau}\ddot{\tau} + b_{\tau\tau}\dot{\tau} + c_{\tau\tau}\tau + [a_{\tau 4}\ddot{\Phi} + c_{\tau 4}\Phi] = 0$$

$$(M_{44} + A_{44})\ddot{\Phi} + B_{44}\dot{\Phi} + C_{44}\Phi + [a_{4\tau}\ddot{\tau} + c_{4\tau}\tau] = Me^{i\omega t}$$

A closer look into the equation can give an idea how to link this equation to the rest of the equation of motion. In the first equation there are 2 parts one which is an equation of τ and the other which is an equation of Φ, $a_{\tau\tau}\ddot{\tau} + b_{\tau\tau}\dot{\tau} + c_{\tau\tau}\tau$ is the basic equation of motion for any oscillating body $a_{\tau 4}\ddot{\Phi} + c_{\tau 4}\Phi$ is the coupling term with the roll. Similarly $(M_{44} + A_{44})\ddot{\Phi} + B_{44}\dot{\Phi} + C_{44}\Phi = Me^{i\omega t}$ is the equation of motion for roll while there is an additional coupling term $a_{4\tau}\ddot{\tau} + c_{4\tau}\tau$. So $a_{4\tau}$ & $c_{4\tau}$ are the coupling terms between the roll motion of the vessel and the movement of water column in the anti roll tank. Hence by modifying the matrices used to solve the equation of motion it's possible to find the effect of anti roll U-tank. The new matrices are as following,

$$\bar{\bar{M}} = \begin{bmatrix} m & 0 & 0 & 0 & mz_g & -my_g & 0 \\ 0 & m & 0 & -mz_g & 0 & mx_g & 0 \\ 0 & 0 & m & my_g & -mx_g & 0 & 0 \\ 0 & -mz_g & my_g & I_{11} & I_{12} & I_{13} & 0 \\ mz_g & 0 & -mx_g & I_{21} & I_{22} & I_{23} & 0 \\ my_g & mx_g & 0 & I_{31} & I_{32} & I_{33} & 0 \\ 0 & 0 & 0 & 0 & 0 & 0 & 0 \end{bmatrix}$$

$$\bar{\bar{A}} = \rho \begin{bmatrix} A_{11} & A_{12} & A_{13} & A_{14} & A_{15} & A_{16} & 0 \\ A_{21} & A_{22} & A_{23} & A_{24} & A_{25} & A_{26} & 0 \\ A_{31} & A_{32} & A_{33} & A_{34} & A_{35} & A_{36} & 0 \\ A_{41} & A_{42} & A_{43} & A_{44} & A_{45} & A_{46} & a_{4\tau}/\rho \\ A_{51} & A_{52} & A_{53} & A_{54} & A_{55} & A_{56} & 0 \\ A_{61} & A_{62} & A_{63} & A_{64} & A_{65} & A_{66} & 0 \\ 0 & 0 & 0 & a_{\tau 4}/\rho & 0 & 0 & a_{\tau\tau}/\rho \end{bmatrix}$$

$$\bar{\bar{B}} = \rho\omega \begin{bmatrix} B_{11} & B_{12} & B_{13} & B_{14} & B_{15} & B_{16} & 0 \\ B_{21} & B_{22} & B_{23} & B_{24} & B_{25} & B_{26} & 0 \\ B_{31} & B_{32} & B_{33} & B_{34} & B_{35} & B_{36} & 0 \\ B_{41} & B_{42} & B_{43} & B_{44} & B_{45} & B_{46} & 0 \\ B_{51} & B_{52} & B_{53} & B_{54} & B_{55} & B_{56} & 0 \\ B_{61} & B_{62} & B_{63} & B_{64} & B_{65} & B_{66} & 0 \\ 0 & 0 & 0 & 0 & 0 & 0 & b_{\tau\tau}/\rho\omega \end{bmatrix}$$

$$\bar{\bar{C}}=\rho g \begin{bmatrix} 0 & 0 & 0 & 0 & 0 & 0 & 0 \\ 0 & 0 & 0 & 0 & 0 & 0 & 0 \\ 0 & 0 & C_{33} & C_{34} & C_{35} & 0 & 0 \\ 0 & 0 & C_{43} & C_{44} & C_{45} & C_{46} & c_{4\tau}/\rho g \\ 0 & 0 & C_{53} & C_{54} & C_{55} & C_{56} & 0 \\ 0 & 0 & 0 & 0 & 0 & 0 & 0 \\ 0 & 0 & 0 & c_{\tau 4}/\rho g & 0 & 0 & c_{\tau\tau}/\rho g \end{bmatrix}$$

$$\bar{F}= \rho g H/2 \ \begin{bmatrix} F_1 & F_2 & F_3 & F_4 & F_5 & F_6 & 0 \end{bmatrix}$$

The values of $a_{\tau\tau}, a_{\tau 4}, b_{\tau\tau}, c_{4\tau}$& $c_{\tau\tau}$ are dependent on the geometry of the tank which is explained in section 3.4.3. Hence by using these matrices in the algorithm explained in section 5 it's possible to find the response of the vessel with anti roll U tank.

6.2. FINDING BEST CONFIGURATION

For an anti roll U tank to be effective the natural frequency of the tank should be equal to the natural period of the vessel. It was seen in section 6 that the natural period of the tank is only a function of the cross section of the tank and the water filled.

If a space is defined to fix a U tank then the first step is to find the configurations that fit the space and have the exact natural frequency of the vessel. To do so, it is necessary to find the variables which are to be varied to obtain all the possible cross-sections. An anti roll U tank can be represented as shown in Figure 26.

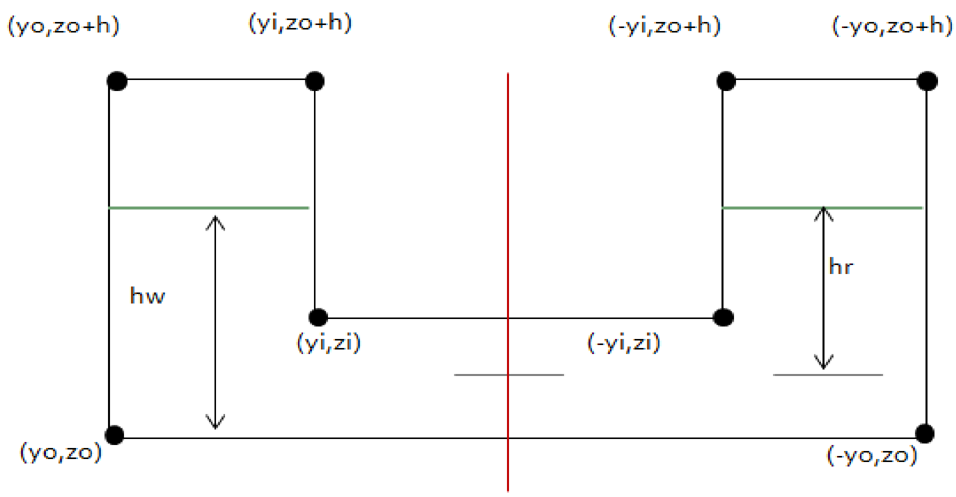

Figure 26. Representation of an anti roll U tank

From the Figure 26 it could be seen that a typical configuration of an anti roll tank can be defined by 5 variables i.e. yo, yi, zo, zi and hr. The 'h' of the tank at the moment can be considered to be not defined. If so, then the only unknown in the equation of natural frequency of tank, will be ‘hr’ for a particular geometry i.e.

$$\omega_t = \sqrt{\frac{2\mathrm{gh_d}}{w\ \mathrm{w_r} + 2\mathrm{h_d}\mathrm{h_r}}}$$

$$\omega_t = \frac{2\pi}{Natural\ Period\ of\ Vessel}$$

$$h_d = abs\ (\ zo - zi)$$

$$w = abs(\ yo + yi)$$

$$w_r = abs\ (\ yo - yi)$$

$\mathrm{h_r}$ of a tank can be found if the geometry is given and if the maximum height possible for the tank is known then only those geometries whose $\mathrm{h_r}$is less than the maximum limit is chosen.

To find all possible geometries, define yo at the extreme limit and change the yi between yo and the inner limit defined. Similarly do the same for zo and zi. If it can be done in a loop then a set of array of geometries whose hr is less than the upper limit of height can be defined.

Now if the longitudinal length of the tank is given, then all the variables required to make the matrices to estimate the roll RAO can be calculated. Also if the coefficients of the vessel for different periods are known then the RAO for different wave period can be found and hence the maximum roll in the whole spectrum can be calculated for comparison. In order to select only realistic configuration, the maximum height limit is compared with the minimum height of the tank needed which is calculated by

$$h = \frac{h_d}{2} + h_r + \frac{w}{2}\ \sin\ (\tau_{max}) \tag{39}$$

where τ_{max} is the maximum response of the water column estimated from the whole spectrum. If h is beyond the upper limit then discard that geometry. Also if one more condition i.e.

$$zi \leq \frac{h_d}{2} + h_r - \frac{w}{2}\ \sin\ (\tau_{max}) \tag{40}$$

is considered then more realistic configurations can be obtained. Finally by using the above algorithm the best suitable configurations for a particular space can be calculated.

6.3 USING BALLAST TANKS

The arrangement of Ballast tanks in a vessel can resemble an anti roll U tank if it's possible to connect those tanks. If any configuration using ballast are effective then the problem of loosing stowage area can be avoided, hence all possibilities are tried.

6.3.1 Midship Tanks

The ballast tanks near the midship region resemble an anti roll U tank, if these tanks are assumed to be connected with valves then these can be considered for the analysis. The details of the tanks can be seen in Table 5. It can be seen that the width of the wing tanks are not the same on both sides so for simplicity the average value is taken.

Table 5. Midship ballast tank details

TANK DETAILS (Ballast tanks)	
Sets of tanks resembling U tank	2
Length of the tank in m (xt)	13.4 m
Distance between axis of side tank (w)	22.25m
Width of the side tank1	5 m
Width of the side tank2	5.5 m
Average Width(wr)	5.25m
Height of the side tank (ht)	10.8 m
Height of the connecting tube (hd)	2.2 m
Height between COG of the ship to the axis of the connecting tank (rd)	8.9 m
Coefficient of linear damping of the tank (qv)	0.17
Righting Moment obtained using per set of tanks	86,868.09 KN.m

These sets of ballast tanks are normally used for counter ballasting during lifting operations. So if these tanks are used for other purpose then the righting moment obtained from these sets of tanks will be lost which in-turn reduce the total lifting capacity of the vessel.

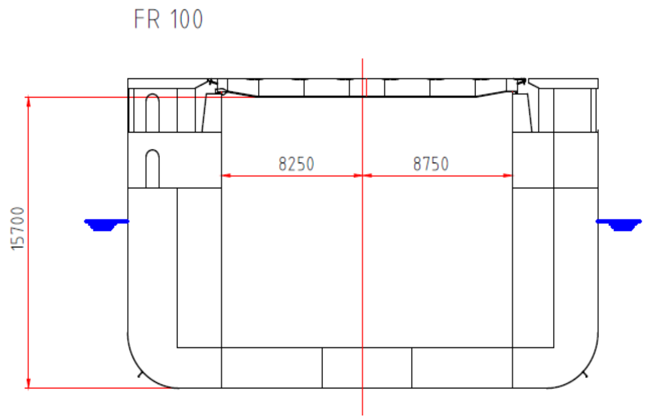

Figure 27. Midship cross- section of SAL 183 with ballast tanks

The natural frequency of a tank depends on its geometry as well as the level of water filled so it is necessary to find out the height until which the water is to be filled. Here the only variable to be calculated is the level of water to be filled. From equation (38)

$$\omega_t = \sqrt{\frac{2gh_d}{w\,w_r + 2h_d h_r}}$$

$$\frac{2\pi}{19.2} = \sqrt{\frac{2\times 9.81\times 2.2}{22.25\times 5.25+2\times 2.2\times h_r}},\quad h_r = 65.05\text{m}$$

The height of the side tank is just 10.8m and its clear that this height of water column can't be accommodated in the current tanks hence the algorithm explained in section6.2 can be used instead another analysis is performed to find the most optimum water height to be filled. The results are discussed below.

6.3.2 Results & Discussion

A code was made to estimate the level of water to be filled in the midship ballast tanks, so that the response of the vessel will be as minimum as possible. Since the natural frequency of the tank can't be made equal to the natural frequency of the vessel, the only option is to check the effectiveness of different water levels on the response on the vessel and the water level which has the least response is chosen. It was found that the least response was seen when the water level in the side tank is 1.1m above the center of the connecting tube or 2.2m from the bottom.

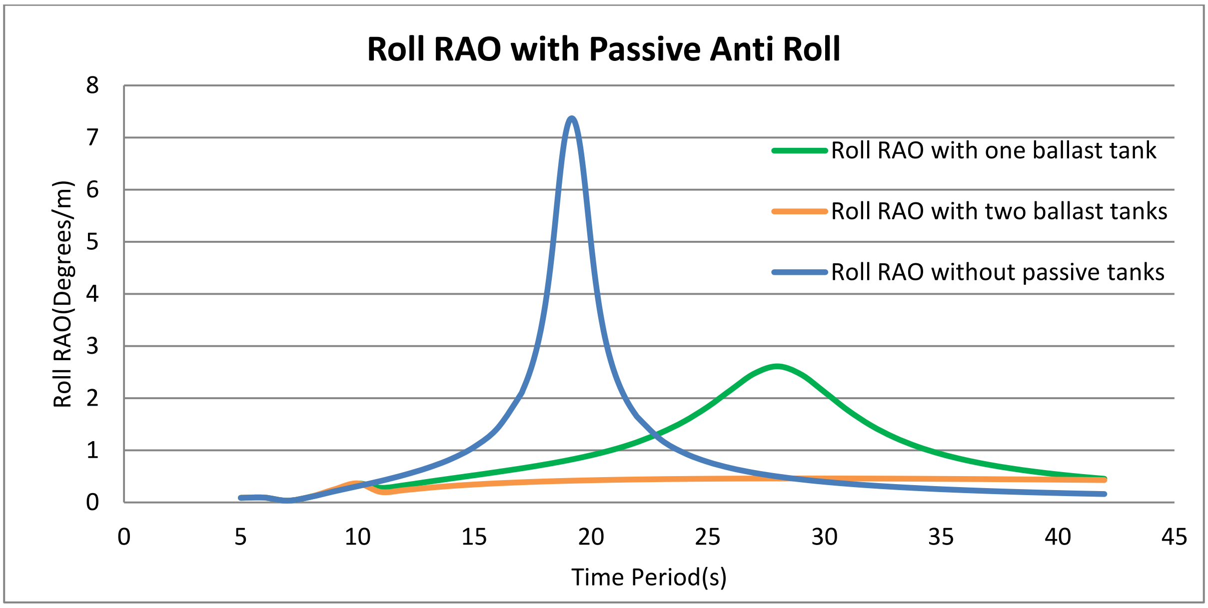

Figure 28. Comparison of roll RAO of the vessel with and without midship tanks as U tanks

The natural frequency of each set of these tanks is 10.48sec. The roll RAO of the vessel when each set of ballast tanks are converted into anti roll tanks is shown in Figure 28. The tank damping considered is 0.17. It was found that as tank damping increases the effectiveness of the tank increases and 0.17 is a tank damping given for a well designed anti roll tank [10]. Here since there are too many structures in the tank it's obvious that the damping will be greater than expected. Anyhow here lower damping is considered so that the over estimation of the effectiveness of the tank won't be done.

It can be seen in Figure 28 that using one set of ballast tanks is not effective enough to reduce the roll RAO. Even though the RAO of the vessel reduces at natural frequency, it is visible that still the vessel has a RAO of 2.6 degrees at wave period of 28secs.

The current results are obtained by considering that these tanks are symmetrical but in reality they are not, so these can cause some other effects which even can be counterproductive, hence if this configuration is to be used a detailed time domain analysis is needed by utilizing other theories.

SAL 183 has a lifting capacity of 2000t with 1000t each, on each crane. This capacity is calculated at the lever of 26.2m from the centerline of the vessel. As discussed before these ballast tanks are used to provide the moment to counteract the moment created due to lifting operation and if one set of these ballast tanks are used then the lifting capacity of the vessel reduces by 338 tons. If both set of tanks are used then it's quite effective, but, the total loading capacity of the vessel reduces to 1324tons.

Another problem will be connecting these tanks with valves which can be operated from the bridge. The whole process is really a complicated process as several pipes and wires are passing through the space between these tanks which make it really complicated to implement.

6.3.3 Forward Tanks

In the forward part of the vessel the arrangement of the ballast tanks are totally different when compared with midship ballast tanks. In the midship region, the wing tanks extend along the whole depth of the vessel as a single tank, and if those tanks are used the whole volume is lost. For an anti roll U tank, tall wing tanks are not necessary, a short tank which is well tuned is enough to be effective, and hence the arrangement of the tanks in the forward became really interesting. The ballast tank arrangement in the forward of the vessel is as shown in Figure 29 and it extends from frame 124 to 153 which is 20m.

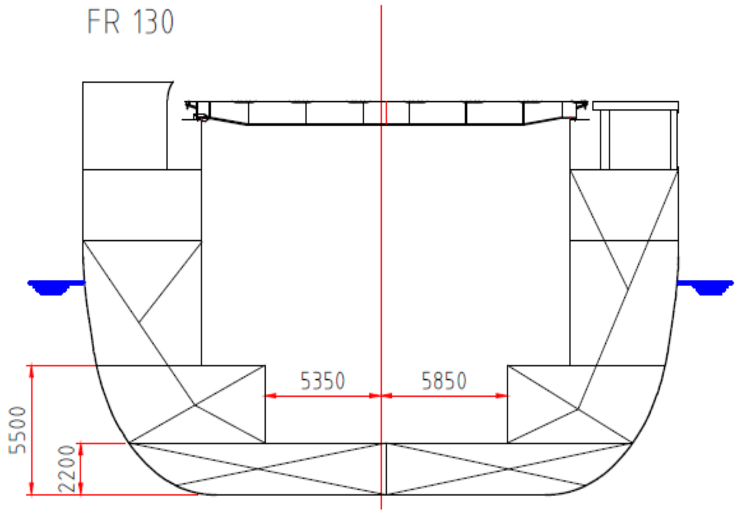

Figure 29. Forward section of the vessel with ballast tanks

If the tanks between 2200mm and 5500m can be joined then it can be an effective solution as those tanks have higher breadth when compared with the midship tanks. Also rest of the tanks can be utilized for ballasting which means that loss of righting moment will be less.

Joining these 2 tanks with a duct in the bottom will be less complex when compared with midship tanks. So using the algorithm explained in section 6.2 the best configurations were found and has been discussed in next section.

6.3.4 Results & Discussion

The analysis was done and 6 configurations were obtained which are listed in Appendix A2. To understand the effectiveness of each configuration 2graphs were plotted with the maximum roll response on one axis and length of the tank & volume of water on the other as shown in Figure 30. The figure shows that the all the tank configurations have the same effectiveness w.r.t length while the volume of water needed for getting the same response is different. Normally the configuration with least volume will be used i.e. configuration 1.

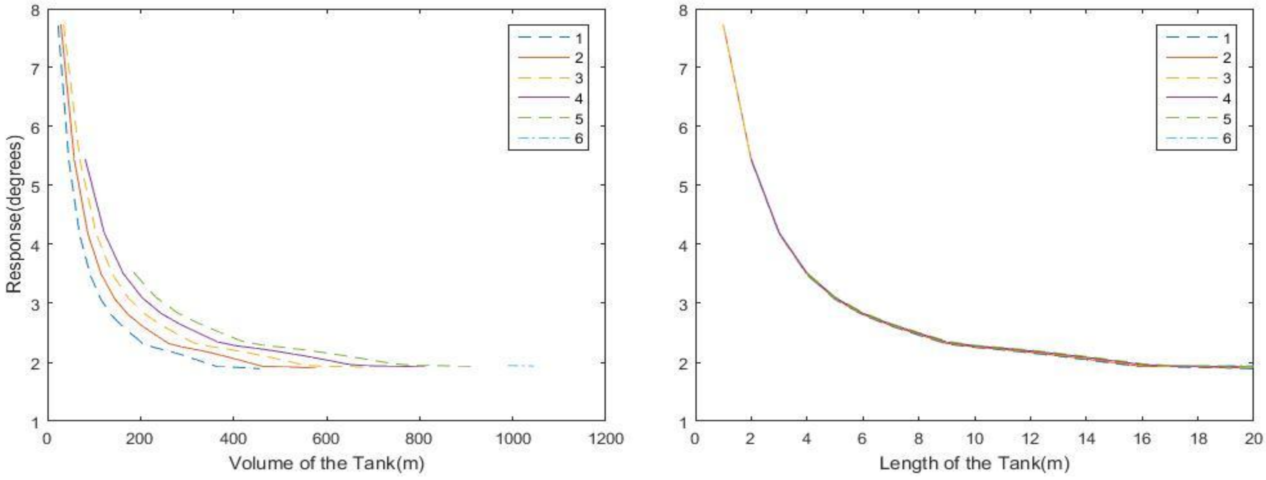

Figure 30. Effectiveness of different configurations of forward ballast tanks

But, since these set of tanks have a low CG, the maximum volume of water possible will be the best choice. If the configuration 4,5 &6 are closely observed, it could be seen that the graphs doesn't extend throughout the range of the graph like other configurations this means that the tank height is not sufficient enough for handling the water inside hence to be in the safer side, configuration 3 is considered as the best configuration and it has been shown in Figure 31.

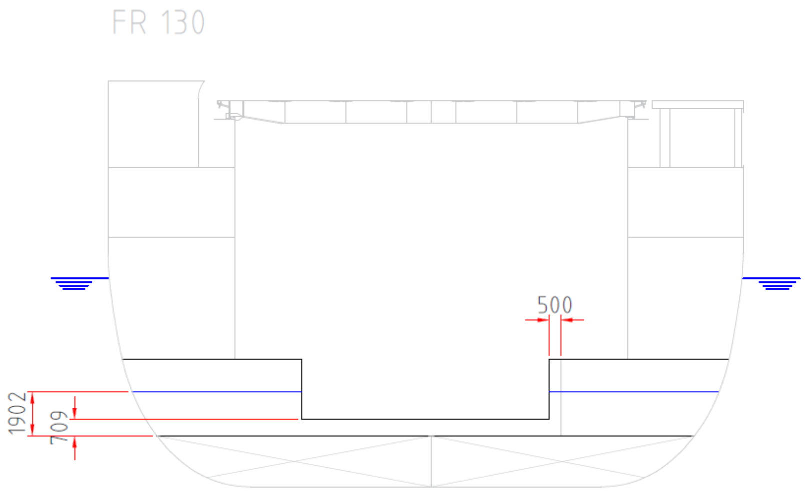

Figure 31. The best configuration possible for forward ballast tanks

To implement the configuration some modifications are to be made on the tanks. U tanks are supposed to have symmetric side tanks but these tanks are asymmetric which make it necessary to extend the smaller tank to 500mm. Then a duct of height 709mm is to be installed to join both tanks so that the water flow is continuous. In addition, for better control air ducts with valves can be provided. The valves control the flow of air which in turn controls the movement of the water between the two side tanks.

But because of this modification cargo space below 5500mm will be lost which accounts to about 739.2m^3, if the whole 20m is used.

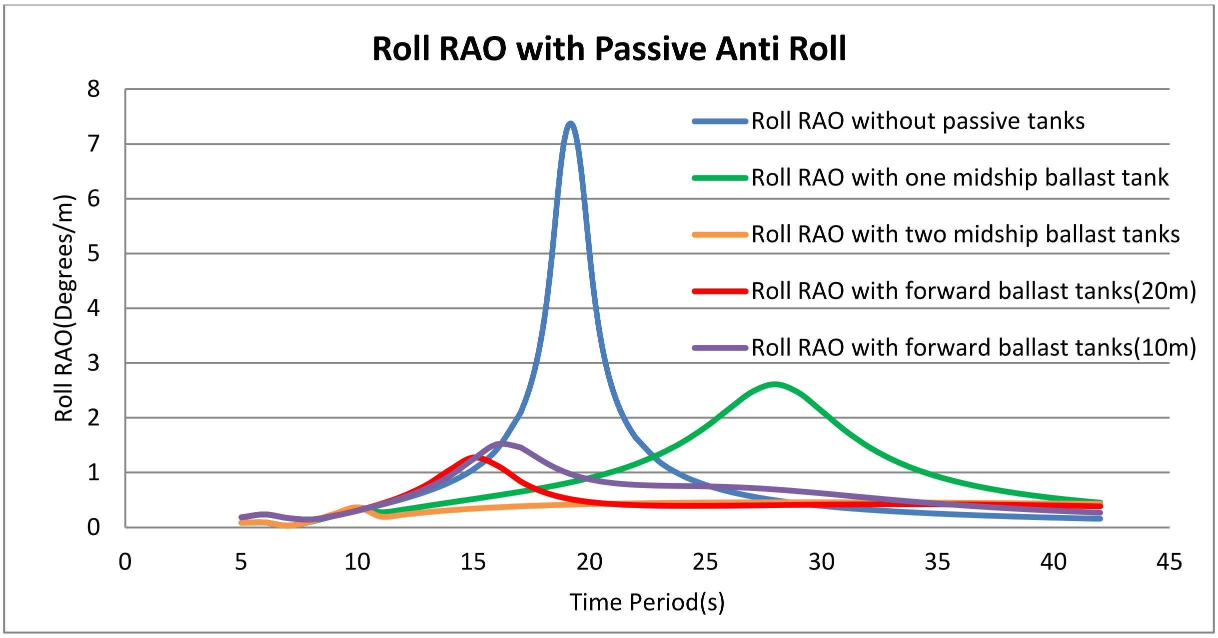

Figure 32. RAO comparison with all possibility using ballast tanks

In addition, the total loading capacity of the vessel reduces to 1872tons as the moment by filling those tanks are lost. These effects can be made half if only 10m length is considered but still the reduction in RAO is significant. Hence to have a comparative study, RAO using both 10m and 20m length of the same configuration is compared with the midship tanks in Figure 32. It could be concluded from using forward ballast tanks as U tanks are really effective when compared with the midship tanks.

6.4 USING NEW SET OF TANKS

Using ballast tanks as anti roll tanks can’t be considered as the best solution because the lifting capacity of the vessel is reduced drastically and some major changes are required to make them anti roll U tank. So it was curious to know how effective a new set of anti roll U tank will be if there is a possibility to fit it into the cargo hold of the vessel.

6.41 Possible locations

The diagram of the cargo hold of the vessel is shown in Figure 33. The vessel has a tween deck and a large cargo hold and the limits in which the U tube tanks can be fitted have been shown in Table 6.

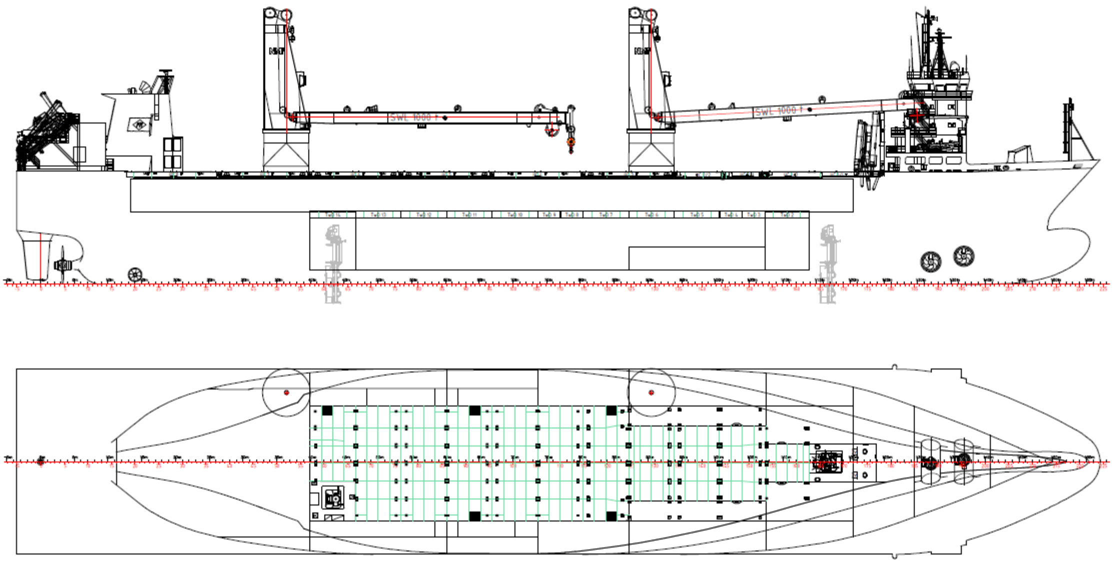

Figure 33. Profile view of the cargo hold (top) tank-top view (bottom)

Table 6. Limits for fitting anti roll U tank

	X - Direction		Y - Direction		Z - Direction	
	Upper Limit	Lower Limit	Upper Limit	Lower Limit	Upper Limit	Lower Limit
Tween Deck	Fr 52	Fr 19	8.25m	0	15.6m	10.8m
	26.6 m					
Cargo Hold	Fr 124	Fr 52			15.6m	2.2m
	47.7m					

Using the algorithm explained in 6.2 the best configurations are found using the limits provided in Table 6.

6.4.2 Results and Discussion

Tween Deck

The analysis was run for the tween deck with x limit up to 26m and about 27 configurations were obtained. The details have been provided in Appendix A2. The effectiveness of each configuration w.r.t the length of the tank and the volume of water in the tank can be seen in Figure 34. The minimum response which can be achieved by fitting a U tank on the tween deck is nearly 3 degrees, which is not as effective as converting the forward ballast tanks.

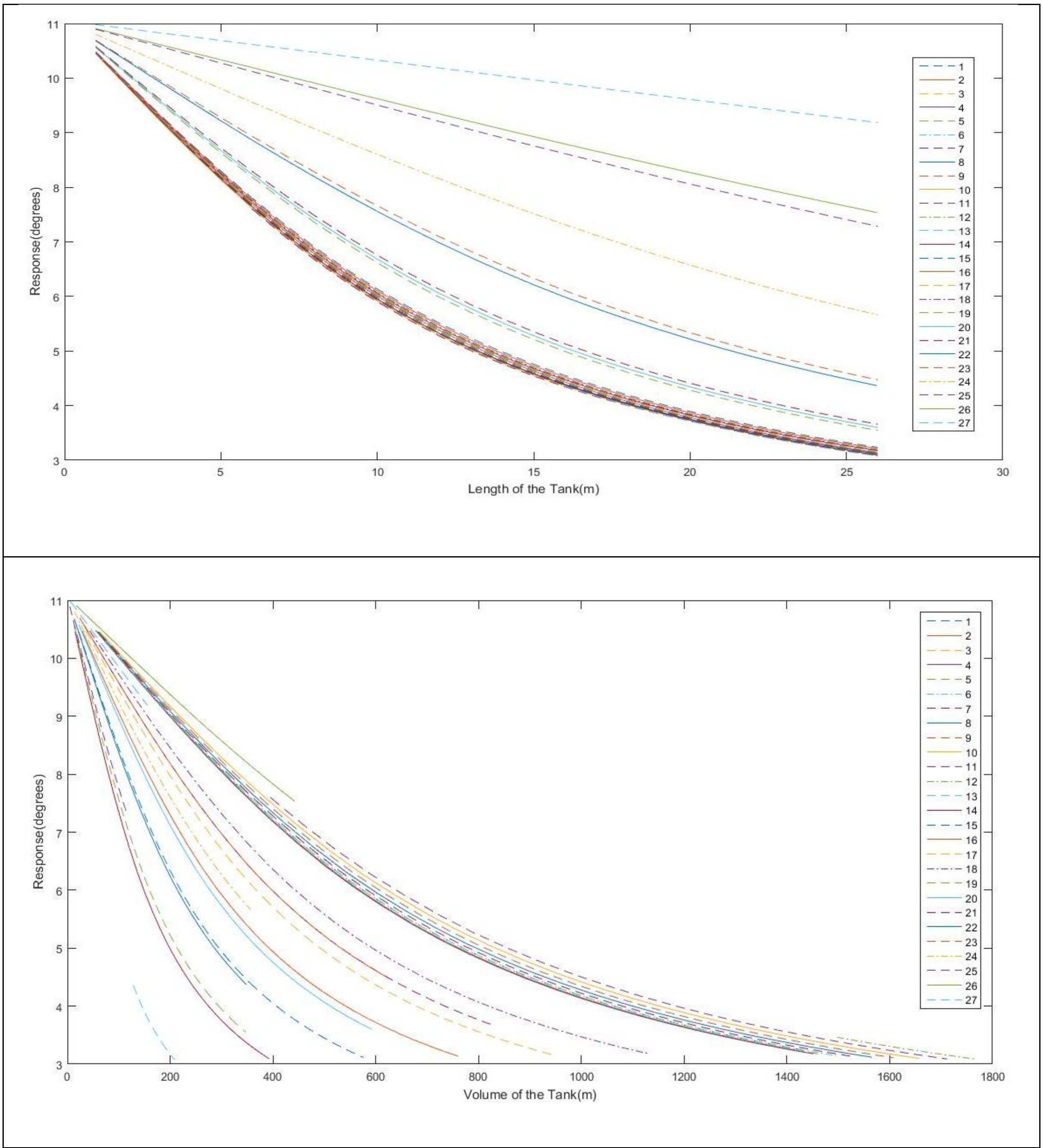

Figure 34. Effectiveness of different configuration on tween deck w.r.t length & volume of tank

Since new set of tanks are implemented, the configuration should have the least volume or water mass and in figure 34 it can be seen that the configuration 14 i.e. the second line from left, is the best choice, the details of the configuration can be seen in table 7.

But when these tanks are used the cargo space is lost and the volume lost depends on the height of the tank. The height of the U tank is about 1.47m due and hence a total cargo volume of 649.74 m^3 is lost. One of the main benefits of using anti roll U tanks is that it can be utilized during the transportation but these tanks can’t be used during transit since the center of gravity of these tanks are high. Hence this configuration can’t be said to be the best solution which made it curious to know the effect of fixing a U tank in the cargo hold where CG can be kept low.

Cargo Hold

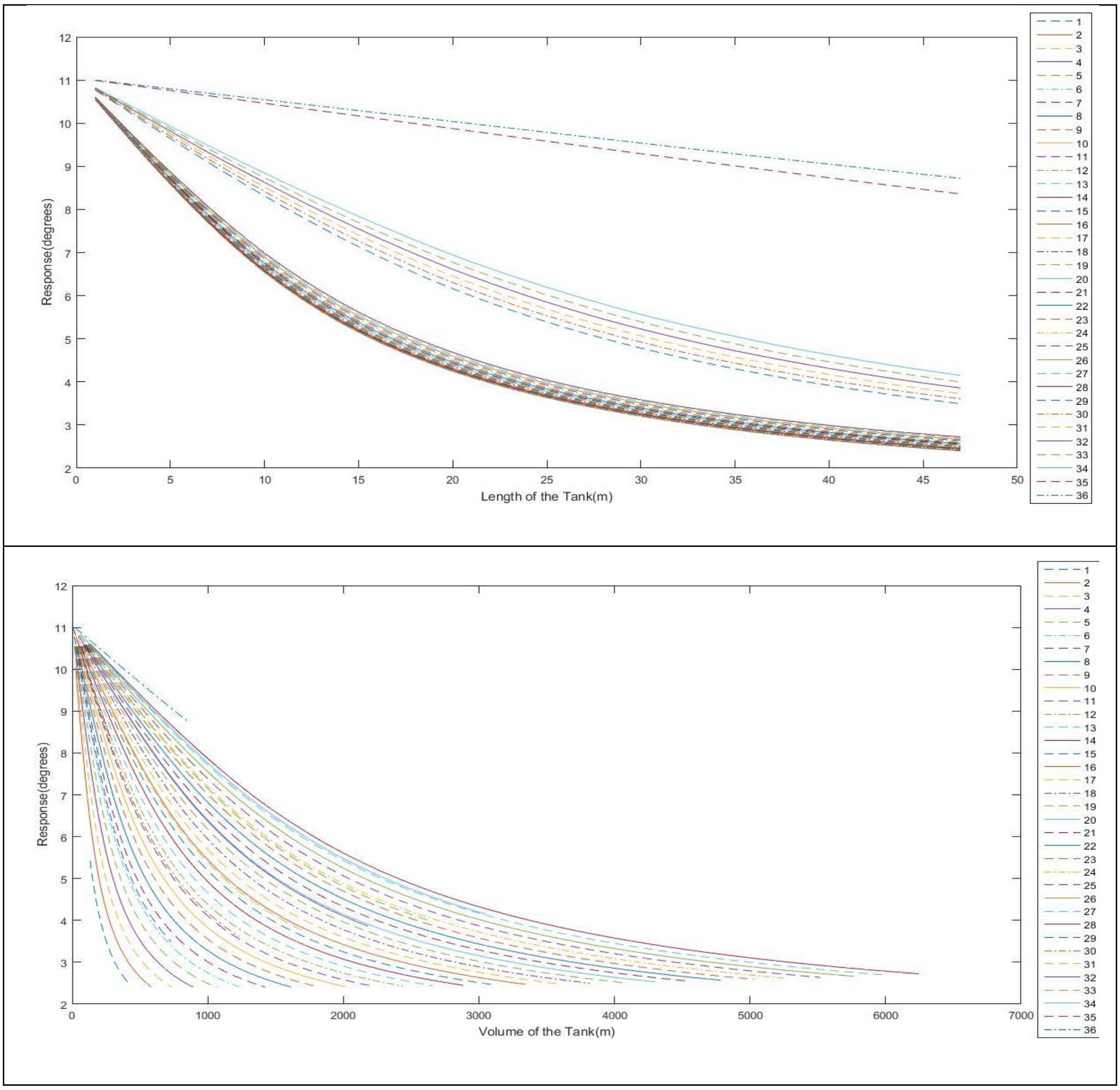

Figure 35. Effectiveness of different configuration in cargo holds w.r.t length & volume of tank

Similar analysis was run for 47m of the cargo hold and 36 different configurations were found. The plots are shown in figure 35 and ID number 3 can be considered as the best configuration. The results from the tween deck and the cargo hold are close, but still for comparison the length needed for obtaining similar response when the U tank is on tween deck, was found and it is 32m. And this configuration has the added benefit of having low CG which makes it suitable during transportation too.

Anyhow, it can be inferred that if the tank is near to the center of gravity of the vessel then the efficiency increases. Similarly, when these tanks are compared with forward tank results, then it can be conclude that side tanks with large width which is placed away from each other is most effective.

Best Configurations

The best configurations for both conditions which were discussed above are shown in figure 36 and the details are shown in table 7.

Table 7. Best anti roll U tank configuration

ID	yo	yi	zo	zi	hr	hw	CG from keel	xt	Volume	Response	Height of the tank
On Tween Deck											
14	8.25	2.63	10.80	11.14	1.02	1.19	11.34	26	392.55	3.09	1.47
In Cargo Hold											
3	8.25	1.07	2.2	2.57	0.85	1.04	2.70	32	501.80	3.07	1.28
								47	737.02	2.40	1.22

As it was discussed before when these tanks are fitted there is a loss of cargo space. Here since the cross sectional area of the tanks are almost the same for both cases the only factor which affect the lost volume is the length of the tank. If the U tank is fixed on tween deck then the volume lost is 649.74m^3 while in the case of fixing it in the cargo hold its about 696.32m^3 and 974.78m^3 for 32m and 47m long tank respectively.

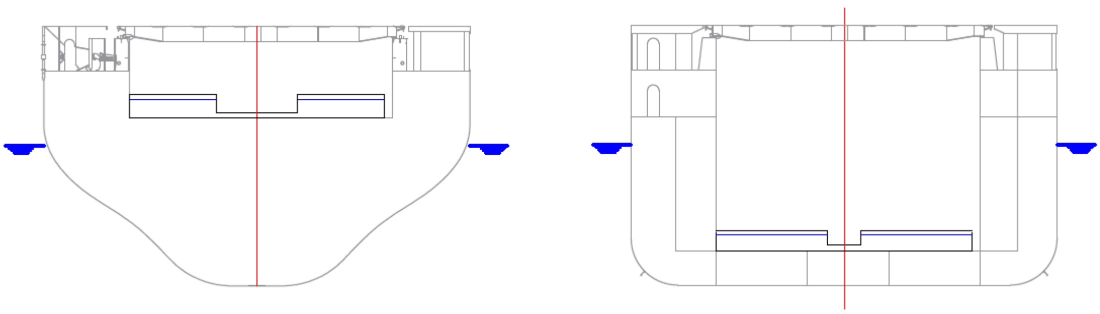

Figure 36. Selected U tank configurations on tween Deck (Left) & in cargo hold (Right)

As the tanks are tuned for the natural frequency a well reduced roll RAO is obtained (see Figure 37). The U tank with 33m in the cargo hold and the U tank on the tween deck have almost similar effect.

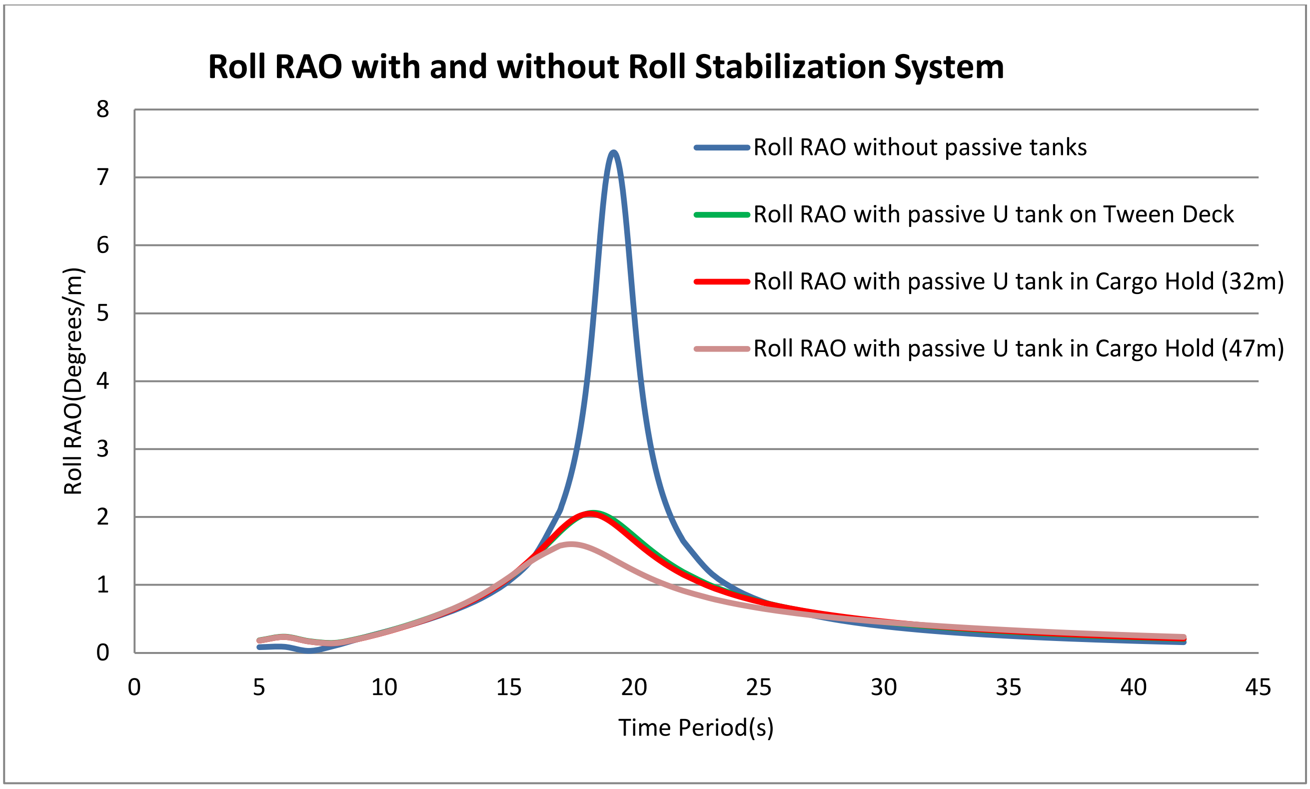

Figure 37. Roll RAO of the vessel with new set of anti roll U tanks

When a new set of tanks are used there is loss of cargo volume and also fixing these tanks cost a lot as the additional cost of tank is also needed which was not needed in the case of using the ballast tanks. Also additional weight is added on board the vessel which accounts to the system weight and also the water in the tank i.e. 392.5t, 501.8t and 737.02t of water for the tween deck configuration and the 33m & 47m long cargo hold configuration respectively. This addition of mass reduces the weight of cargo which can be carried by the vessel. Hence using new sets of anti roll U tanks have many issues.

7. DESIGN AND OPTIMIZATION OF NEW SYSTEM

While executing really heavy lift operations with cargo weight close to the limit of the vessel, SAL 183 attaches a pontoon on the same side of the cargo so that an extra righting moment can be obtained. The arrangement can be seen in Figure 36.

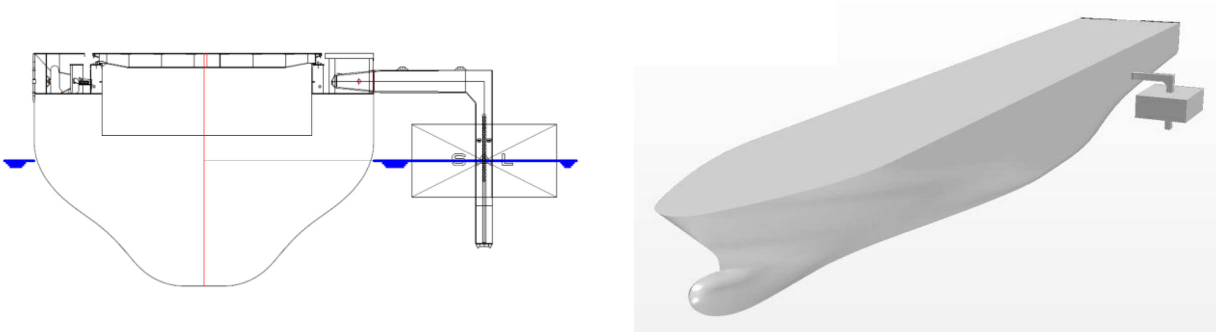

Figure 38.SAL 183 with the pontoon

However, during offshore installation process the cargo operation doesn't require high righting moment. Hence there is no requirement to fit the pontoon on to the vessel. So during this period the stabilizing arm used to fit the pontoon is free which can be utilized for some other purpose and the engineering experts in SAL Heavy Lift came up with the idea of fitting a plate on to this arm while performing an offshore project.

But effectiveness of such arrangement is unknown and there can be many different configurations possible. The plate can be of any geometry with any dimensions and there are 'n' numbers of ways of fixing the plate onto the arm and each of these configurations can have different effects on the roll of the vessel. Hence a detailed investigation is required to design such a system.

7.1 EFFECTS DUE TO THE PLATE

When a plate is fixed near the hull form there can be different effects and they are

- Change in Froude Krylov force - the pressure is integrated around the plate too
- Diffraction - the plate affects the incident wave.
- Radiation - due to the movement of the plate waves can be generated.
- Viscous drag - Due to viscosity there is drag force on the plate.

The first 3 effects can be calculated using a potential solver while the viscous drag can't be estimated since the solver use the assumption of invicid fluid.

In the equation of motion the addition viscous drag due to the plate will be added to the damping coefficient, so if the damping coefficient due to the drag part can be computed then the equation of motion can be solved accurately.

7.2 DAMPING COEFFICIENT DUE TO THE PLATE (VISCOUS)

The equation of motion for roll is as following

$$(M_{44} + A_{44})\ddot{\Phi} + B_{44}\dot{\Phi} + C_{44}\Phi = F_4 e^{i\omega t}$$

Each term is a moment term hence $B_{44}\dot{\Phi}$ is a moment acting on the vessel and its possible to estimate the moment due to the drag force acting on the plate. The general drag force equation can be written as

$$F_d = \frac{1}{2}\rho A C_d V^2 \tag{41}$$

Where,

ρ - Density of the fluid

C_d - Drag coefficient

V – Velocity of the fluid on the plate

Hence to find the drag force a plate the primary term to be estimated is the velocity of the fluid on the plate or the velocity of the plate. So let's considers Figure 37.

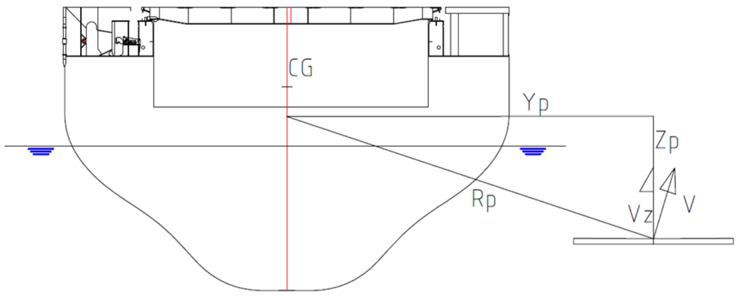

Figure 39. Velocity on the plate

When the vertical distance between center of gravity and center of flotation is high, then the center of rotation can be assumed to be the midpoint between them. Hence we can write velocity V as

$$V = R_p\,\dot{\varphi} \tag{42}$$

$$R_p = \sqrt{Y_p^2 + Z_p^2} \tag{43}$$

The velocity is perpendicular to the line joining the center of rotation and the middle point of the plate as shown in Figure 37.

Then the moment acting on the vessel is

$$M_d = \left(\frac{1}{2}\rho A C_d (R_p\,\dot{\varphi}\,)^2\,\right)\sin\,(tan^{-1}(Y_p/\,Z_p))\,Y_p$$

$$M_d = \left(\tfrac{1}{2}\rho A C_d R_p^2\right)\sin\,(tan^{-1}(Y_p/\,Z_p))\,Y_p\,\dot{\varphi}^2 \qquad (44)$$

We know that the damping moment can be written as

$$B_\Phi = B_1\dot{\Phi} + B_2\dot{\Phi}^{\,2} + B_3\dot{\Phi}^{\,3}$$

$$B_{44} = B_1 + \frac{8}{3\pi}\,\omega\Phi_a B_2 + \frac{3}{4}\omega^2\Phi_a^2 B_3$$

Comparing Equation (44) and the above equation

$$B_2 = \left(\tfrac{1}{2}\rho A C_d R_p^2\right)\sin\,(tan^{-1}(Y_p/\,Z_p))\,Y_p \qquad (45)$$

The linearized damping coefficient from the drag of the plate can be written as

$$B_{44p} = \tfrac{8}{3\pi}\,\omega\,\Phi_a\left(\tfrac{1}{2}\rho A C_d R_p^2\right)\sin\,(tan^{-1}(Y_p/\,Z_p))\,Y_p \qquad (46)$$

In the above equation all the variables other than C_d is known for a given configuration and roll angle. C_d in general is a function of plate geometry, angle of attack and type of fluid flow. There have been several experimental studies done on drag coefficients of a plate in steady flow condition; however, in the current case the fluid flow is oscillating. Most of the studies in oscillating flow are done on rectangular plates and hence in this thesis only rectangular plates with different aspect ratios are considered. The drag coefficient in an oscillating flow is called oscillatory drag coefficient.

The main work done in oscillating flow is by Kuelegan and Carpenter, mainly for estimating the wave induced forces on vertical pilings and submerged objects in offshore. Following their work Martin investigated the case of a plate with an infinite aspect ratio, i. e., the case of two dimensional flows. Ridjanovic later extended this study in order to determine the effect of aspect ratio (see Figure 38.) on oscillatory drag coefficients which were intend to study the roll damping effect due to bilge keel on a vessel [7].

The oscillatory drag coefficient is found to be a function of aspect ratio and also the ratio between the amplitude of oscillation and breadth of the plate. The studies in oscillating flow are performed only for one angle of attack i.e. 90 degree, but in the current case it's required to estimate damping coefficient for different angle of attacks of the plate. There are no data available on any study done in oscillating fluid for plates with different angle of attack. But, data are available for plate in steady flow condition as shown in Figure 38 (C_d is calculated using the area of the plate instead of using projected area).

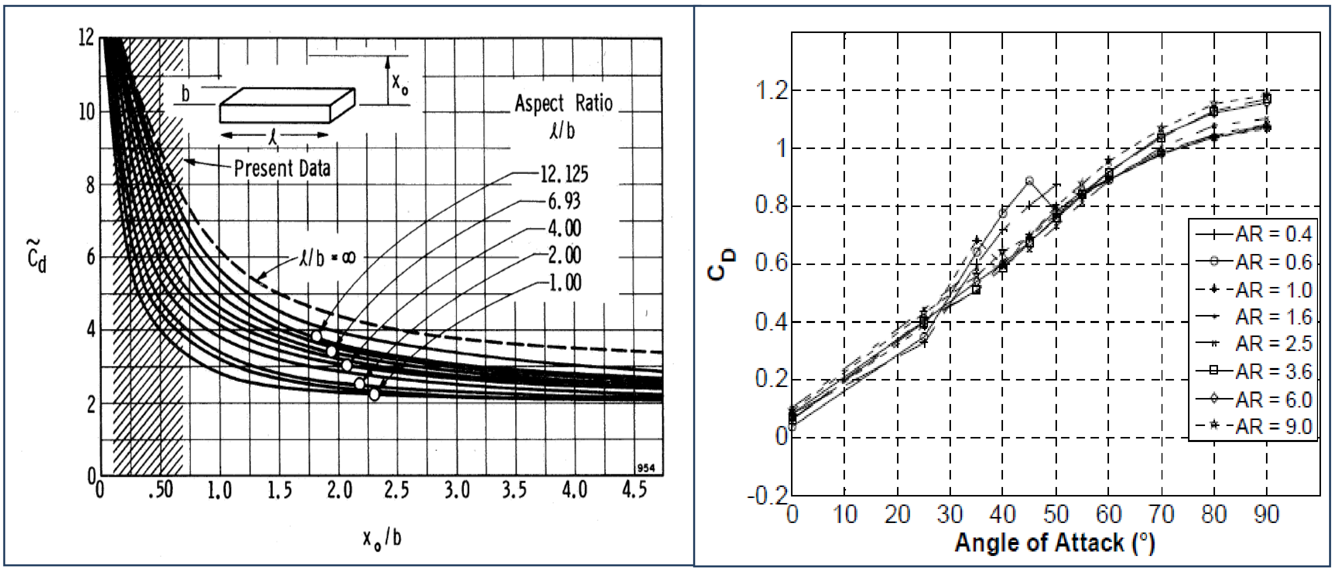

Figure 40. Oscillating drag coefficient [7] (Left) & drag coefficient for a steady flow [9] (right)

In DNV-GL recommendation [14], a method to extrapolate the steady flow drag coefficient to oscillatory drag coefficient was suggested for cylindrical structures, where a variable 'Wake Amplification Factor'(WAF) was defined.

$$\text{Wake Amplification Factor} = \frac{Oscillatory\ Drag\ Coefficient}{Steady\ Drag\ Coefficient} \tag{47}$$

Since we know both oscillatory and steady drag coefficient for 90 degree condition, the wake amplification factor can be estimated and used for extrapolation. This approach is used to find C_d and finally the damping coefficient due to a plate on the vessel.

7.3 OPTIMIZATION PROCESS

A plate with different dimensions can be fitted on the pontoon arm in different angles and at different depths which will have different effects on the vessel. So there are infinite numbers of configurations and the objective is to find the most optimum configuration among them. In the current case optimum configuration means the arrangement of the plate which minimize roll RAO of the vessel, as well as, have minimum weight. It's logical that a larger plate can reduce the roll RAO drastically; however as the plate dimension increases the cost also increases. So a multi-objective optimization process has to be performed to obtain the best configuration and genetic algorithm is best suited in such cases. A multi-objective problem doesn't have just one solution instead it has a set of solutions and the details are discussed in the following section. Multi Objective Genetic Algorithm (MOGA) is one of the optimization processes programmed in modeFRONTIER and hence it has been used for this thesis.

7.3.1 Genetic Algorithm

Genetic algorithm (GA) is inspired by the evolutionist theory explaining the origin of species. It was developed by Holland and his colleagues in the 1960s and 1970s. The concept used is that in nature, weak and unfit species within their environment are faced with extinction by natural selection. The strong ones have greater opportunity to pass their genes to future generations via reproduction. In the long run, species carrying the correct combination in their genes become dominant in their population. Sometimes, during the slow process of evolution, random changes may occur in genes. If these changes provide additional advantages in the challenge for survival, new species evolve from the old ones. Unsuccessful changes are eliminated by natural selection.

In a problem the variables are called genes in GA terminology and the solution is called an individual or a chromosome. In the original implementation of GA by Holland, genes are assumed to be binary numbers. In later implementations, more varied gene types have been introduced. GA operates with a collection of chromosomes, called a population. The population is randomly initialized. As the search evolves, the population includes fitter and fitter solutions, and eventually it converges. Holland presented a proof of convergence to the global optimum where chromosomes are binary numbers.

GA uses two operators to generate new solutions from existing ones: crossover and mutation. In crossover, generally two chromosomes, called parents, are combined together to form new chromosomes, called offspring. The parents are selected among existing chromosomes in the population with preference towards fitness so that offspring is expected to inherit good genes which make the parents fitter. By iteratively applying the crossover operator, genes of good chromosomes are expected to appear more frequently in the population, eventually leading to convergence to an overall good solution.

The mutation operator introduces random changes into characteristics of chromosomes. Mutation is generally applied at the gene level. In typical GA implementations, the mutation rate is very small, typically less than 1%. Therefore, the new chromosome produced by mutation will not be very different from the original one. Mutation plays a critical role in GA. As discussed earlier, crossover leads the population to converge by making the chromosomes in the population alike. Mutation reintroduces genetic diversity back into the population and assists the search escape from local optima.

Reproduction involves selection of chromosomes for the next generation. In the most general case, the fitness of an individual determines the probability of its survival for the next generation. There are different selection procedures in GA depending on how the fitness values are used. Proportional selection, ranking, and tournament selection are the most popular selection. The general algorithm of GA is shown in Figure 39.

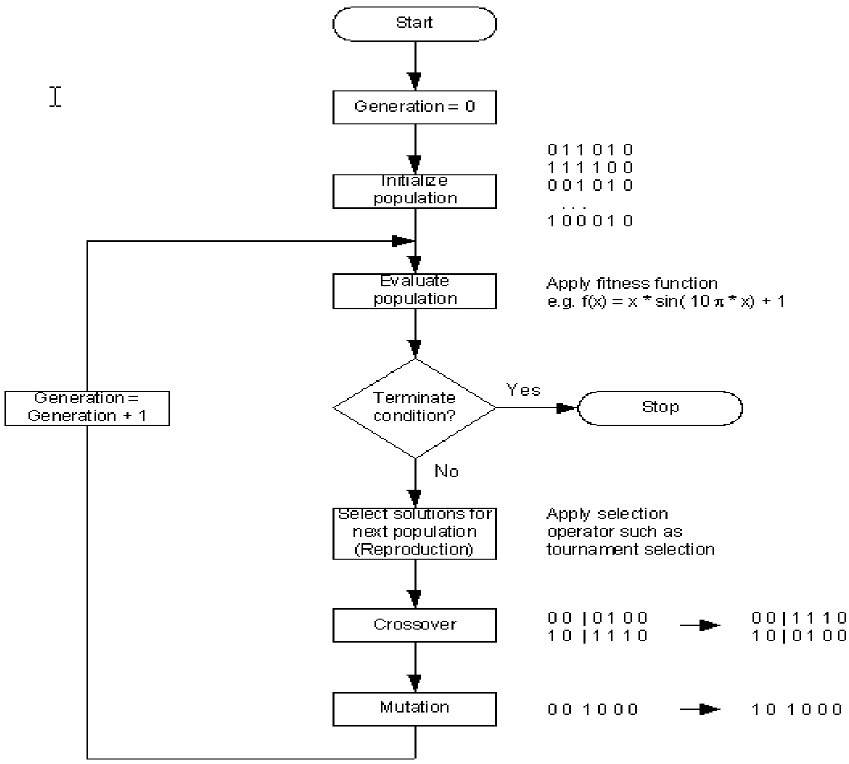

Figure 41. Flowchart of genetic algorithm

GA being a population based approach is well suited to solve multi-objective optimization problems. The ability of GA to simultaneously search different regions of a solution space makes it possible to find a diverse set of solutions for difficult problems with non-convex, discontinuous, and multi-modal solutions spaces. For a multi objective problems there are several numbers of optimum solutions and they are called Pareto optimal set, it is a set of solutions that are non-dominated with respect to each other. While moving from one pareto solution to another, there is always a certain amount of sacrifice in one objective to achieve a certain amount of gain in the other. The pareto solutions for different objectives are clearly shown in Figure 40.

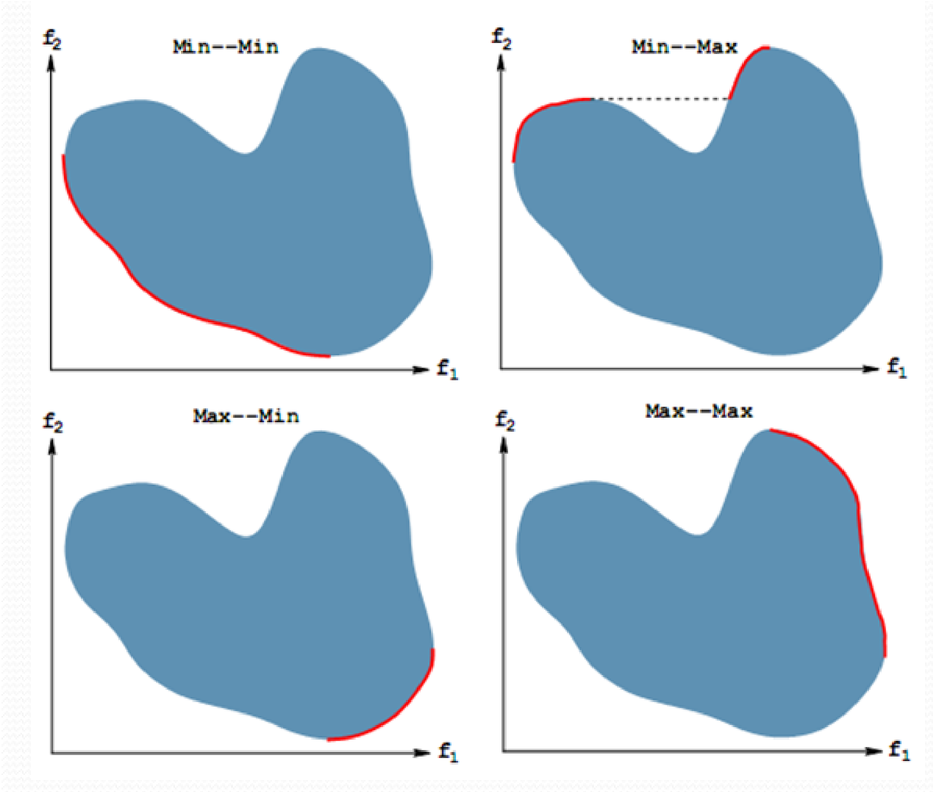

Figure 42. Pareto optimal solution sets for different objectives

If f_1 & f_2 are the solutions then the blue colored region in Figure 40 is the solution area. The red lines are the pareto optimal sets of a given problem, and different combination of maximum and minimum of f_1 and f_2 are discussed in each quadrant. In the current case since both the solutions are to be minimized the top right quadrant will be the pattern of the solution expected.

7.3.2 Flow Chart

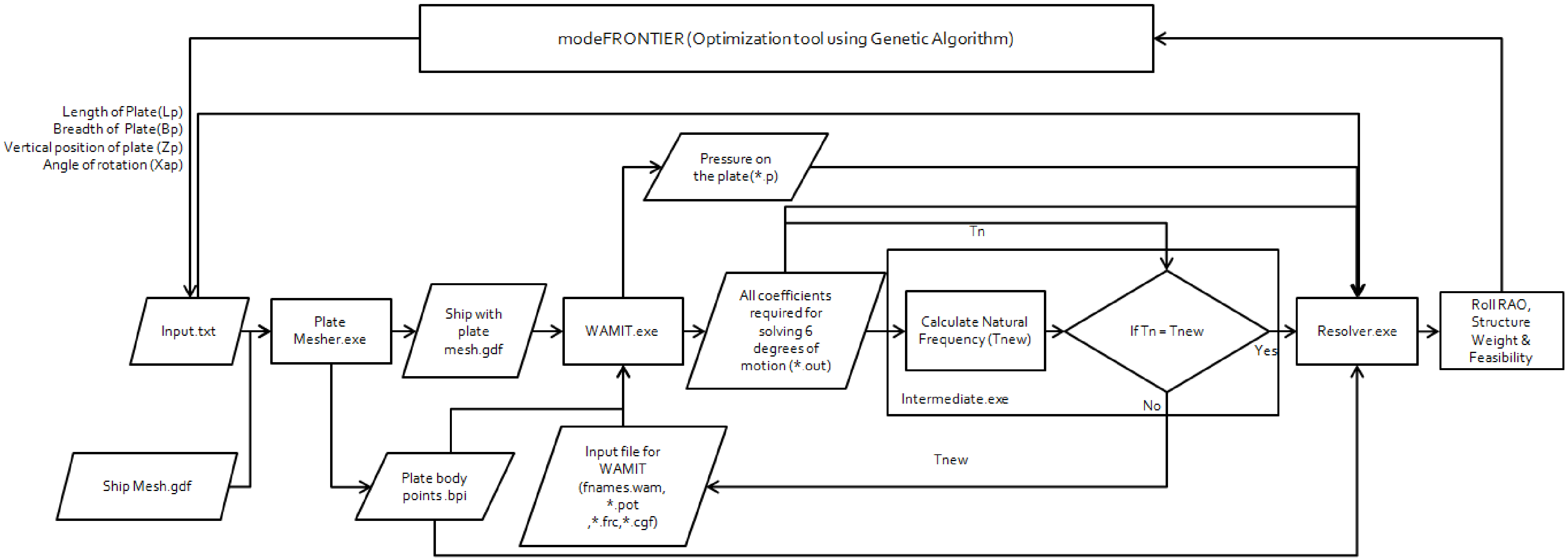

7.3.3 Description

The flow chart shown in section7.3.2 gives the whole overview of the optimization process used to design the plate system in this thesis. The details of the flow chart will be discussed in this section.

Input.txt

This is a text file which contains all the inputs required for running the whole analysis as shown in Figure 41. modeFRONTIER modifies this file and then the analysis is done. The details of how modeFRONTIER works is given in section 7.6.

```
SAL183                          Title of the ship mesh
plate                           Title of the plate mesh
final                           Title of the ship with plate mesh

-1.5                            Center of rotation
3                               Wave Height for which motions is to be analysed(m)

0                               Polygon geometry(1) or rectangular geometry(0)
10        10        0.01        Length, Breadth & thickness (rectangule) or Radius, Number of sides & thickness(Polygon)
25        25        2           Dicritization along x,y,z
-42.3     22.685    -11         Position of the center of the plate
-18       0         0           Orientation about x,y,z axis


2                               Damping coefficient using Ikeda or Star CCM(ikeda-1 Star-CCM2)

1                               Ikeda using bilge keel damping (1-yes)

0.1103                          a of just ship from Star CCM roll decay test
-0.0114                         b of just ship from Star CCM roll decay test
0.0010                          c of just ship from Star CCM roll decay test

4.436160E+05                    A44 of just ship from WAMIT(Output of WAMIT)
9.416854E+01                    B44 of just ship from WAMIT(Output of WAMIT)


Feasibility check

10                              Limiting angle(degrees)
-3                              Limiting line

Structure

315                             Reh(N/mm^2) - Yield stress - DNV recommendation
15                              Maximum Number of stiffners
```

Figure 43. Input.txt file

Shipmesh.gdf

It is the surface mesh of the vessel which is inputted as the hull form in WAMIT. In this case the center of reference is the same as the center of gravity of the vessel. (See Figure 42)

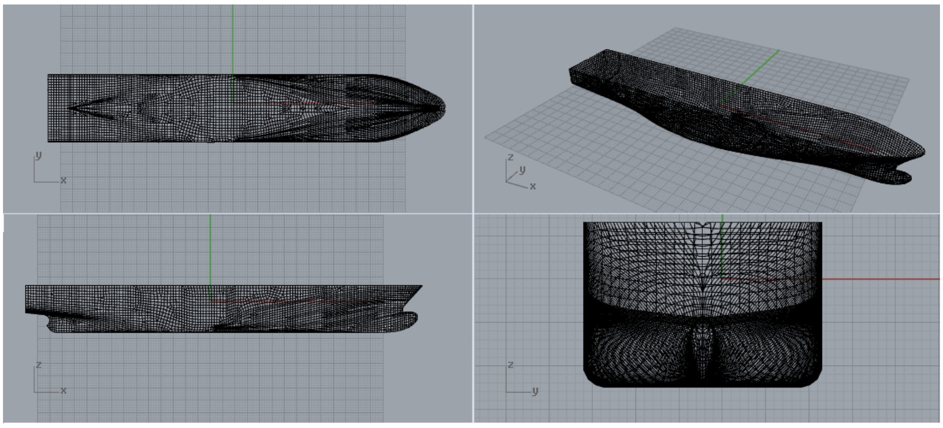

Figure 44. Surface mesh of SAL 183

Platemesher.exe

Platemesher.exe is a code made to append the mesh of the plate specified in Input.txt file to the hull mesh. The code reads the length, breadth and thickness of the plate and discritize the whole plate along each axis as mentioned in Input.txt file. The initial discritization is done for the whole volume, but since it's a surface mesh only the outer points are selected and are rotated to the required angle using the rotation matrix.

A surface can be represented using 4 nearby points, so by following the standard representation of *.gdf files, the points are outputted. Representation of the coordinates of the four points which are at the corners of one surface are not random, there is a pattern which has to be followed as per WAMIT requirement so that it can determine direction at which water medium is present. So if the representation is right then the normal from the surface should be to the outside as shown in Figure 43.

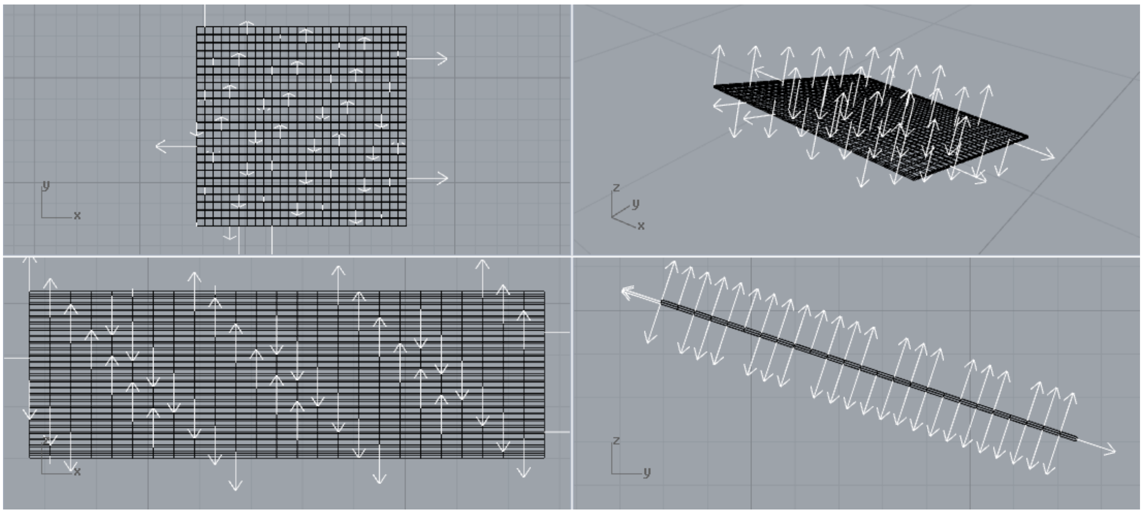

Figure 45. Plate mesh with its normal

After the plate mesh is created the code reads the vessel mesh from the title provided in Input.txt and creates a new mesh file by appending the plate mesh into the hull mesh. Finally the mesh as shown in Figure 44 is obtained.

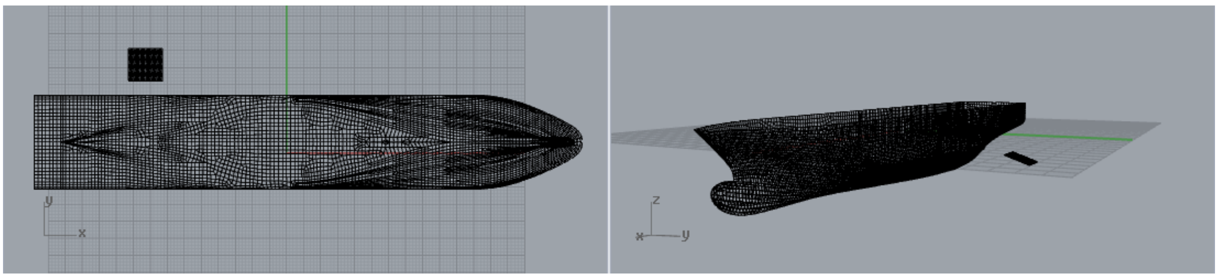

Figure 46. Vessel with a rectangular plate

Platemesher could also create mesh of plates with polygonal geometry if the number of sides and the radius distance from the center to the edges are known (Figure 45). But since the drag estimation for such geometries are not available this part of the code is not utilized for the current optimization process.

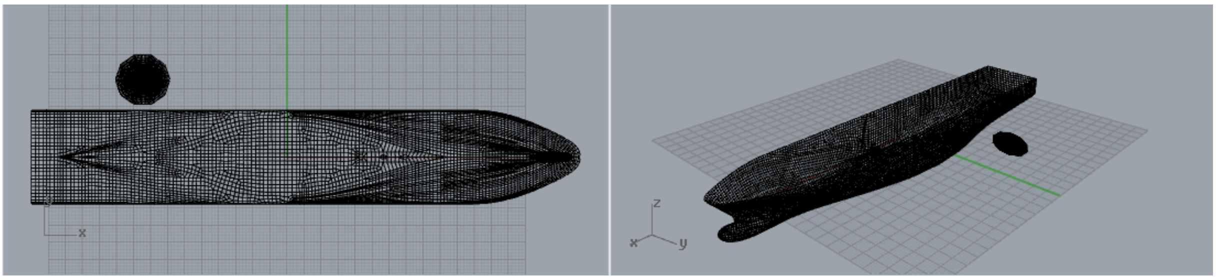

Figure 47. Vessel with a polygonal plate

The code also create a *.bpi file which contain the coordinates of the plate body at which the pressure has to be estimated. This pressure is later utilized to calculate the load for structure analysis.

Input files for WAMIT

In addition to the mesh file of the vessel with plate (* .gdf) and the body point (*.bpi) there are other input files required for running WAMIT. The primary file is *.pot, which consist of the details required for the potential solver like wave period, wave direction, modes to be analyzed, number of bodies and name of the mesh file etc. The next file is the *.frc file were the center of gravity of the vessel, mass, moment of inertia etc is represented and finally we have *.cfg were the other setting like type of solver, number of rams used, the output files needed etc are inputted. WAMIT understand the name of the files to be read from a file called fnames.wam where the names of the above 3 are given.

WAMIT.exe

The potential solver WAMIT.exe is run using the mesh file (*.gdf), body points file (*.bpi), fnames.wam, *.pot,*.frc and *.cfg files. There are several output files which can be seen after the WAMIT run however the main output file is *.out where all the coefficients i.e. Added mass, damping coefficient, stiffness coefficient, exciting forces and also other values like volume, center of buoyancy etc are outputted. Also another output which is of importance is the *.p file which contains the pressure on each point given in the*.bpi file. Using these 2 files the rest of the analysis can be done.

Intermediate.exe

When a plate is fixed to the hull form the natural frequency of the whole system changes due to the change in added mass, so it is necessary to find out the natural frequency of the new system and then do the analysis. The objective of this process is to find out the maximum motion of the vessel which occurs at natural frequency. So the intermediate.exe code reads the output file of WAMIT, *.out, and from the added mass & the stiffness coefficient the new natural frequency is calculated. Then the code check whether both r same, if not, the code creates a new set of input files for WAMIT, mainly the wave period in *.pot file is changed to the new wave period. After the new files are created WAMIT is again run and then the new *.out and *.p are used in the code ‘ resolver.exe’.

Resolver.exe

Resolver.exe inputs the data from Input.txt, *.out & *.p files and run the analysis. It has mainly 2 parts, hydrodynamic analysis and structure optimization. In hydrodynamic analysis the code analyze the RAO of the vessel after taking into account the damping coefficient due to the plate and also the viscous damping of the vessel. The structure optimization part finds the best scantling for a given pressure distribution and estimates the weight of the structure. It also checks whether the pontoon arm will be able to handle the weight and force acting on the arm, if it doesn’t satisfy then this solution is unfeasible. Hence the output of this code is the response of the vessel, weight of the structure and whether this is a feasible solution.

From these outputs the modeFRONTIER calculates the next set of variables using genetic algorithm for the next iteration and this keeps on going. And finally a set of optimum values are obtained called pareto optimal set as explained in section 7.3.1.

7.4 HYDRODYNAMIC ANALYSIS

Hydrodynamic Analysis part of the resolver.exe is the combination of the algorithm used to find the roll RAO (section 5) and the concept of damping due to the plate (section 7.2). Here the damping coefficient of the plate and the vessel is found for a roll angle and the equation of motion is solved and then the roll angle is compared with the initial value and unless both r equal minimization algorithm is ran and the result is obtained. The detailed algorithm can be seen in the flow chart shown below.

7.4.1 Flow Chart

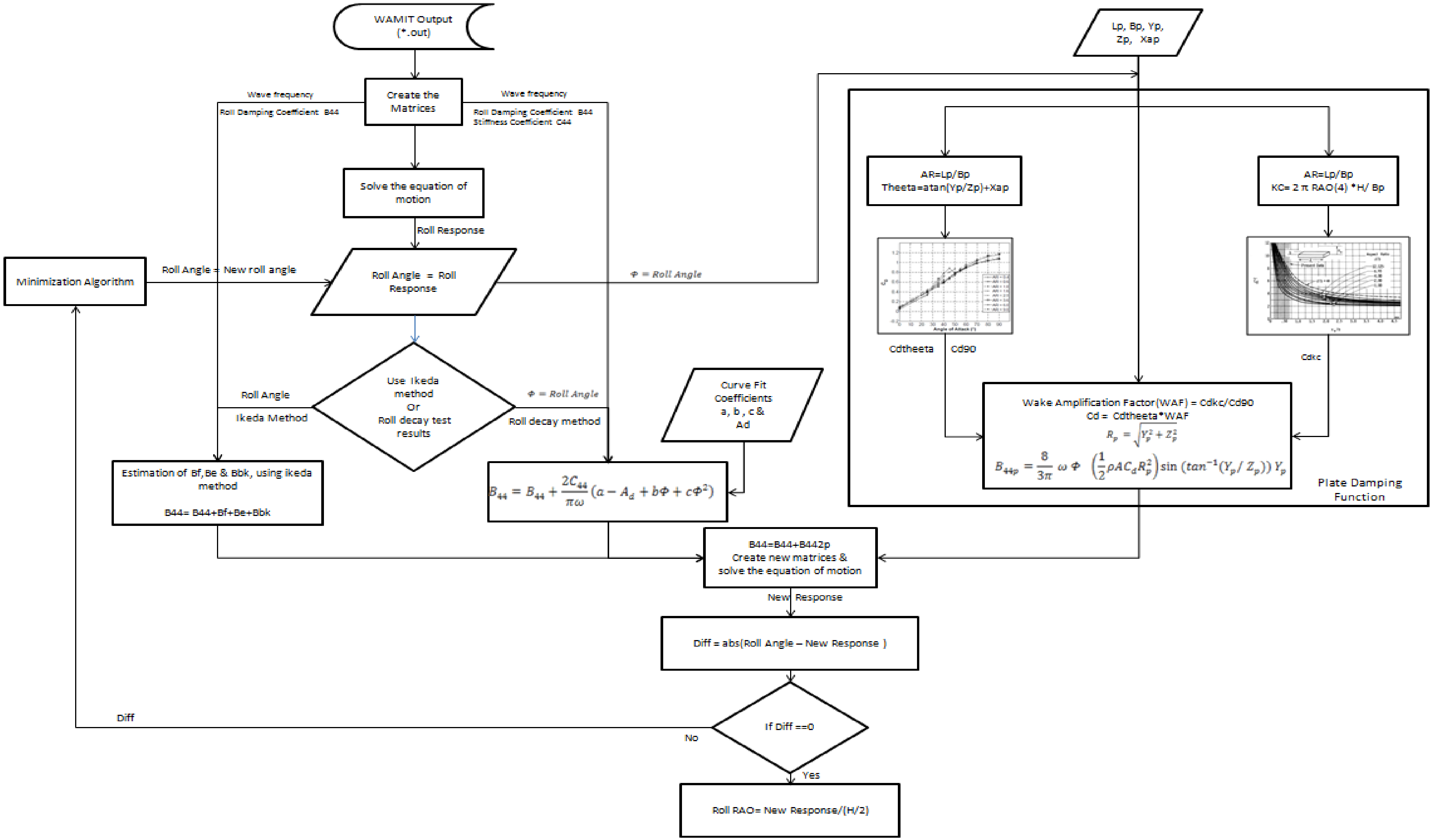

7.4.2 Description

The flowchart shown above is similar to that of the flow chart used for estimating the roll RAO but an extra part which is known as the plate damping function is been added into this. The plate damping function inputs the length of the plate (L_p), breadth of the plate (B_p), position of the plate (Z_p) and the orientation of the plate (X_{ap}) from the input.txt file. Then using the concept explained in section 7.2 the damping due to the plate is found for which the C_d has to be estimated. To find the C_d initially the aspect ratio (AR) is calculated along with the angle of attack. The C_d corresponding to the AR and angle of attack ($C_{dtheeta}$) is found through interpolation along with C_d for 90 degrees (C_{d90}).

Then the KC number is found which a function of amplitude of roll motion and breadth of the plate. So the C_{dkc} is found, then it's possible to find the wake amplification factor as it's the ratio between C_{dkc} and C_{d90}. The wake amplification factor is used to extrapolate the C_d of steady flow to oscillating flow by just multiplying this factor. Hence the finally it's possible to estimate damping coefficient due to plate and this is added to the damping coefficient estimated using the roll RAO algorithm. Finally the equations of motion with new matrices are solved for obtaining the roll motion of the vessel with the plate.

7.5 STRUCTURE OPTIMIZATION

In the hydrodynamic analysis the plate was assumed to have just a constant thickness and it's not sufficient enough to take up the load, as it acts as a sheet of paper in water, it's necessary to define a structure for the plate. Also since the whole optimization is done for a plate which is to be fitted on the current pontoon arm, it's necessary that find out whether the weight of the plate can be handles by the pontoon arm. If the weight along with other loads is too high for the arm then those solutions are not feasible.

So the primary objectives of this section of code are to estimate the pressure distribution on the plate and find an optimum structure that pressure distribution and finally check whether the pontoon arm is able to handle the loads on the plate along with the weight of the plate structure. The flowchart of the algorithm has been shown in the next section.

7.5.1 Flow Chart

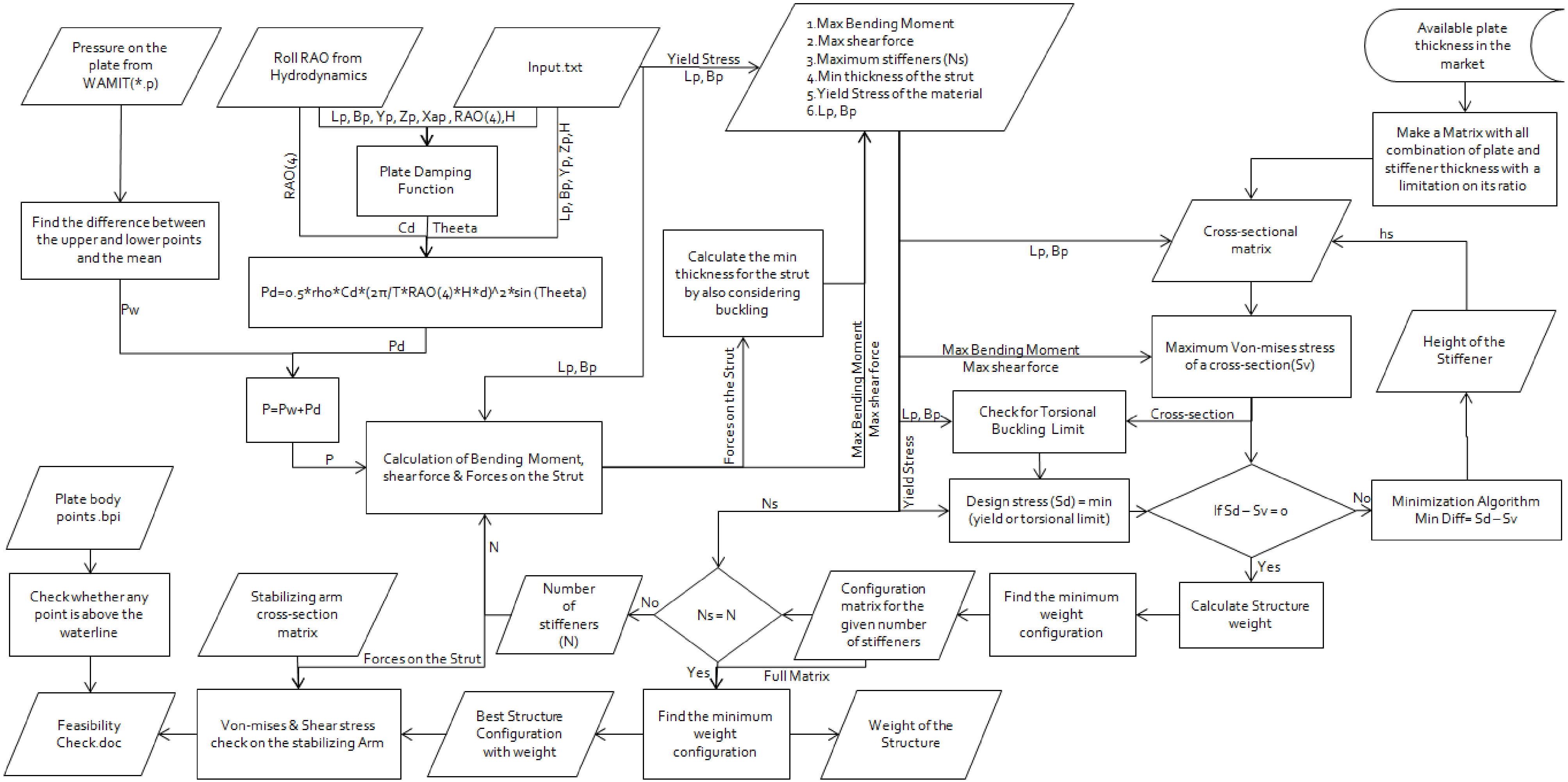

7.5.2 Description

The algorithm shown in section 7.5.1 has 3 main objectives and they are

- Calculating the load on the plate
- Calculating the best optimum plate structure for the given pressure
- Checking whether the pontoon arm can take up the load and weight of the plate

They have been discussed in detail below.

Assumptions

In this algorithm a simplified model has been used so that the computation time will be less as well as the results have closer values to the reality. The most commonly used simplified theory for computing the stress in a structure is the simple beam theory. But the theory is valid only for slender beams and not suitable for shell structures. By considering some assumptions the whole structure arrangement shown in Figure46 can be simplified to use simple beam theory.

The box structure provided in the center is used to connect the plate to the pontoon arm. Since the pontoon arm has higher stiffness than the rest of the structure the box structure can be considered to be a fixed support. Here a large continuous stiffener is provided along one side of the plate so that the whole model can be simplified as a cantilever beam. And also only simple plate stiffeners are provided along the other side of the plate so that the model can be further simplified.

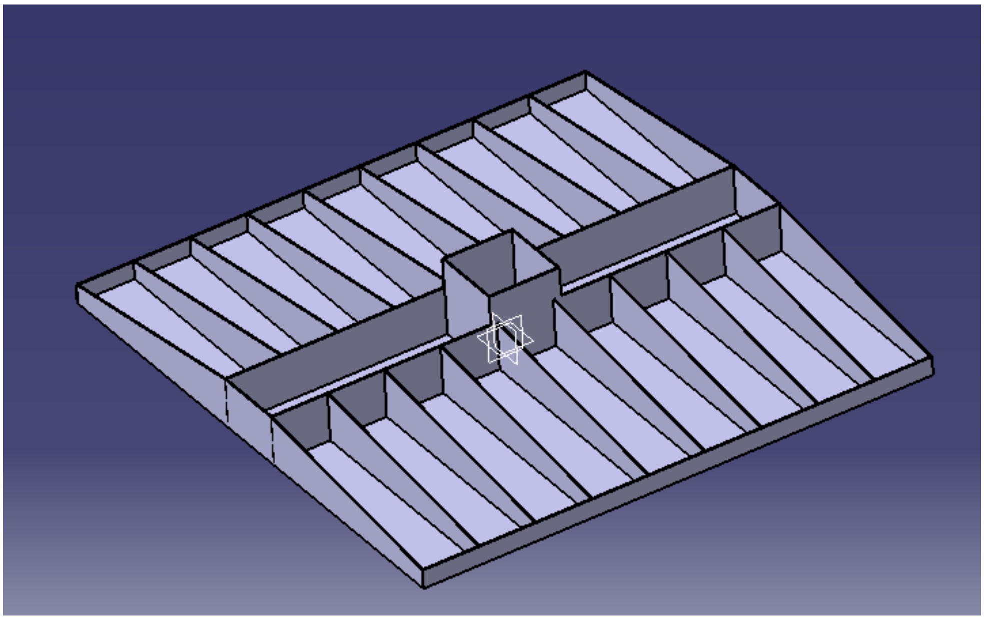

Figure 48. Plate structure

Another main assumption is that the pressure load on the plate is constant throughout. This make it possible to split the whole structure into equally divided beams whose cross section is a T section i.e. stiffener with plate. Finally the whole model can be simplified into a cantilever beam with uniformly distributed load with a T shape cross section as shown in Figure 47.

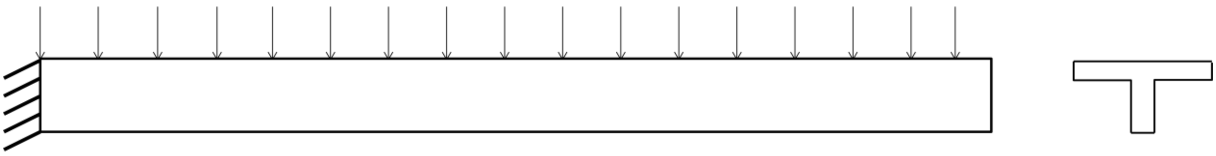

Figure 49. Simplified model of the structure

Load Estimation

The initial step of a typical structure analysis is to estimate the load. The main loads on the structure here are due to the wave which is calculated using potential solver WAMIT and also the viscous drag component due to the oscillation of plate in the fluid.

The pressure due to the wave potential is estimated in WAMIT and to do it *.bpi file is used as an input file. When it is inputted WAMIT provides the pressure on the points mentioned in *.bpi and it's outputted in *.p file. This file contains the amplitude and phase of the pressure on the points mentioned. If the pressure on both sides of the plate is known, as shown in Figure 48, then the resultant will be the difference between those.

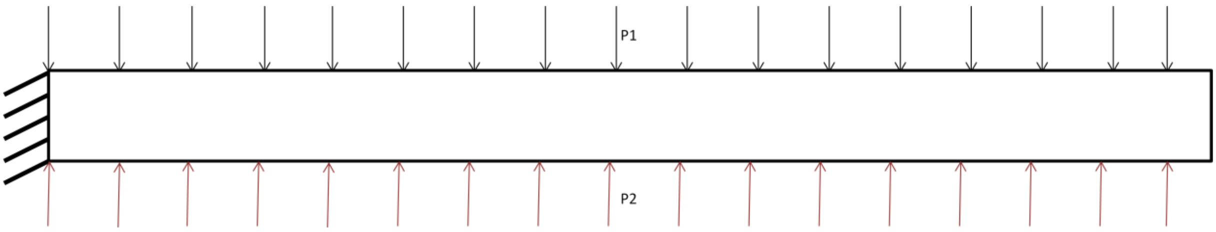

Figure 50. Pressure on the plate

The plates can be in inclined angle and the difference of the pressure should be found between points which are exactly opposite to each other. So the pressure on top and bottom of the plate is found separately and the difference between the mean of those values will give the pressure due to the wave. i.e. $P_w = |\text{mean } (P_{top)}\text{- mean } (P_{bottom})|$.

The next component is the pressure due to the drag or viscosity. Let's write pressure P_d as

$$P_d = \frac{F}{A} = \frac{\frac{1}{2}\rho A C_d V^2}{A} = \frac{1}{2}\rho C_d V^2 \tag{47}$$

$$V = R_p\,\dot{\varphi}$$

$$\dot{\varphi} = i\omega\varphi$$

$$P_d = \frac{1}{2}\rho C_d V^2 = \frac{1}{2}\rho C_d (R_p\, i\omega\varphi)^2 = \frac{-1}{2}\rho C_d (R_p\, \omega\varphi)^2 \qquad (48)$$

After the hydrodynamic analysis the RAO φ of the vessel is known so with the corresponding C_d it's possible to find the pressure due to drag force. The C_d is obtained from the plate damping function and the RAO is the output of the hydrodynamic analysis part. So total Pressure can be written as $P=P_d+P_w$

If the number of stiffeners (N) is known then the distributed load can be written as

$$w = P\frac{B_p}{N} \qquad (49)$$

Then, shear forces (F) and bending moment (M) are

$$F = wx = P\frac{B_p}{N}\,x \qquad (50)$$

$$M = w\frac{x^2}{2} = P\frac{B_p}{N}\frac{x^2}{2} \qquad (51)$$

The maximum will be at $x = \frac{Lp-Bs}{2}$ where, Bs is the breadth of the pontoon arm and the cantilever configuration is calculated from the continuous beam which is Bs/2 distance away from the center of the plate. So if the maximum bending moment and shear force is known then the only unknown is the cross section of the plate structure.

Structure definition

It can be seen in equation (51) that the bending moment M is a second order function of the distance from the free end, so for the most optimum configuration the stiffener shape should be as shown in Figure 49. But, for simplicity of production and calculation only a linear slope is given which make the calculation further simplified as the only cross-section to be considered for the stress analysis will be the one near the pontoon arm or at the fixed end.

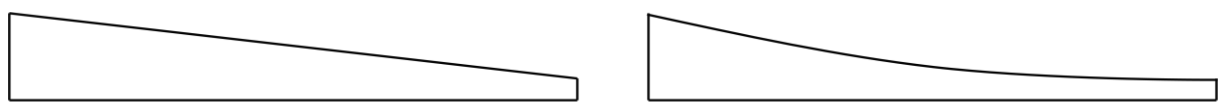

Figure 51. Simplified linear stiffener profile (left) and optimized stiffener profile (right)

For a T section the main variables are the breadth of the element plate (b_p), thickness of the plate (t_p), stiffener height (h_s) and stiffener thickness (t_s).

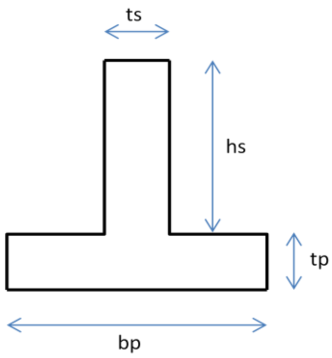

Figure 52. Cross section of the plate with stiffener

Breadth of the plate $b_p = B_p$/number of stiffeners. Since the plate and stiffeners are to be made from standard plates available in the market only the thicknesses which are available are used for this optimization. So a matrix of b_p and all the combinations of t_p & t_s is made. There are some practical difficulties in using some of these combinations so it's important to eliminate those combinations, so few conditions are used. The primary one is the weldability, in the industry if a stiffener is to be has to be welded on to the plate following $0.5 \leq \frac{t_s}{t_p} \leq 1.4$ condition should be met. This eliminates many numbers of combinations. And one more limitation which is used in the industry for a web stiffener is as following

$$t_s \leq \frac{h_s\sqrt{f_y}}{190} \tag{52}$$

where, $f_y$is the yield stress of the material.

This condition helps in choosing only those thicknesses which are suitable for a given height of the stiffener. Hence these 2 conditions reduce the number of possible configurations and now h_s is unknown so this condition is checked after the stress analysis is done.

Stress Analysis

Using simple beam theory the stresses are estimated as following

Bending stress $\sigma_b = \frac{M\,y}{I}$ (53)

Shear stress $\tau = \frac{FQ}{It}$ (54)

Vonmises Stress $$\sigma = \sqrt{\sigma_b{}^2 + 3\tau^2} \tag{55}$$

where,

y - The distance from the neutral axis

Q- Moment of area

I – Moment of Inertia

Here M and F is known Q, I and y depends on the geometry so a code was made which will find the moment of inertia and moment of area of any rectangular geometry, provided the dimensions are entered in a matrix form. If Q and I are known then the maximum von mises can be calculated. So the input for this code will be the moment M, shear force F and the geometry in matrix form.

In reality the stress distribution in a stiffened plate structure due to shear lag is as shown in Figure 51. So if the total breadth of the plate is considered for finding stress then the stress calculated will be underestimated, hence for accurate estimation effective breadth is considered. The formulation used in DNV-RP-C201 has been used for finding the effective breadth for each configuration. So now instead of the sectional plate breadth b_p the effective breadth b_e is used which is a constant multiplied by $b_{p.}$

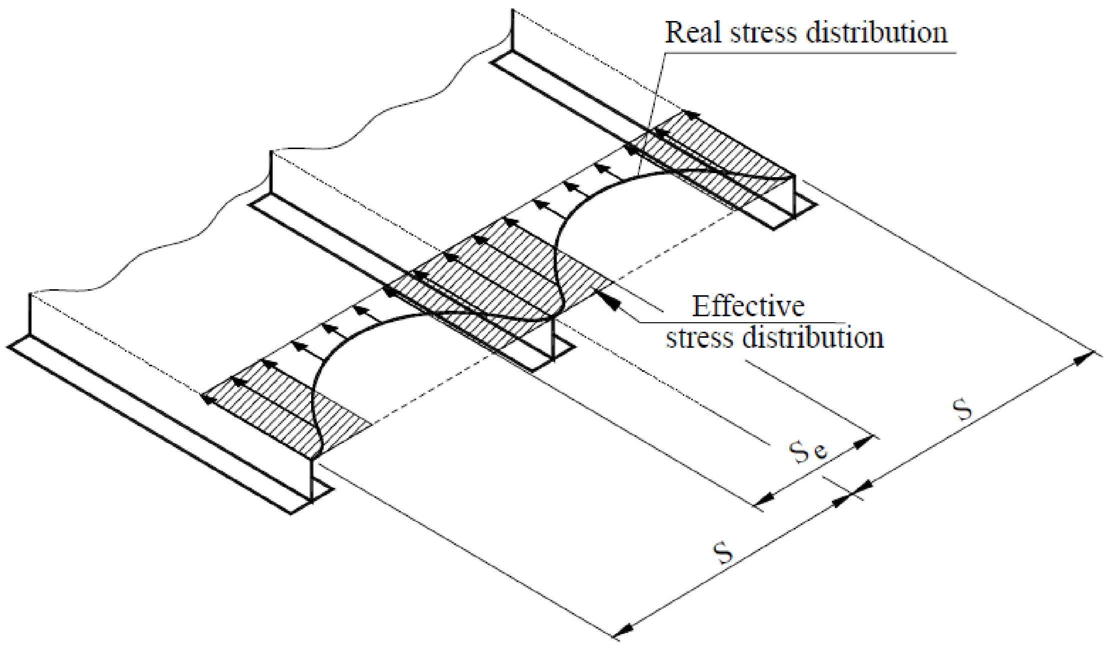

Figure 53. Stress distribution in a plate with stiffener

A design is said to be safe when the maximum von mises stress in a structure is less than or equal to the allowable stress. Using the code explained above the maximum von-mises stress can be determined if all the geometric parameters are known, but now the variable h_s is unknown. To find out h_s the allowable stress is to be estimated.

As per the GL rules the allowable stress is given by 0.9 $R_{eh,}$ where R_{eh} is the permissible stress for steel. But, in such kind of long structures there are chances for torsional buckling of stiffeners so if torsional buckling happens then the allowable stress of the structure will be less than the calculated value. Hence using DNV-RP-C201 rules the torsional buckling check is performed and if torsional buckling happens allowable stress is replaced with the new torsional stress.

Using the allowable stress and the other geometric parameters, h_s for each configuration is found out using an iterative method. Now since h_s is also known the main structure scantlings are known. But, this alone won't be sufficient to keep the structure stiff, it can be seen that the continuous beam structure is not capable of providing enough transverse stiffness for the plate, hence similar analysis is done in the transverse direction assuming that the plate between the continuous beam and the free end is also supported by a stiffener on the free end. So the height of the stiffener on the free end can be determined by considering a freely supported beam between the large stiffeners so the length of the beam to be calculated will be equal to b_p. If the continuous beam is assumed to have the same height and thickness as the stiffener then the whole scantling of the plate structure is known.

But to find the complete structure the scantling of the box structure which joins the plate and the pontoon arm is to be found out. It is a box structure whose thickness is unknown to calculate it the simple normal stress equation $\sigma_a = \frac{F_n}{A}$ can be used where, σ_a is the allowable stress, F_n is the normal force from the plate and A is the area. Along with this the buckling check is also done so that all possibilities are taken into account.

Now all the scantlings for different combinations of plate thicknesses are known and hence the weight of structure can be calculated for each case and the configuration which has minimum weight is chosen. This analysis is continued for different number of stiffeners and finally minimum structural weight is selected and outputted.

Feasibility check

It is necessary to find whether the pontoon arm can hold the plate weight and the loads acting on it. The pontoon arm is fixed to the hull as shown in Figure 52.

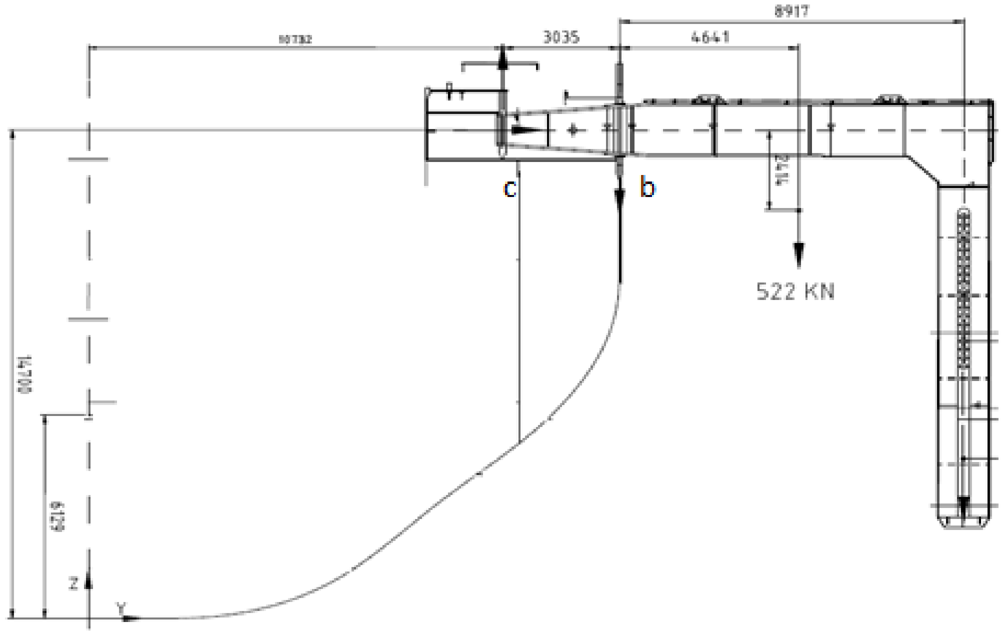

Figure 54. Detailed drawing of SAL 183 with pontoon arm.

The simple body diagram of the above arrangement can be seen in the Figure 53. The self weight of the pontoon arm is given as 522KN.

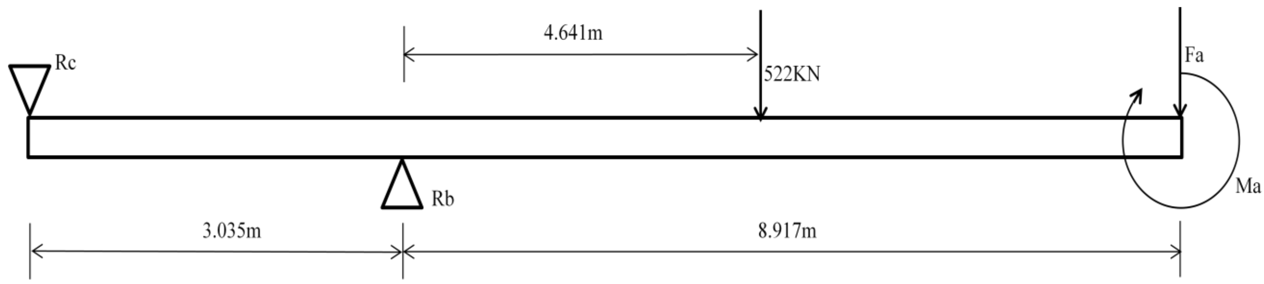

Figure 55. Free body diagram of the pontoon arm arrangement

F_a is the force acting along the axis of the pontoon arm and the moment M_a is due to the inclined forces acting because of the orientation of the plate. When the above arrangement is solved then the moment and forces acting on point c and b can be found. Using the von-mises algorithm used in previous section the von-mises stress is calculated by inputting the cross-section given in Figure 54. Finally the value obtained is compared with the allowable stress. If it's safe then it's outputted as a feasible solution.

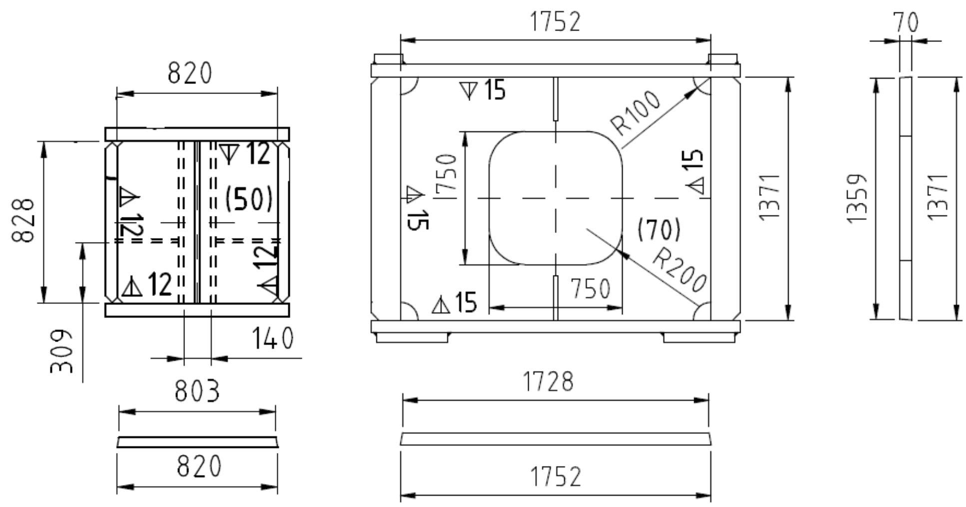

Figure 56. Plate at c (left) and b (right) points of the pontoon arm

In this part one more feasibility check is done that is to find whether the plate will remain submerged throughout the oscillation. To do so the water surface is considered as the limit and the point which has the highest 'z' is taken and using the rotation matrix the point is rotated to the RAO angle and checked whether the z is below the water line. It's done because the whole calculation is performed considering that the plate will remain submerged throughout the whole process.

7.6 OPTIMIZATION USING modeFRONTIER

As discussed before an optimization process is required to design the best plate suitable for the vessel SAL183 and the software modeFRONTIER is used for this purpose. The concept behind modeFRONTIER is that it's a program were many optimization algorithms are programmed in it. If a function 'F' is to be optimized for n variables $X_1, X_2, X_{3,..}, X_n$ then it's necessary to find the solution $F(X_1, X_2, X_{3,..}, X_n)$. This solution can be found using user defined algorithm and modeFRONTIER provides a platform to integrate different softwares for that algorithm.

So the primary step to perform the optimization in modeFRONTIER is preparing a flowchart which represents the algorithm needed and the flowchart used in the current case has been shown in Figure 55. Now the software executes each program in the sequence mentioned and the solution is obtained. Here since genetic algorithm is used the solution can be called chromosomes. The program behind modeFRONTIER is concerned only about the final output of the algorithm so that the input for next iteration can be calculated using the optimization algorithm.

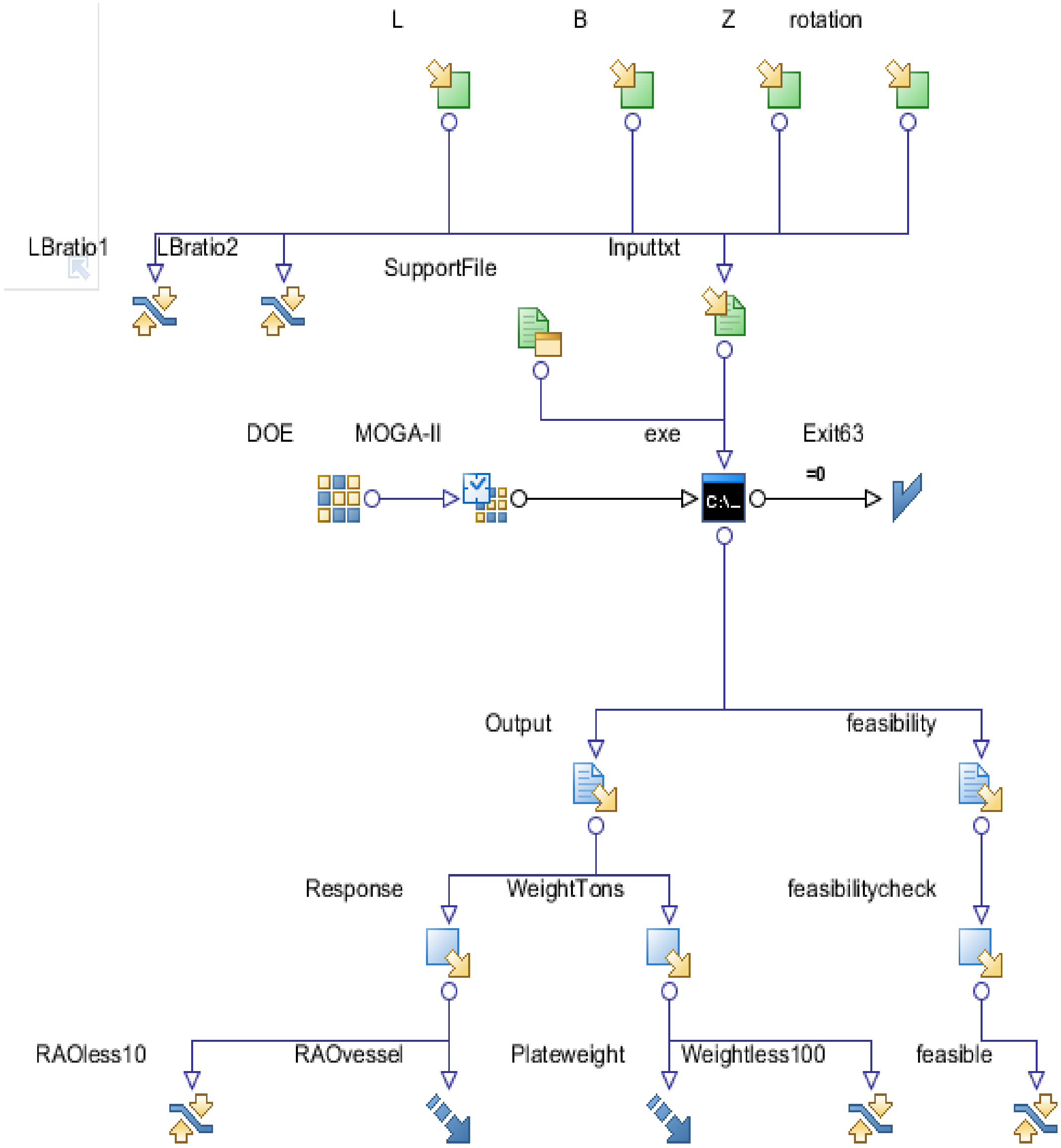

Figure 57. Flow chart in modeFRONTIER

The input and output of the optimization algorithms are just numbers which are solutions and variables respectively. Since optimization is done for the plate, the variables here will be the length of the plate, breadth of the plate, position of the center of the plate and finally the orientation of the plate. The objective of this optimization will be to minimize roll RAO and the structure weight. The details of all the variables and files used in modeFRONTIER have been shown in Table 6.

Table 8. Key elements used in modeFRONTIER

Input Variables	L	$1.75 \leq L \leq 30$; $\Delta L = 0.01$, Length of the plate
	B	$1.75 \leq B \leq 16$; $\Delta B = 0.01$, Breadth of the plate
	Z	$-13.5 \leq Z \leq -7$; $\Delta Z = 0.01$, Position of the plate
	Rotation ®	$-90 \leq$ ® ≤ 90 ; Δ® $= 0.1$, Orientation of the plate
Input File	Input.txt	Contains all the variables required for the run
Support Files	Ship.gdf	Surface mesh of the ship
	Platemesher.exe	Code used to append the mesh of the plate to Ship.gdf
	.pot,.cfg & *.frc	Input files to run WAMIT
	WAMIT.exe	Potential solver
	Intermediate.exe	Alter the wave period in input files of WAMIT
	Resolver.exe	Hydrodynamic and structure solver-section 7.4 & 7.5
	Other WAMIT files	Support files needed to run WAMIT
DOS Batch	Platemesher.exe	The executable files are executed in the given order
	WAMIT.exe	
	Intermediate.exe	
	WAMIT.exe	
	Resolver.exe	
Optimization	MOGA-II	Initialize random 10 cases Generations = 200 Crossover probability = 0.5 Mutation probability = 0.01
Output files	Output.doc	Output after running resolver.exe
	Check.doc	Output after running resolver.exe
Output Variables	Response	Response of the vessel – obtained from output.doc
	Weight tons	Weight of the plate – obtained from output.doc
	Feasibility check	Feasible check (section 7.5)-obtained from Check.doc
Constraints	LBratio	$0.08 \leq L/B \leq 12$ - Constrained aspect ratio
	RAOless10	Response≤ 10
	Weightless10	Weight tons≤ 100
	feasible	Feasibility check=1

In input variable section we define the limits of the variables so that the numbers used will be between the limit. The pontoon arm has a dimension of 1.73mX1.73m hence the lower limits for the length and breadth are kept as 1.75m. The upper limit of breadth has to be limited to 16m since beyond that the plate will intersect the hull. The axis of the whole body has been defined at the center of gravity which is 11.5m above keel and the waterline is at -3m from COG. Since throughout the whole motion complete immersion of the plate is needed the limit has been kept -7m and as the plate can't be fit far below the keel the other limit was kept -13.5m. The orientation of the plate was kept between 90 to -90 so that all the possible rotation can be considered.

The program modeFRONTIER creates folders for each iteration and all the support files are copied into that folder. Then the input file is created in the folder with the new variables and then the executable files are run in the given sequence. When the whole run is done the program check for the output file name provided and extract the output variables needed and those are the solutions or chromosomes. From these solutions the next set of variables are defined using the optimization algorithm. It is possible to provide constraints on both input variables, as well as, output variables so that it's possible to define other limitations which will help in obtaining solutions which meet all the requirements.

7.7 RESULTS & DISCUSSION

Several optimizations were run and the final optimization which was done using the decay coefficient and the structure code has been discussed here.

7.7.1 Optimization

The optimization was run for 200generations with 10 population which accounts to 2000 iterations and the following results were obtained.

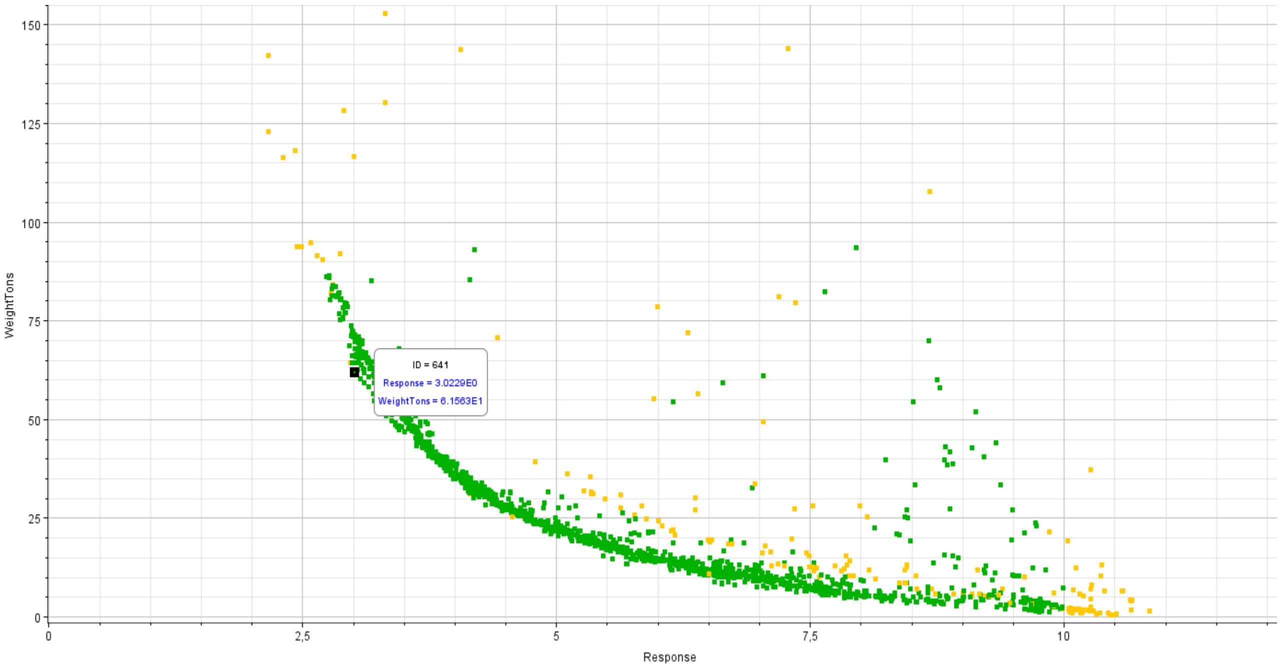

Figure 58. Optimization results with the best result chosen being highlighted

It was explained that the best results from an optimization run lies in the pareto frontier or pareto set and hence the pareto set was extracted from the obtained results and it's shown in Figure 56. Details of all the designs on the pareto set has been attached in appendix A3.

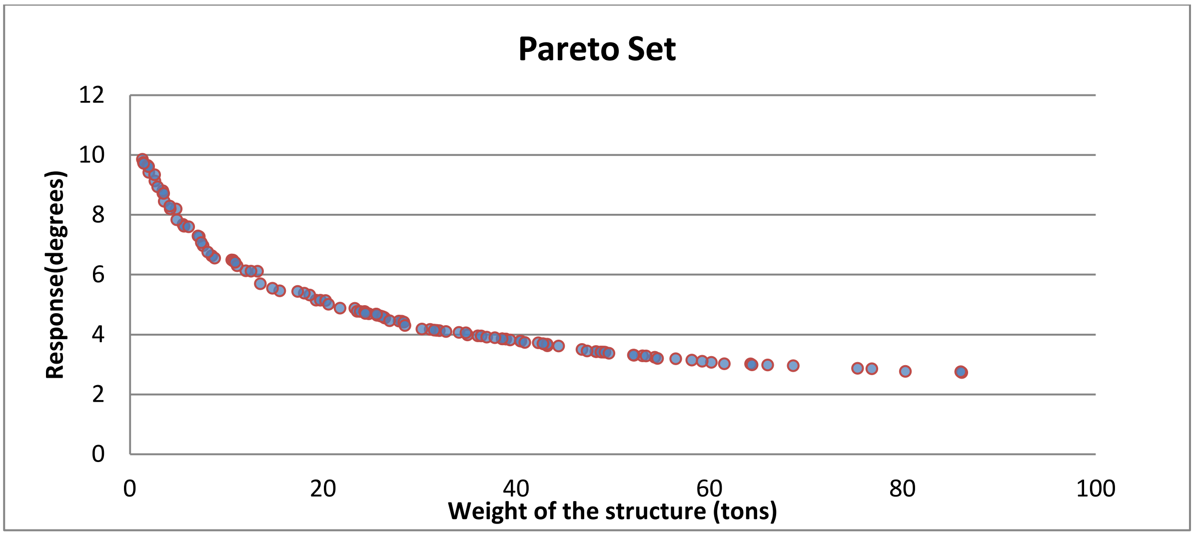

Figure 59. Pareto set of the optimization run

It could be seen that above 60 tons the effectiveness of the plate is almost constant hence the configuration 641 which is one of the best configuration near 60tons is chosen.. The details have been shown in Table 7. The mesh representation of design 641 has been shown in Figure 58.

Table 9. Details of configuration 641

ID	Length	Breadth	Vertical position	Rotation	Response	Weight	Aspect ratio
	m	m	m	Degrees		Tons	
641	12.64	12.93	1.91 above keel	17.2	3.023	61.56	1.023

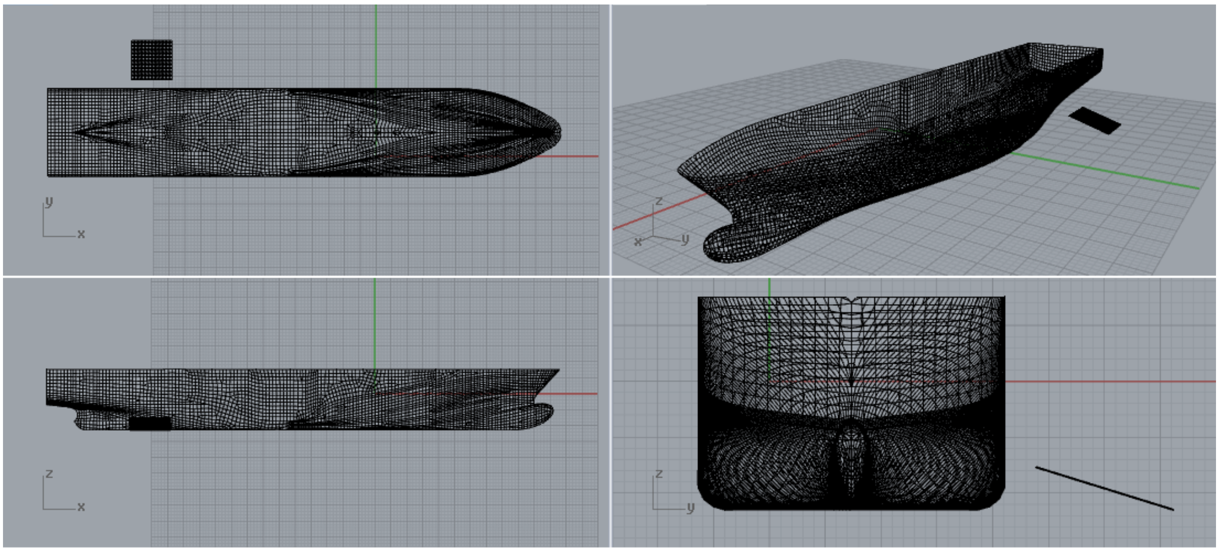

Figure 60. Configuration 641

From the graph of oscillatory drag coefficient and KC number (Figure 38), it's obvious that as the aspect ratio increases the damping increases hence the optimized structure is expected to have higher aspect ratio. To study the optimum range of aspect ratio for the given problem, the Pareto frontier data was analyzed and plotted (Figure 58).

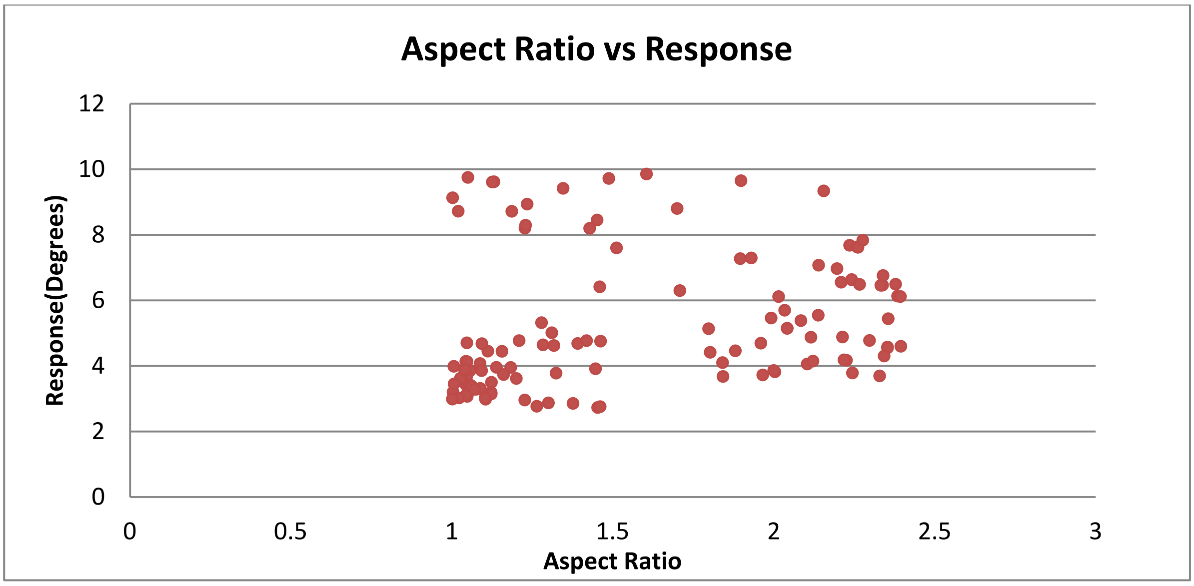

Figure 61. Aspect ratio of the designs in pareto set

It could be seen from figure 59 that the optimum range of aspect ratio for the current case is between 1 and 2.5 and as the response reduces it converges near to 1. In the initial stage several optimizations were ran for minimizing the response and the area of the plate in which the structure optimization algorithm was not considered. It gave values which were having higher aspect ratio.

This change in optimization results was because of the consideration of the structure for the plate. The major weight in the structure is the weight of the plate and for higher aspect ratio the plate becomes long which make the bending moment to increase drastically. To support the stress due to this bending moment higher thickness stiffeners and plates are required which increase the weight drastically. And this increase in weight is providing any significant increase in the damping and hence the results got converged to an aspect ratio of 1.

Hence in such kind of optimizations, structure design has to be taken into account or else the optimization might provide a result which is incorrect.

7.7.2 Roll RAO with the Plate

For the optimization run the roll RAO was estimated only for the natural frequency of the new system while it was curious to know how the plate will affect the behavior of the vessel in other frequencies. So the roll RAO was calculated for different wave periods and has been shown in figure 62. It was also curious to know how much roll deduction would have been calculated if the viscous damping of the plate is not considered. Even when the damping of the plate is not considered the roll RAO is less which means that the radiation wave generated by the new system is more which cause the reduction in roll.

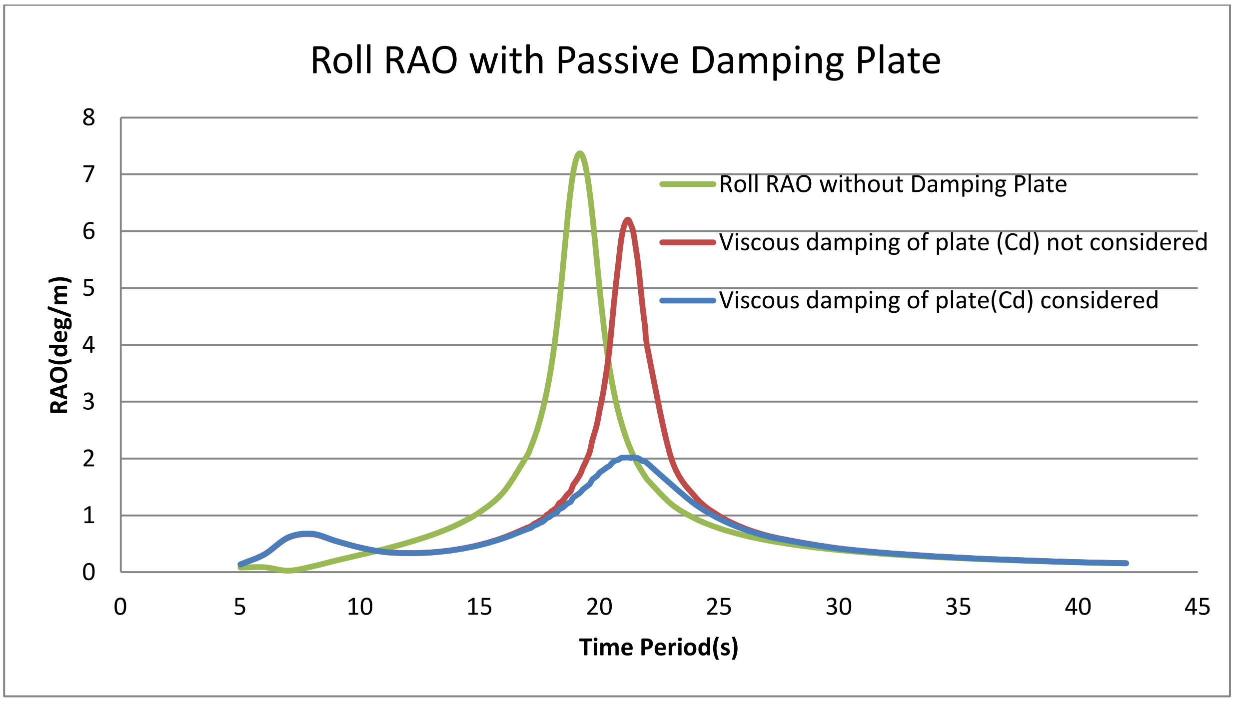

Figure 62. Roll RAO with the optimum plate

From the graph it could be seen that the plate increases the roll of the system in lower time period range between 5secs and 10 secs which is a drawback since the number of waves between 5 and 10 secs in Real Ocean is large. So even though the magnitude of the roll is reduced by the plate the vessel tends to always experience roll motion in all sea conditions.

7.7.3 Plate Structure

The most optimum structure for the configuration 641 is as shown in figure 63. The details of the structure can be seen in table 10. Stiffener 1 is the stiffener along the length and the shape can be seen in figure 64. Stiffener 2 is the long high beam extending along the breadth; it is considered as a beam extending after the box structure hence 4 stiffeners. Stiffener 3 is the long beam on the free end and box structure in the center can be represented as 4 plates as shown in table.10

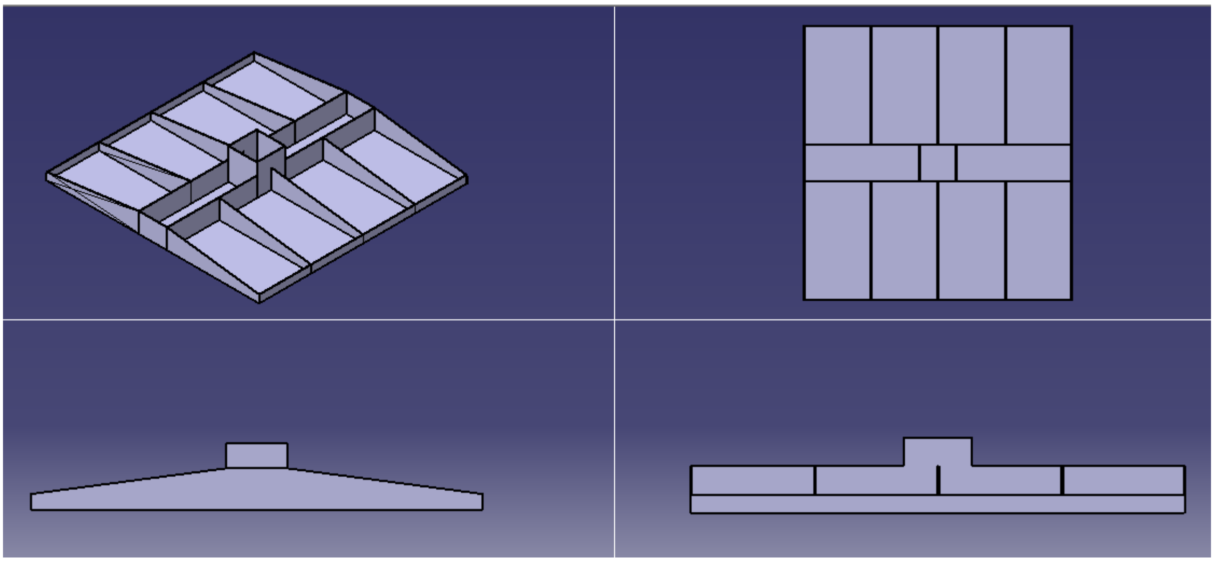

Figure 63. Plate with structure for configuration 641

Table 10. Structure details

	Number	Length	Breadth/Height		Thickness	Total Mass
		Meters				Tons
Plate	1	12.93	12.64		0.026	33.12
Stiffener 1	10	4.66	h1=1.275	h2=0.435	0.036	13.63
Stiffener 2	4	5.45	1.274		0.036	7.79
Stiffener 3	2	12.64	0.435		0.036	3.08
Box– each side	4	1.75	1.985		0.036	3.94
Mass of the structure	61.56 tons					
Pressure	18852.318 Pa					
Allowable stress ($0.9R_{eh}$)	283.5 MPa					

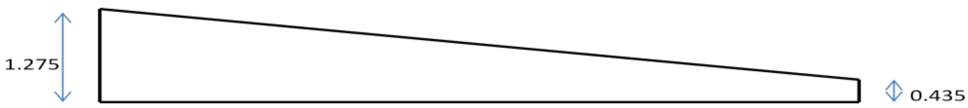

Figure 64. Stiffener 1

It’s necessary to check the stress on the plate structure with FEA software and hence the above structure is modeled as a 3-D object and analyzed in Hyperworks using tetra mesh and solid element property. The top surface of the box structure was constrained in all DOF and a uniform pressure load was provided on the plate surface. The results can be seen in figure 65.

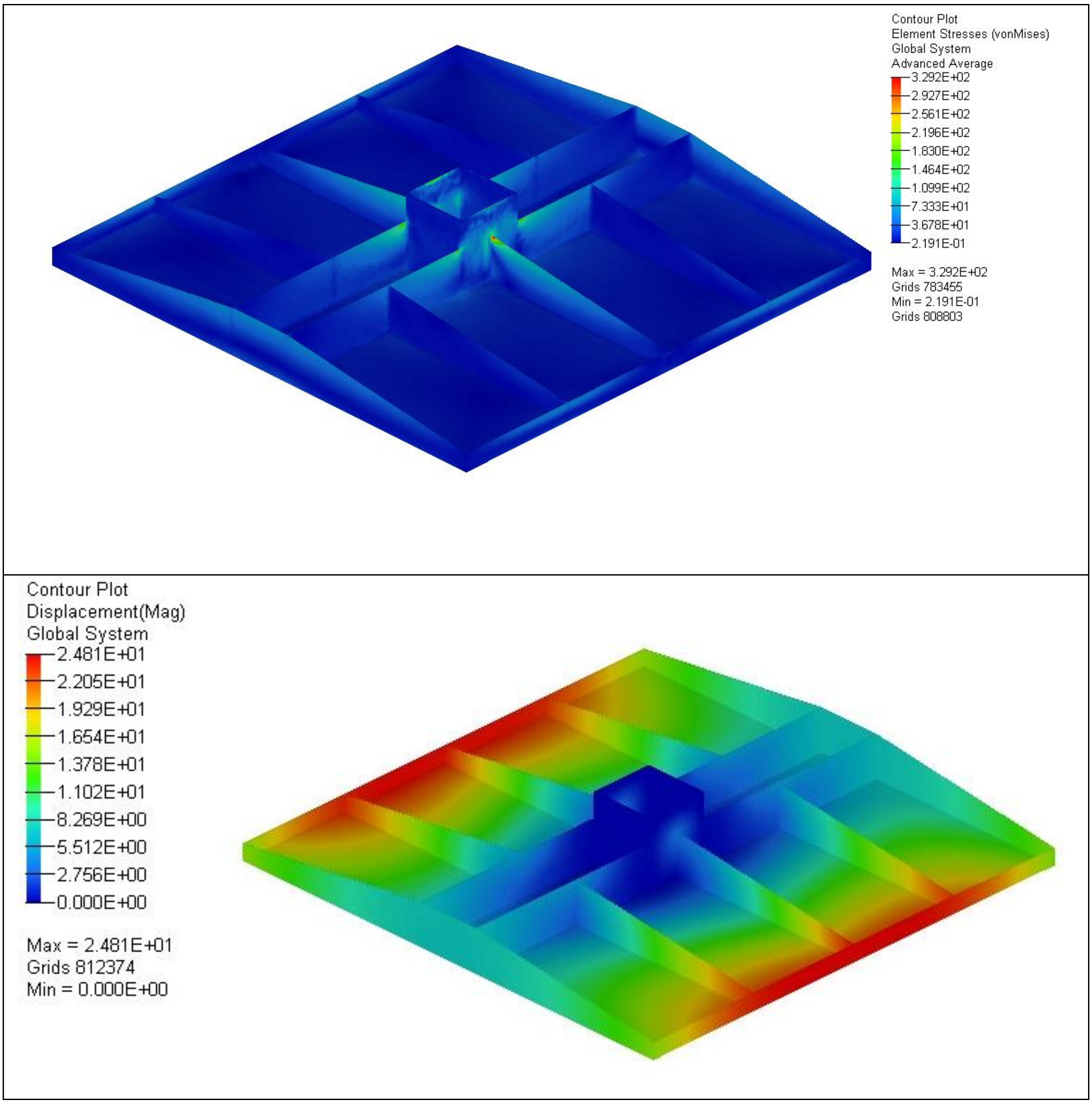

Figure 65. FEA results

The FEA results in Figure 65 show that the maximum Vonmises stress is around 329.2MPa and this is 16% higher than the allowable stress calculated. But this maximum stress is due to the stress concentration (see figure 65) which is a concern during fatigue analysis. Here the structure optimization algorithm was indented to find the weight of the structure for a given pressure distribution and hence fatigue was never a concern. And this extra stress due to stress concentration can be reduced with a proper designing of the available material. So it could be said that the structure optimization algorithm is giving good results and also the plate used is safe.

8. FINAL COMPARISION

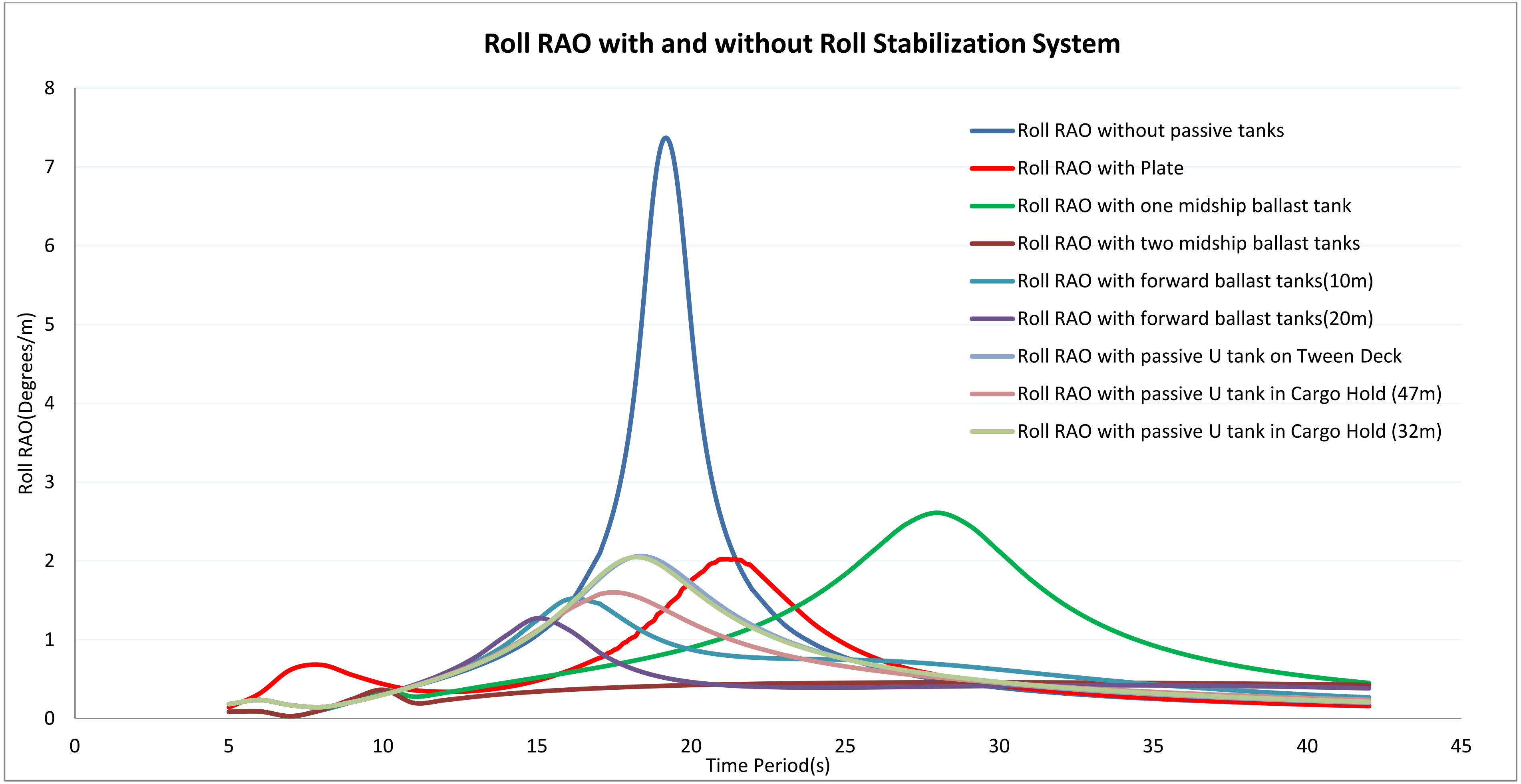

Figure 66. Final comparison of roll RAO

Table 11. Final comparison

<table>
<tr><th colspan="4"></th><th colspan="2">Maximum Response of the Vessel (degrees)</th><th colspan="2">Extra Weight Added</th><th>Lost Lifting Capacity (tons)</th><th>Lost Stowage Volume (m^3)</th><th>Complexity in Construction</th><th>Time Lost During Operations</th><th>Utilized During Transportation</th><th>Initial Cost</th></tr>
<tr><td rowspan="7">Anti Roll U tanks</td><td rowspan="2">Midship Ballast Tanks</td><td colspan="2">1 set of Tanks</td><td>3.91</td><td>64.61% reduction</td><td colspan="2" rowspan="2">Weight of the valves</td><td>338 (16.9%)</td><td rowspan="2">Nil</td><td rowspan="2">High</td><td rowspan="7">Nil</td><td rowspan="7">Yes</td><td>Medium</td></tr>
<tr><td colspan="2">2 set of Tanks</td><td>0.69</td><td>93.75% reduction</td><td>676 (33.8%)</td><td>Medium</td></tr>
<tr><td rowspan="2">Forward Ballast Tanks</td><td colspan="2">Length 10m</td><td>2.27</td><td>79.45% reduction</td><td colspan="2" rowspan="2">Weight of extra Steel and valves</td><td>64 (3.2%)</td><td>369.6 (2%)</td><td rowspan="2">Medium</td><td>Medium</td></tr>
<tr><td colspan="2">Length 20m</td><td>1.91</td><td>82.71% reduction</td><td>128 (6.4%)</td><td>739.2 (4%)</td><td>Medium</td></tr>
<tr><td rowspan="3">New Set of Tanks</td><td>Tween Deck</td><td>26m</td><td>3.09</td><td>72.04% reduction</td><td>392.55t (1.79%)</td><td rowspan="3">+ Steel & Component Weights</td><td rowspan="3">Nil</td><td>649.74 (3.5%)</td><td rowspan="3">Medium</td><td rowspan="3">High</td></tr>
<tr><td rowspan="2">Cargo Hold</td><td>32m</td><td>3.07</td><td>72.56% reduction</td><td>501.80t (2.3%)</td><td>696.32 (3.8%)</td></tr>
<tr><td>47m</td><td>2.4</td><td>79.13% reduction</td><td>737.02t (3.37%)</td><td>974.78 (5.3%)</td></tr>
<tr><td colspan="4">Passive Damping Plate</td><td>3.02</td><td>72.64% reduction</td><td colspan="2">61.56 tons of steel</td><td>Nil</td><td>Nil</td><td>Low</td><td>~ 6hrs (for fixing)</td><td>No</td><td>Low</td></tr>
</table>

Very Good Good Satisfactory Bad

All the cases studied in this thesis have been compared in table 11 along with RAO comparison in Figure 66.

The aim of the study is to find the most economical and feasible roll stabilization system for SAL 183. And from table 11 it could be seen that the most expensive configuration of all is adding new set of tanks as the whole system has to be build and installed, and the response obtained by adding those are not that impressive. Also large amount of weight is added onboard along with loss of volume loss hence due to all the disadvantages this configuration can’t be considered as a good solution.

The next high priority parameter is the loss of lifting capacity. As the loss of lifting capacity is too high while using midship ballast tanks as anti roll U tank these designs are discarded. In addition, converting these tanks into anti roll U tank using valves is really a complex process.

So finally the configurations left are passive damping plate and modifying forward ballast tanks to anti roll U tanks. When the initial cost is considered the passive anti roll U tank is really cheap as the plate can be constructed anywhere around the world and can be loaded on to the vessel when the fabrication is over. While for modifying the forward ballast tanks, the vessel has to be idle as steel structures are cut and welded in the cargo hold of the ship and this can be done only with a support of the shipyard which might increase the initial cost. But in long run this difference in the initial costs might get reduced as in the case of damping plate 6hrs are lost whenever these plates has to be attached to the vessel, since time is money this loss of time has to be considered as an money spend as installment for fixing this system. So the initial cost alone can’t be considered as a selection criteria here.

If only 10m configuration is considered then the extra material added will be almost the same as the damping plate since the main plate to create the connecting tube will be 10x17m with really less stiffening and thickness when compared with the plate. The 10m configuration has the added advantage of effective roll reduction and possibility of using it during the transit. While the plate increases the motion of the vessel in higher frequency waves, and can’t be used during transit due to very high increase in resistance, as well as, is 6.8% less effective compared with the 10m configuration. However using the 10m configuration will reduce the lifting capacity of the vessel by 3.2% and the cargo volume by 2%. Hence it could be said that both the passive damping plate, as well as, modifying 10m of the forward ballast tanks are feasible and economical solution for vessel SAL 183 with its own pros and cons.

9. CONCLUSION

All the possibilities of installing a roll stabilization system on heavy lift vessel SAL type 183 were studied. The solution with really less initial investment will be fixing a plate of dimension 12.64 m x 12.94 m on the pontoon arm with an angle of 17.2 degrees at 1.9 m above the keel. This arrangement reduces the roll motion up to 72.6 % and doesn't affect the vessel particulars, but this increases the motion of the vessel at lower wave periods where the occurrences of waves are high. In addition, this system can't be used during transit because it induces high resistance to the vessel.

So another solution which is more effective than the above is to modify the ballast tanks in the forward of the vessel to an antiroll U tank. The best choice will be to just modify 10 m of the ballast tank which provides a reduction of 79.45 % in roll motion and also it has the added advantage that it can be used during transit. But a compromise on the cargo volume as well as lifting capacity has to be considered as 2 % of the cargo volume will be lost if this system is used and also 3.2 % of the lifting capacity as these tanks were used for obtaining counter moment while lifting. In addition, this modification can be done only in a shipyard during which the vessel remains idle and, hence, it results in higher initial cost.

Thus, the company may choose their suitable system, as both systems possess advantages and disadvantages which can't be compared. During this study it was found that Ikeda method gives good roll prediction for SAL type 183 hull forms for the considered metacentric height which can be considered as an additional inference for future calculations.

Finally, the further extension of this project will be to perform experimental studies on the vessel with the plate for better understanding and also studying the effect of holes in the plate which will increase the effectiveness of the current plate as it increases the damping due to eddy dissipation. Furthermore, the damping plate's efficiency in seaways higher than 1.5 m significant wave height need to be assessed if offshore installations carried out with heavy lift vessels become common practice in future.

10. REFERENCES

[1] Prof. Dr.-Ing. habil. Nikolai Kornev, 2012, *Ship Dynamics in Waves* , Rostock: Faculty of Mechanical Engineering and Marine Technology Chair of Modelling and Simulation, University of Rostock

[2] Yuki KAWAHARA, Kazuya MAEKAWA, Yoshiho IKEDA ,2009, A Simple Prediction Formula of Roll Damping of Conventional Cargo Ships on the Basis of Ikeda's Method and Its Limitation, *Proceedings of the 10th International Conference on Stability of Ships and Ocean Vehicles*, 6, 387-398

[3] Martin Irvine, Jr., Joseph Longo, and Frederick Stern, 2013, Forward Speed Calm Water Roll Decay for Surface Combatant 5415: Global and Local Flow Measurements, *Journal of Ship Research*, 57(4), 1–18.

[4]Robert V. Wilson , Pablo M. Carrica, Fred Stern, 2006, Unsteady RANS method for ship motions with application to roll for a surface Combatant, *Computers & Fluids*, 35, 501–524.

[5] YANG Boa, WANG Zuo-chao, WU Ming, Numerical Simulation of Naval Ship's Roll Damping Based on CFD, *Procedia Engineering*, 37, 14 – 18.

[6] Ahmed F. Abdel Gawad , Saad A. Ragab, Ali H. Nayfeh, Dean T. Mook, 2001, Roll stabilization by anti-roll passive tanks, *Ocean Engineering*, 28 , 457–469

[7] William E, Woolam,1973. *Drag Coefficients for Flat Square Plates Oscillating Normal To Their Planes In Air.* Texas .Southwest Research Institute

[8] Garbis H. Keulegan and Lloyd H. Carpenter, 1958, Forces on Cylinders and Plates in an Oscillating Fluid, *Journal of Research of the National Bureau of Standards*, 60(5), 423-440.

[9] Xavier Ortiz, David Rival, David Wood , 2015, Forces and Moments on Flat Plates of Small Aspect Ratio with Application to PV Wind Loads and Small Wind Turbine Blades, E*nergies*, 8, 2438-2453.

[10]Khaled S. Youssef, Saad A. Ragab, Ali H. Nayfeh *, Dean T.Mook, 2002, Design of passive anti-roll tanks for roll stabilization in the nonlinear range, *Ocean Engineering*, 29, 177–192.

[11] Reza Moaleji, Alistair R. Greig, 2007, On the development of ship anti-roll tanks, *Ocean Engineering*, 34, 103–121.

[12]ITTC, 2011, Recommended Procedures - Numerical Estimation of Roll Damping

[13] WAMIT User Manual Version 7.1.

[14] Det Norske Veritas , 2010, Recommended Practice DNV-RP-H103Modelling and Analysis of Marine Operations.

[15] Det Norske Veritas , 2010, Recommended Practice DNV-RP-C201 Buckling Strength Of Plated Structures.

APPENDIX A1

OUTPUT FROM WAMIT

```
-----------------------------------------------------------------------

WAMIT  Version 7.102(x64)

Copyright (c) 1999-2015 WAMIT Incorporated
Copyright (c) 1998 Massachusetts Institute of Technology

-----------------------------------------------------------------------

The WAMIT software performs computations of wave interactions with
floating or submerged vessels.  WAMIT is a registered trademark of
WAMIT Incorporated.  This copy of the WAMIT software is licensed to

SAL Heavy Lift GmbH
Brooktorkai 20
20457 Hamburg
Germany

for lease.                    Release date: 17 Jun 2015

-----------------------------------------------------------------------


Low-order panel method  (ILOWHI=0)

Input from Geometric Data File:        SAL183.gdf
Rhino->WAMIT file export (mesh)

Input from Potential Control File:      shipwithoutplate.pot
shipwithoutplate.pot


POTEN run date and starting time:        06-Nov-2015  --  14:57:41
Period       Time           RAD      DIFF  (max iterations)
19.2000    14:59:10        -1 (-1)  -1 (-1)

Gravity:     9.80665               Length scale:        1.00000
Water depth:        infinite
Logarithmic singularity index:             ILOG =     0
Source formulation index:                  ISOR =     1
Diffraction/scattering formulation index: ISCATT =     0
Number of blocks used in linear system:   ISOLVE =     1
Number of unknowns in linear system:        NEQN =  5628

BODY PARAMETERS:

Total panels:    5628  Waterline panels:    374      Symmetries: none
Irregular frequency index: IRR = 0

XBODY =    0.0000 YBODY =    0.0000 ZBODY =    3.0000 PHIBODY =   0.0
Volumes (VOLX,VOLY,VOLZ):          21317.6      21316.9      21316.7
```

Center of Buoyancy (Xb,Yb,Zb): -0.370687 -0.000001 -6.799070
Hydrostatic and gravitational restoring coefficients:
C(3,3),C(3,4),C(3,5): 3384.0 0.92803E-02 21759.
C(4,4),C(4,5),C(4,6): 32629. 0.27849 0.0000
C(5,5),C(5,6): 0.47404E+07 0.0000
Center of Gravity (Xg,Yg,Zg): -0.370687 -0.000001 0.000000
Radii of gyration: 11.000000 0.000000 0.000000
0.000000 40.000000 0.000000
0.000000 0.000000 40.000000

Output from WAMIT

FORCE run date and starting time: 06-Nov-2015 -- 14:59:10

I/O Files: shipwithoutplate.frc shipwithoutplate.p2f shipwithoutplate.out
shipwithoutplate.frc

****

Wave period (sec) = 1.920000E+01 Wavenumber (kL) = 1.092035E-02

ADDED-MASS AND DAMPING COEFFICIENTS

I	J	A(I,J)	B(I,J)
1	1	1.209216E+03	1.059662E+02
1	2	1.325220E-03	1.196461E-04
1	3	9.094962E+02	-2.792090E+01
1	4	-3.930008E-02	1.811835E-03
1	5	2.452290E+05	2.215602E+04
1	6	-1.873207E-01	1.336869E-03
2	1	7.055998E-04	-6.445199E-04
2	2	1.904260E+04	4.409684E+02
2	3	3.576815E-02	3.050756E-02
2	4	1.762226E+04	-1.054890E+02
2	5	3.805008E-01	3.021250E-01
2	6	1.266579E+05	1.353293E+03
3	1	9.094838E+02	-2.802710E+01
3	2	-2.432898E-03	4.653111E-04
3	3	6.100597E+04	3.186151E+04
3	4	-2.109986E-01	2.312771E-02
3	5	4.890322E+05	2.118222E+05
3	6	-1.495743E-02	-1.107437E-02
4	1	-3.022671E-02	-4.203081E-03
4	2	1.771771E+04	-1.027390E+02
4	3	-7.672977E-02	1.484356E-01
4	4	4.436161E+05	9.416854E+01
4	5	-6.552795E+00	6.628952E-01
4	6	1.188418E+06	7.369728E+02
5	1	2.452282E+05	2.215679E+04
5	2	1.318884E-01	1.525319E-02

5	3	4.889784E+05	2.116827E+05
5	4	-1.189702E+01	9.559901E-02
5	5	6.078842E+07	6.123488E+06
5	6	-1.691821E+01	6.782640E-01
6	1	-6.498260E-01	-7.456398E-02
6	2	1.266486E+05	1.352323E+03
6	3	-4.155197E-01	-3.144226E-01
6	4	1.189836E+06	7.304816E+02
6	5	-8.114062E+01	-1.466577E+01
6	6	2.335523E+07	2.010713E+04

HASKIND EXCITING FORCES AND MOMENTS

Wave Heading (deg) : 90

I	Mod[Xh(I)]	Pha[Xh(I)]
1	9.652312E+00	-178
2	4.086067E+02	89
3	2.518188E+03	8
4	1.010371E+02	-91
5	1.642585E+04	8
6	1.294557E+03	89

RESPONSE AMPLITUDE OPERATORS

Wave Heading (deg) : 90

I	Mod[RAO(I)]	Pha[RAO(I)]
1	9.12836E-04	179
2	3.01337E+00	-87
3	1.00379E+00	0
4	5.52476E+00	93
5	3.67231E-05	180
6	1.10230E-01	-87

APPENDIX A2

BEST CONFIGURATIONS FOR ANTI ROLL U-TANK

Forward Ballast Tanks						
Config No	yo	yi	zo	zi	hr	hw
1	12.5	5.35	2.2	2.902202	0.726826	1.077928
2	12.5	5.35	2.2	2.905405	1.139492	1.492194
3	12.5	5.35	2.2	2.908609	1.548426	1.90273
4	12.5	5.35	2.2	2.911812	1.95368	2.309586
5	12.5	5.35	2.2	2.915015	2.355303	2.71281
6	12.5	5.35	2.2	2.918218	2.753343	3.112452

On Tween Deck						
Config No	yo	yi	zo	zi	hr	hw
1	8.25	0.082323	10.8	11.18485	3.184576	3.377
2	8.25	0.164646	10.8	11.18485	3.210991	3.403415
3	8.25	0.24697	10.8	11.18485	3.255015	3.447439
4	8.25	0.329293	10.8	11.18485	3.31665	3.509074
5	8.25	0.411616	10.8	11.18485	3.395894	3.588318
6	8.25	0.493939	10.8	11.18485	3.492748	3.685172
7	8.25	0.576263	10.8	11.18485	3.607212	3.799636
8	8.25	0.658586	10.8	11.18485	3.739285	3.93171
9	8.25	0.740909	10.8	11.18485	3.888969	4.081393
10	8.25	0.823232	10.8	11.18485	4.056262	4.248686
11	8.25	0.905556	10.8	11.18485	4.241165	4.43359
12	8.25	0.987879	10.8	11.18485	4.443678	4.636103
13	8.25	2.55202	10.8	11.13737	0.384572	0.553259
14	8.25	2.634343	10.8	11.13737	1.01734	1.186026
15	8.25	2.716667	10.8	11.13737	1.670195	1.838882
16	8.25	2.79899	10.8	11.13737	2.343138	2.511825
17	8.25	2.881313	10.8	11.13737	3.036169	3.204856
18	8.25	2.963636	10.8	11.13737	3.749288	3.917975
19	8.25	3.951515	10.8	11.0899	1.144286	1.289236
20	8.25	4.033838	10.8	11.0899	2.278095	2.423044
21	8.25	4.116162	10.8	11.0899	3.435281	3.580231
22	8.25	4.939394	10.8	11.04242	1.544598	1.66581
23	8.25	5.021717	10.8	11.04242	3.235912	3.357124
24	8.25	5.762626	10.8	10.99495	2.209407	2.306882
25	8.25	6.421212	10.8	10.94747	0.636889	0.710626
26	8.25	6.503535	10.8	10.94747	4.24431	4.318047
27	8.25	7.079798	10.8	10.9	1.908626	1.958626

On Tween Deck						
Config No	yo	yi	zo	zi	hr	hw
1	8.25	0.905556	2.2	2.568687	0.411587	0.59593
2	8.25	0.987879	2.2	2.568687	0.622977	0.80732
3	8.25	1.070202	2.2	2.568687	0.852749	1.037092
4	8.25	1.152525	2.2	2.568687	1.100903	1.285246
5	8.25	1.234848	2.2	2.568687	1.367438	1.551782
6	8.25	1.317172	2.2	2.568687	1.652356	1.836699
7	8.25	1.399495	2.2	2.568687	1.955655	2.139998
8	8.25	1.481818	2.2	2.568687	2.277336	2.461679
9	8.25	1.564141	2.2	2.568687	2.617398	2.801742
10	8.25	1.646465	2.2	2.568687	2.975843	3.160186
11	8.25	1.728788	2.2	2.568687	3.352669	3.537012
12	8.25	1.811111	2.2	2.568687	3.747877	3.93222
13	8.25	1.893434	2.2	2.568687	4.161466	4.34581
14	8.25	1.975758	2.2	2.568687	4.593438	4.777781
15	8.25	2.058081	2.2	2.568687	5.043791	5.228134
16	8.25	2.140404	2.2	2.568687	5.512526	5.696869
17	8.25	2.222727	2.2	2.568687	5.999643	6.183986
18	8.25	2.305051	2.2	2.568687	6.505141	6.689484
19	8.25	2.387374	2.2	2.568687	7.029021	7.213365
20	8.25	2.469697	2.2	2.568687	7.571283	7.755627
21	8.25	2.55202	2.2	2.568687	8.131927	8.316271
22	8.25	2.634343	2.2	2.568687	8.710953	8.895296
23	8.25	2.716667	2.2	2.568687	9.30836	9.492703
24	8.25	2.79899	2.2	2.568687	9.924149	10.10849
25	8.25	2.881313	2.2	2.568687	10.55832	10.74266
26	8.25	2.963636	2.2	2.568687	11.21087	11.39522
27	8.25	3.04596	2.2	2.568687	11.88181	12.06615
28	8.25	3.128283	2.2	2.568687	12.57112	12.75547
29	8.25	5.10404	2.2	2.434343	1.96731	2.084482
30	8.25	5.186364	2.2	2.434343	3.774784	3.891956
31	8.25	5.268687	2.2	2.434343	5.611178	5.728349
32	8.25	5.35101	2.2	2.434343	7.476491	7.593663
33	8.25	5.433333	2.2	2.434343	9.370724	9.487895
34	8.25	5.515657	2.2	2.434343	11.29388	11.41105
35	8.25	7.079798	2.2	2.3	1.908626	1.958626
36	8.25	7.162121	2.2	2.3	7.77083	7.82083

APPENDIX A3

DAMPING PLATE OPTIMIZATION RESULTS

Pareto Set							
ID	L	B	Z	rotation	Response	WeightTons	Aspect Ratio
40	5.013787086	10.10546075	-10.3656	-7.4	6.115445	13.226806	2.015534481
71	5.842059337	12.36211604	-10.3656	-5.9	4.875307	23.303858	2.116054516
194	10.72294939	11.3116041	-10.1633	-16.8	3.849458	38.930596	1.054896716
201	10.68350785	11.29215017	-10.12	-16.7	3.852633	38.604955	1.056970269
210	11.0877836	11.60341297	-10.2356	-16.3	3.682268	42.883824	1.046504278
250	4.97434555	4.989078498	-10.2789	-14.6	9.131646	2.602283	1.002961786
256	3.771378709	5.07662116	-9.83111	-15.1	9.419273	1.970142	1.34609159
360	7.35069808	14.45341297	-9.81667	-18.4	3.724083	42.296729	1.966263994
387	5.615270506	11.46723549	-10.0767	-17.9	5.148514	19.293866	2.042151929
400	5.615270506	11.46723549	-10.5389	-18	5.146127	19.742543	2.042151929
403	5.565968586	12.32320819	-9.73	-16.6	4.882178	21.774607	2.214027622
474	11.54136126	12.05085324	-9.65778	-18.2	3.426043	48.322391	1.044144878
480	10.09188482	10.98088737	-10.2067	-17.7	4.071718	34.087172	1.088090835
481	11.89633508	12.54692833	-9.65778	-17.8	3.240038	54.360774	1.054688544
490	11.54136126	12.05085324	-9.6	-18.4	3.429947	48.257477	1.044144878
507	11.5117801	12.15784983	-9.62889	-18.2	3.412147	49.045682	1.056122487
509	10.23979058	10.6890785	-9.57111	-17.3	4.139116	31.783431	1.043876671
513	10.89057592	12.23566553	-9.61444	-17.8	3.500318	46.824758	1.123509502
517	11.54136126	12.95546075	-9.6	-18.4	3.190971	56.532428	1.122524498
519	10.23979058	10.72798635	-9.57111	-17.3	4.130249	32.049597	1.047676343
520	9.983420593	11.36996587	-9.57111	-17.4	3.956553	36.040374	1.13888479
523	11.64982548	13.08191126	-9.6	-18.5	3.144927	58.197063	1.12292766
525	11.5117801	12.15784983	-9.51333	-17.3	3.413227	48.873178	1.056122487
544	12.23158813	13.51962457	-9.55667	-18.5	2.982539	66.050509	1.105304105
549	11.5117801	12.1383959	-9.57111	-17.3	3.416338	48.780732	1.054432572
551	11.54136126	14.1616041	-9.57111	-17.7	2.958111	68.698049	1.227030658
556	11.30471204	11.61313993	-9.6	-17.2	3.623613	43.241316	1.027283127
558	11.5117801	12.18703072	-9.57111	-17.3	3.410604	49.206738	1.058657358
563	11.5117801	12.23566553	-9.57111	-17.3	3.3738	49.616463	1.062882145
571	11.66954625	12.56638225	-9.55667	-17.1	3.288461	53.092347	1.076852689
575	5.506806283	5.397610922	-9.77333	-17.2	8.721219	3.42915	1.020230314
581	10.45671902	11.42832765	-9.71556	-18	3.855472	38.567303	1.092917159
584	12.13298429	13.39317406	-9.51333	-17	3.019809	64.28374	1.103864782
600	7.863438045	10.94197952	-9.74444	-14.9	4.683992	25.508281	1.391500697
602	12.33019197	12.38156997	-9.58556	-17.2	3.200814	54.647073	1.004166845
605	2.883944154	4.629180887	-9.70111	-17.2	9.856921	1.30898	1.605156217
615	9.756631763	11.54505119	-9.51333	-17.3	3.953046	36.384219	1.183302955
625	12.33019197	12.92627986	-9.58556	-17.2	3.070029	60.218087	1.048343764

633	12.33019197	12.87764505	-9.58556	-17.2	3.106591	59.270936	1.044399396
641	12.63586387	12.92627986	-9.58556	-17.2	3.022852	61.562542	1.022983469
653	11.5117801	12.53720137	-9.6	-17.5	3.30867	52.220514	1.089075821
659	6.206893543	12.16757679	-9.67222	-17.5	4.693031	24.749005	1.960332767
660	11.5117801	12.5274744	-9.6	-17.5	3.311942	52.150025	1.088230863
661	9.312914485	12.33293515	-9.6	-17.5	3.778943	40.501752	1.324283088
681	10.22993019	12.28430034	-9.68667	-17.2	3.616111	44.403598	1.200819567
750	7.508464223	10.98088737	-9.67222	-16.5	4.754231	24.369481	1.462467829
761	5.536387435	12.72201365	-9.65778	-17	4.776351	23.545625	2.297890782
803	11.30471204	10.86416382	-9.65778	-16.6	3.850162	38.920068	1.040550587
854	4.717975567	6.739931741	-9.64333	-16	8.198231	4.804091	1.428564359
867	8.208551483	10.81552901	-9.64333	-16.7	4.621192	25.947946	1.317592883
870	8.52408377	10.30972696	-9.31111	-15.4	4.771549	23.85913	1.209482126
871	7.626788831	9.755290102	-8.96444	-17.5	5.31972	18.632171	1.279082235
940	9.194589878	10.63071672	-9.70111	-16.3	4.444918	28.161662	1.156192594
944	11.84703316	11.75904437	-9.64333	-18.2	3.450905	47.353154	1.007482648
990	10.79197208	10.86416382	-9.64333	-16.8	3.987022	34.971356	1.006689393
993	7.656369983	10.86416382	-9.80222	-15	4.770072	24.318242	1.418970589
995	3.712216405	6.311945392	-9.64333	-14.9	8.804203	3.426087	1.700317197
1015	8.326876091	10.6890785	-9.64333	-15.7	4.64292	25.598935	1.283684107
1041	4.027748691	4.230375427	-9.48444	-15.4	9.752533	1.40418	1.050307691
1061	4.451745201	8.442150171	-8.27111	-13.3	7.273418	7.197339	1.89636868
1065	9.460820244	10.52372014	-9.67222	-11.9	4.449819	27.876032	1.112347541
1069	4.293979058	9.62883959	-8.12667	-13.6	6.632369	8.493782	2.242404879
1072	4.461605585	6.477303754	-8.12667	-13.6	8.452552	3.56885	1.45178762
1081	3.731937173	8.344880546	-7.88111	-13.5	7.680924	5.51679	2.236072088
1084	2.755759162	5.23225256	-10.4522	-14.7	9.652327	1.846364	1.898661041
1089	4.293979058	9.62883959	-8.18444	-13.6	6.632623	8.491884	2.242404879
1096	3.731937173	8.432423208	-7.79444	-12.9	7.630937	5.60446	2.259529788
1097	4.372862129	8.442150171	-7.73667	-13.7	7.294431	7.065306	1.930577713
1098	2.765619546	5.961774744	-10.4089	-14.2	9.341052	2.572553	2.155674215
1100	4.165794066	9.15221843	-8.25667	-13.6	6.969729	7.592906	2.196992526
1102	3.731937173	8.442150171	-7.79444	-13.7	7.619279	5.619117	2.262136199
1116	4.412303665	10.52372014	-9.67222	-13.1	6.130531	12.015364	2.385085193
1138	4.412303665	10.56262799	-10.2789	-12.3	6.117479	12.555901	2.393903228
1152	6.177312391	11.10733788	-10.2211	-12.6	5.135907	20.276691	1.798085831
1219	5.694153578	13.40290102	-9.99	-9	4.575396	26.336334	2.35380041
1233	5.694153578	13.40290102	-9.99	-11.3	4.551335	26.409628	2.35380041
1295	5.595549738	13.40290102	-10.1633	-11	4.598712	26.168065	2.395278686
1474	7.833856894	10.27081911	-8.35778	-11.5	5.01157	20.578894	1.311080768
1507	5.388481675	11.2337884	-10.2067	-11.3	5.381631	18.071689	2.084778064
1566	4.92504363	11.60341297	-10.2067	-11	5.440725	17.38873	2.356002066
1570	4.215095986	10.02764505	-10.2067	-11.3	6.492975	10.562131	2.378983796
1605	4.363001745	9.891467577	-10.2067	-11.4	6.487113	10.686759	2.267124369
1616	13.01055846	12.98464164	-10.2067	-12.1	2.987233	64.435622	1.00199596

1621	4.284118674	10.01791809	-10.2067	-11.4	6.464029	10.710159	2.338384824
1625	11.84703316	14.97866894	-10.2067	-11.9	2.768198	80.309663	1.264339244
1634	4.293979058	10.01791809	-10.2067	-11.5	6.459198	10.730663	2.333015125
1659	5.023647469	7.595904437	-8.22778	-11.5	7.601826	6.095726	1.512029752
1664	4.796858639	4.240102389	-10.2067	0.2	9.620318	1.936051	1.131307265
1672	4.796858639	4.259556314	-10.2067	0.2	9.611792	1.942504	1.126140444
1679	5.260296684	6.457849829	-7.67889	-10.6	8.203275	4.188401	1.22765886
1680	5.260296684	6.467576792	-7.67889	-1	8.293126	4.145231	1.229507988
1686	5.822338569	4.716723549	-7.34667	-10.1	8.937547	2.88838	1.234403184
1688	4.392582897	9.70665529	-8.35778	-11.4	6.553636	8.790852	2.209783063
1692	4.195375218	8.977133106	-7.53444	-10.7	7.072624	7.409959	2.139768826
1695	5.487085515	10.93225256	-7.67889	-10.2	5.460962	15.527131	1.992360522
1699	5.989965096	5.047440273	-8.51667	-10.9	8.71781	3.510046	1.18673323
1700	6.926701571	12.48856655	-9.48444	-11.6	4.415387	28.385014	1.802960099
1702	5.487085515	9.375938567	-7.67889	-10.2	6.298601	11.115769	1.708728348
1709	4.106631763	9.609385666	-8.32889	-11.6	6.757709	8.0726	2.339967696
1719	3.613612565	8.228156997	-8.01111	-11.5	7.83574	4.870254	2.276989259
1723	11.04834206	15.21211604	-9.32556	-12.7	2.855431	76.836478	1.37686867
1729	5.161692845	11.03924915	-7.98222	-11.6	5.545953	14.778021	2.138687729
1733	8.652268761	12.51774744	-7.96778	-9.6	3.913177	36.958187	1.44675897
1741	11.00890052	16	-9.28222	-12.8	2.730007	86.151285	1.453369477
1743	10.94973822	16	-9.47	-13.5	2.756868	86.042658	1.461222148
1753	6.65061082	13.99624573	-9.65778	-11.8	4.058084	34.807734	2.104505302
1761	6.068848168	8.860409556	-8.47333	-11.4	6.413926	10.901083	1.459982078
1763	5.220855148	10.62098976	-7.76556	-11.6	5.697995	13.520028	2.034339099
1769	7.173211169	13.20836177	-8.27111	-11.6	4.101248	32.742705	1.841345732
1773	6.295636998	14.01569966	-8.58889	-11	4.171409	31.105135	2.226256003
1786	5.151832461	3.461945392	-8.22778	-11.6	9.720692	1.446929	1.488132214
1791	7.163350785	14.35614334	-8.95	-12.7	3.818651	39.379788	2.004110056
1801	7.114048866	14.22969283	-8.93556	-12.7	3.859575	38.55713	2.000224219
1803	7.77469459	14.32696246	-9.31111	-11.5	3.676958	43.225094	1.842768522
1805	6.680191972	12.56638225	-8.89222	-11.1	4.46124	26.907136	1.881140887
1806	5.960383944	13.96706485	-8.27111	-11.5	4.301807	28.492179	2.343316299
1812	6.295636998	13.96706485	-8.27111	-11.5	4.183768	30.251086	2.218530841
1814	11.72870855	12.56638225	-10.1633	-11.2	3.284332	53.458387	1.071420796
1815	6.739354276	15.69846416	-8.77667	-12.8	3.694402	42.781746	2.329372151
1818	6.512565445	13.82116041	-8.56	-12.1	4.146805	31.523257	2.122229792
1823	6.759075044	15.17320819	-8.83444	-12.4	3.784353	40.435617	2.244864585
1901	10.26937173	11.92440273	-9.08	-11.5	3.73568	40.904071	1.161161856
1909	9.283333333	10.15409556	-9.91778	-11.3	4.67898	25.554753	1.093798445
1911	11.41317627	14.84249147	-9.73	-11.3	2.871216	75.36111	1.300469836
1921	10.87085515	11.32133106	-9.78778	-6.1	3.893872	37.802408	1.041438866
1981	9.529842932	9.979010239	-8.87778	-10.3	4.7045	24.395206	1.047132708